BIOFIDELIC CONSIDERATIONS FOR IMPROVING STANDARDIZED AIRFLOW AND FIRMNESS TESTING FOR INFANT SLEEP PRODUCTS

by

Wyatt D. Davis

A thesis

submitted in partial fulfillment

of the requirements for the degree of

Master of Science in Mechanical Engineering

Boise State University

May 2022

BOISE STATE UNIVERSITY GRADUATE COLLEGE

DEFENSE COMMITTEE AND FINAL READING APPROVALS

of the thesis submitted by

Wyatt D. Davis

Thesis Title: Biofidelic Considerations for Improving Standardized Airflow and Firmness Testing for Infant Sleep Products

Date of Final Oral Examination: 11 March 2022

The following individuals read and discussed the thesis submitted by student Wyatt D. Davis, and they evaluated the student's presentation and response to questions during the final oral examination. They found that the student passed the final oral examination.

Erin Mannen, Ph.D.	Chair, Supervisory Committee
Trevor Lujan, Ph.D.	Member, Supervisory Committee
Krishna Pakala, Ph.D.	Member, Supervisory Committee
Safeer Siddicky, Ph.D.	Member, Supervisory Committee

The final reading approval of the thesis was granted by Erin Mannen, Ph.D., Chair of the Supervisory Committee. The thesis was approved by the Graduate College.

CONFIDENTIALITY STATEMENT AND IN PROGRESS PROJECT STATUS

All contents of this thesis are considered strictly confidential. Portions of this project are funded by the United States Consumer Product Safety Commission. The overall funded project is incomplete, and the data presented in this report should not be considered as finalized for the purpose of the overarching projects.

ACKNOWLEDGMENTS

I am extremely grateful to my family, Scott, Libby, and Wally, and my friends for the love and support they have provided throughout the years. I must also express my deepest thank you to Dr. Erin Mannen and Dr. Safeer Siddicky for all of the help and advice given during my time in the BABI Lab, as well as all of the support provided by my colleagues. I would also like to thank the Mechanical and Biomedical Engineering Department and the Engineering Design Studio at Boise State University for their continued support of my research. I would also like to acknowledge the help of Scott Tavernini and Dr. Andrew Martin from the University of Alberta for providing the files of the idealized models used in this study. Lastly, this project would not have been possible without the support of the Consumer Product Safety Commission.

ABSTRACT

Background

Over the last 30 years, 83 infant fatalities (113 reported, 30 incidental) directly involving crib bumpers have been reported to the Consumer Product Safety Commission. Of these reports, 90% are for infants under a year old, with 61% occurring for infants between 1 and 4 months of age (Safety, 2020). There are currently a few regulations governing the design of crib bumper products, but none test the suffocation risk associated with these products using biofidelic methods.

Goals

We sought to explore the development of new testing methods that can determine the safety of different products and are physiologically representative of this age range. These test methods were derived from the British Standard BS 4578:1970*, Test for Hardness of, and for Air Flow Through Infant Pillows*, and further developed through application of medical literature and anthropometric measures.

Methods

In the process of modifying BS 4578:1970, airflow tests and firmness tests were developed and conducted. In airflow testing, we modified the original flowrate to 2 L/min to model a 2 to 4-month-old and examined the effects of increasing probe complexity to be more representative of an infant's airway system. We sought to find the simplest probe that maintains physiologically representative results for ease of implementation. We also

conducted force vs. displacement testing and characterized products based on stress relaxation.

Results and Discussion

We found that a simple model made of a 3-inch diameter hemisphere with two 3.125-mm air channels representing the nares was the best suited for our criteria. This probe was able to distinguish between safe and unsafe product categories, recording mean pressure values of 0.254 ± 0.019 in. H_2O and 2.038 ± 0.417 in. H_2O respectively. These higher values fit with the expected initial pressure in an infant's esophagus during occlusion (3.74 ± 1.96 in. H_2O) (Cohen and Henderson-Smart, 1986). This led to a recommendation for a threshold to be developed at 0.311 in. H_2O for airflow testing. Our firmness testing was able to characterize the different product categories, finding that each category retained a certain percentage of the initial applied force. The most meaningful data to come from this testing was finding the linear relationship between applied force and measured pressure at levels above 2 N, particularly for the traditional products. All R-squared values for this category were above 0.98.

Conclusion

Our goal in this project was to explore the creation of a new and simple testing standard that can be applied to infant sleeping products. We were able to develop a threshold in airflow testing that can differentiate between safe and unsafe products, while showing that our model is physiologically representative. However, it can currently only be shown that this threshold is applicable to crib bumpers and new thresholds may be developed for different product categories. We also found the relationship between force and pressure for the specific products tested, which can allow for approximations of pressure readings under varied loads.

TABLE OF CONTENTS

LIST OF FIGURES

LIST OF TABLES

LIST OF ABBREVIATIONS

CPSC	Consumer Product Safety Commission

INTRODUCTION

Background

For infants less than 1 year old, the greatest risk of injury or death lies in unintentional suffocation. In an analysis of the Sudden Unexpected Infant Death Case Registry from 2011 to 2014, it was found that 14% of cases were categorized as suffocation (Lambert et al., 2019). Furthermore, the number of fatalities involving crib bumpers tripled to 23 deaths during 2006-2012, as compared to the three previous time periods with an average of 8 deaths per time period (Scheers et al., 2016). Overall, the Consumer Product Safety Commission (CPSC) has received 113 reports of fatal incidents involving crib bumpers between 1990-2019, as well as another 113 reports of nonfatal incidents between 2008-2019 (Safety, 2020). For the fatal incidents, all reports involved traditional bumpers. Upon further examination of the fatal reports, 30 were determined to be "incidental" and unrelated to the crib bumper. However, 75 of the remaining 83 reports involved infants less than a year old. Of the 113 nonfatal incidents, it has been determined that 60 involved an injury and 15 involved a mesh liner. While only 78 of the nonfatal incidents reported the involved child's age, 47 of the cases involved children less than 1 year old (Safety, 2020). Table 1 is able to further break down the incident reports by age. During the years of 1990-2012, there were a total of 71 fatalities, 46 of which were infants aged between 1-4 months (Consumer, 2013). It has been hypothesized that these incidents are related to a combination of a lack of oxygen and carbon dioxide rebreathing when a seal is created between the product and an infant's face.

Table 1 Incidents Reports Involving Crib Bumpers Between January 1990-October 2012 Separated by Age. (Consumer, 2013).

Age	Fatalities	Injuries	No Injury	Unknown
1 to 4 months	46	21	22	1
5 to 8 months	12	24	40	1
9 to 12 months	6	20	15	1
13 to 23 months	4	7	5	0
2 years and older	3	1	2	1
Unknown Age	0	7	44	0
Total	71	80	128	4

To gain a better understanding of these incident reports, it is important to define crib bumpers and the different variations that exist within this product category. The definition can be broad, as it refers to any infant bedding accessory attached to the interior perimeter of a crib for the purpose of acting as a barrier between the infant and the sides of the crib to limit the danger of the infant's limbs being caught between crib slats (Figure 1).

Figure 1 Representative Samples of Two Common Crib Bumper Categories, Traditional Bumper (Left) and Mesh Liner (Right)

The attachment method can be varied, though it is most commonly via ties or a hook and loop system. Traditionally, they are rectangular pieces, filled with either cotton or polyester fiber. This allows them to also provide padding against impacts with the side of a crib, and less importantly, provide visual aesthetics to the crib. However, there are other variations, including vertical bumpers that attach to individual crib slats and mesh liners. These mesh liners have limited padding, as they are not designed to protect against impact injuries. However, as they are much thinner, they are often marketed as "breathable" (Safety, 2020; Consumer, 2013). While crib bumpers can be categorized into these broad groups, there is still plenty of variation between different products and brands.

Current Testing Standards and Regulations

While there have been several reports related to the potential risk of crib bumpers, there are few testing standards regarding the design or sale of these products. Within the United States, manufacturers are only able to refer to one voluntary standard, ASTM F1917-12, *Standard Consumer Safety Performance Specification for Infant Bedding and Related Accessories*, when designing crib bumpers. This standard provides general requirements for a bumper's attachment method, stating that bumpers should be "'capable of being secured at or near all corners and at the midpoints of the long sides of the crib'" (Safety, 2020). It also lists performance requirements for "unsupported vinyls, maximum bumper thickness, and bumper pad tie strength" (Safety, 2020). In these requirements, the maximum bumper thickness is limited to approximately 2 inches and the strength requirement only relates to ties, but not any other form of attachment. However, this standard is lacking, as it does not provide a definition for a crib bumper, leaving room for interpretation, and only addresses suffocation risk by limiting the product's thickness, with no guidance related to firmness nor airflow (Safety, 2020).

Because many injury and death incidents involving crib bumpers report that the infant's face was found in the bumper, indicating suffocation, it is important to consider how best to test for this scenario. While there are many different factors that contribute to these incidents, it is commonly believed that permeability and firmness are two of the most important. The permeability of a product determines how easily air can flow through the material. With higher values of permeability, fresh air can more easily be accessible through the product, limiting the risk of suffocation due to either lack of oxygen or rebreathing of exhaled carbon dioxide when an infant's face is in contact with the product. This value is found through airflow testing, which either pulls or blows air through a product. The other factor to consider is the firmness of the product. When a product is firm, it requires more force to deform. In crib bumpers, this applies to how easily the product can conform to the infant's face. With higher conformability, there is a greater risk of a seal forming around the infant's airways, causing occlusion to occur.

There are a few state and local jurisdictions that have currently banned the sale of crib bumpers. These include Chicago, Il; Maryland; Watchung, NJ; and Ohio, listed in chronological order of when the ban took effect. Several of these regulations took care to exclude mesh liners from the effect of the ban and leave room for replacing the ban with a new ASTM standard. There have been other attempts to ban crib bumpers in the United States, including the "Safe Cribs Act of 2019" that also excludes mesh liners from the ban. Outside of the United States, only BS EN 16780:2018, *Textile child care articles – Safety requirements and test methods for children's cot bumpers* contains performance requirements for crib bumpers. While this standard does address several categories, including suffocation on materials and falls from the crib, it lacks test methods to determine adherence to the requirements (Safety, 2020). With the limited standards on crib bumpers, there is also a large variation in quality of products available on the market. Several retails sell mass produced products, but there are still some that are handmade or for secondhand use available and are often marketed as such.

Although the Safe Cribs Act of 2019 failed to pass through Congress, there is currently a revised form of this bill is currently working its way through the process. This edition, S. 1256 – Safe Cribs Act, is sponsored by Senator Tammy Duckworth (D-IL), who proposed it on 4/20/2021. It calls for the banning of the sale of padded crib bumpers and that mesh liners must meet specific requirements to be fit for sale. The most recent action regarding this bill was the filing of a written report, Report No. 117-62, by Senator Maria Cantwell (D-WA) from the Committee on Commerce, Science, and Transportation on February 1st, 2022 (All, n.d.). While there is a growing concern with infant sleep products, these regulations serve to completely ban the sale of similar products. The creation of a new testing standard that can determine the inherent risk of products will remove these bans but continue to prevent the sale of unsafe products.

Testing Standard Development

The CPSC began the process of investigating the safety of crib bumpers in 2012 and is seeking to develop a broad standard that can distinguish between safe and unsafe infant products (Scheers et al., 2016). Specifically, there is a focus on developing a test method that is capable of setting thresholds based on the firmness and permeability of these products.

To develop a new testing standard in the United States, one needs to follow the process used by ASTM. This process can be initiated by any stakeholder that submits a request to ASTM staff which provides a variety of information that is used to evaluate the amount of interest and support behind creating a new standard. Once the request is received, a search for existing relevant standards is conducted to prevent parallel standardization and to determine the need for standards. However, if this first step shows a need of standards in the field of interest, the request will be transferred to a relevant ASTM Technical Committee and a task group or subcommittee will be formed. If it is found that there is not a technical committee for the field in question, then a new committee will be formed by another process. A hierarchy system is then formed with three levels within the Technical Committee. These include the main committee, the subcommittee(s), and task groups, which are the research teams that perform the work that provides the basis for drafting the standard. Upon receiving reports from the task groups, key stakeholders will meet to provide input and the standard draft will be put forward to the subcommittee for approval. This approval process will repeat two more times with the main committee and the Society before gaining an official designation as an ASTM standard (ASTM, n.d.).

The development of this new standard has relied on modifying several current standards, including the British Standard BS 4578:1970*, Specification for Methods of Test for Hardness of, and for Air Flow Through Infant Pillows* (BS 4578:1970), and combining different tests. The initial modification of BS 4578:1970 primarily relies on altering the airflow rate to be more physiologically representative at 2 L/min. However, this project serves to conduct investigation into further altering the BS 4578:1970 standard to be more physiologically representative of a breathing infant and to involve a more in-depth firmness test, while having a broader application to multiple products.

BS 4578:1970

The BS 4578:1970 test was originally designed in response to occasional reports of accidental suffocation by children in bedding, specifically involving infant pillows. It provides the methodology for testing both the firmness and permeability to air. Both forms of testing can be conducted using the same probe apparatus, a metal tube that is 150 mm in length, has an internal diameter of 36 mm, and an attached metal flange with a diameter of 100 mm on the bottom (Figure 2). This apparatus also has a connection on the side for connection to an inclined manometer.

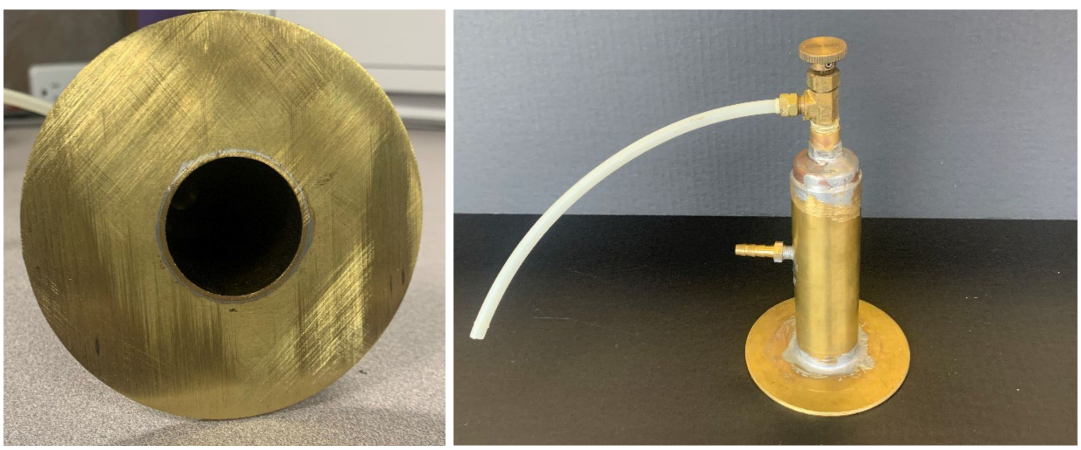

Figure 2 Different Views of Metal Apparatus Described in BS 4578:1970

For the firmness testing, 10 N of force is applied through this apparatus to the center of the product and the deformation of the product is measured. The current BS 4578:1970 does not provide a justification as to why 10 N of force was chosen. Fortunately, it is a close comparison for the weight of a newborn's head weight of about 1 kg, which is 23% of the total body weight (Coats and Margulies, 2008). More components are required for the permeability testing, including a vacuum, a flowmeter with a diaphragm-type valve, an inclined manometer, and a method for applying the 10 N of force. During permeability testing, the flow rate is adjusted to 12 L/min (200 mL/s) and the apparatus is applied to any part of the product at a force of 10 N. The pressure differential is then recorded from the inclined manometer (British, 1970).

Limitations of BS 4578:1970

While the BS 4578:1970 serves its intended purpose of measuring the permeability of infant pillows, it still has significant limitations when considering its use to evaluate crib bumpers or other infant products. Due to the high rate at which flow is designed to occur from a vacuum pump, it is possible for the outer layer of fabric of some products to become attached to the probe. When this is applied to a thin product, such as a mesh liner, it can even pull the product off of the testing surface. This leads to unrealistic testing, as a firm seal can be created in any of these mentioned scenarios, whereas this seal is not always formed by an infant's breathing in with a lower volumetric flow rate. Also, the design of the metal apparatus can also be improved upon to make the probe more applicable to other products, and not just pillows. The current apparatus has a large diameter of 36-mm. This is nearly 10 times the size of an infant's nare size, which can range from 3–7mm in diameter (Mazmanyan et al., 2020; Haase et al., 2021; Sivieri et al., 2013). When applying the original metal apparatus to crib bumpers, the flange can cover over 75% of width of the product. This will leave a channel for atmospheric air to enter the probe and alter the pressure readings during testing. Aside from the limitations posed by the high flow rate and metal apparatus used, this standard is also limited in its addressing of firmness. Currently, the displacement is measured only under a single load and there are no indications as to how meaningful that measurement is. More robust testing may be required to characterize whether a product can be defined firm.

<u>Initial Modification to BS 4578:1970</u>

To make this standard more relevant for infants, the CPSC staff proposed to alter the airflow rate to 2 L/min, a more physiological representative flow rate for infants 2 to 4 months old (U.S. EPA, 2009; Carleton et al., 1998; Maltese and Leshner, 2019; Safety, 2020). With this new flow rate, the overall testing setup was constructed following the guidelines in the standard (Figure 3). This included a flowmeter (E500; Matheson Tri-Gas, Inc., Irving, TX) with an included diaphragm-type valve for adjustment of the flow rate. The outlet of this flowmeter was connected to the vacuum side of an AC linear piston vacuum pump (VP0125; Nitto Kohki USA, Inc., Roselle, IL). This connection was also attached to a needle valve that allowed for gross control of the flow rate. The inlet of the flowmeter was connected to the metal apparatus described above. A digital differential manometer (EM201B; UEi Test Instruments, Portland, OR) was connected to the side of the metal apparatus. The metal apparatus itself was attached to a vertical lifter mechanism (Leshner & Associates, Inc., Elkton, MD) that allowed the assembly to be lowered such that the product experienced a thrust of 10 N. A weight scale (ZK14-S; Ozeri) was used to verify the magnitude of this force.

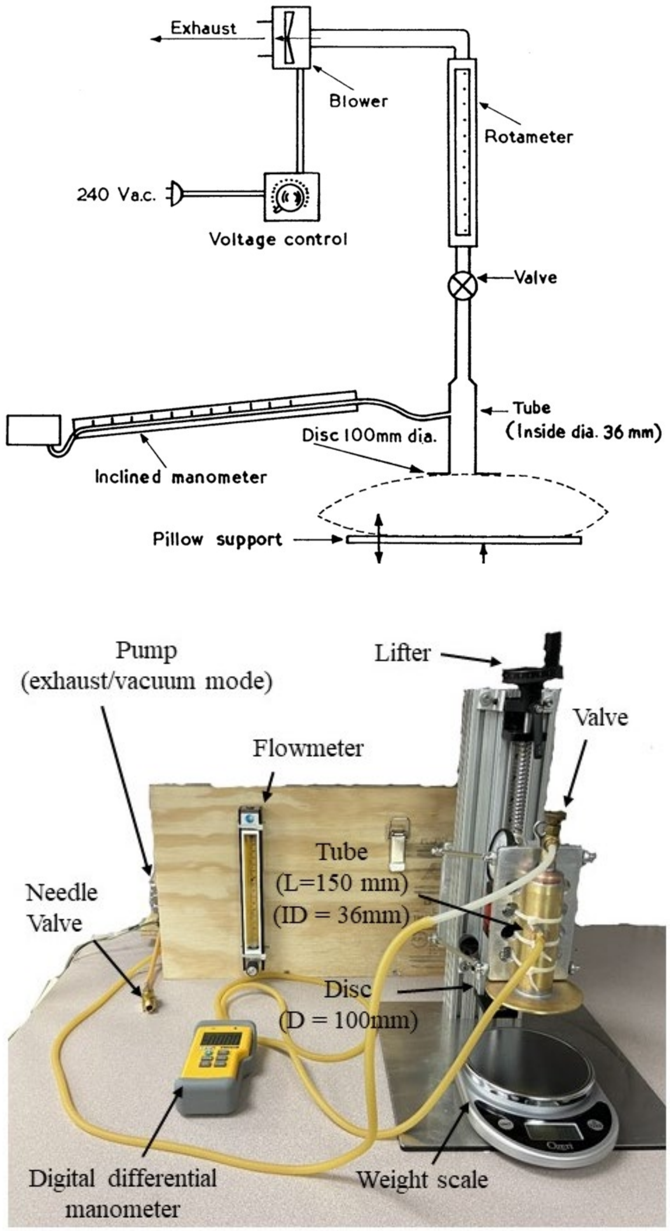

Figure 3 BS 4578:1970 Schematic (Top) and Experimental Setup for Airflow Testing (Bottom).

<u>Limitations of Initial Modification</u>

While lowering the flow rate to 2 L/min was an initial modification to make this standard more physiologically representative, it also resulted in additional limitations.

The most noticeable of these was that the pressure differential was extremely low for the traditional bumpers and below the measurable threshold of the digital manometer for the mesh products. This could have been the result of several variables, namely the diameter of the apparatus opening, and the seal created by the apparatus. Permeability is calculated by the following equation (1),

$$K = \frac{LQ\mu}{PA} \tag{1}$$

where *K* represents the permeability value, *L* is the thickness of the products, *Q* is the air flow rate, μ is the dynamic viscosity of air, *P* is the pressure differential, and *A* is the area of the opening in the probe. The flow rate and pressure differential have a direct correlation, assuming all other factors remain the same. Because of this, having a low flow rate with the current large diameter of 36 mm leads to low pressure differentials, especially if the product has a high permeability. Furthermore, as previously mentioned in describing the original standard, the size of the probe's flange would have limited the seal created by this current probe, as its outer edge was close to the edge of some bumper designs.

Objectives of Project

The objectives of this research are to primarily establish a threshold which can be used to evaluate the safety of an infant product featuring soft goods by use of a simple probe that adheres to a physiological model for use in airflow testing. A secondary objective is to establish a method for the characterization of different product categories based on firmness testing. We hypothesize:

(1) increased complexity of the probe geometry in airflow testing will result in more physiologically accurate results and allow the establishment of a threshold value that distinguishes between safe and unsafe products, and

(2) improvements to the static firmness testing will enable us to better characterize different product categories and provide greater insight into the relationship between the applied force and relative pressure created during the creation of a seal.

METHODS

Product Selection and Characterization

A small number of products were chosen from two common categories of crib bumpers for this project, specifically from traditional bumpers and mesh liners. A total of 6 products were chosen from various manufacturers, which can be further categorized into 4 traditional bumpers and 2 mesh liners (Figure 4). For the purpose of this report, manufacturer information was covered during all rounds of testing and the products themselves were assigned unique identifiers, Traditional 1–4 and Mesh 1–2. They are also referred to as T1–T4 and M1–M2 respectively within this report. After the products were decided upon, several characteristics were recorded, which are detailed in Table 2.

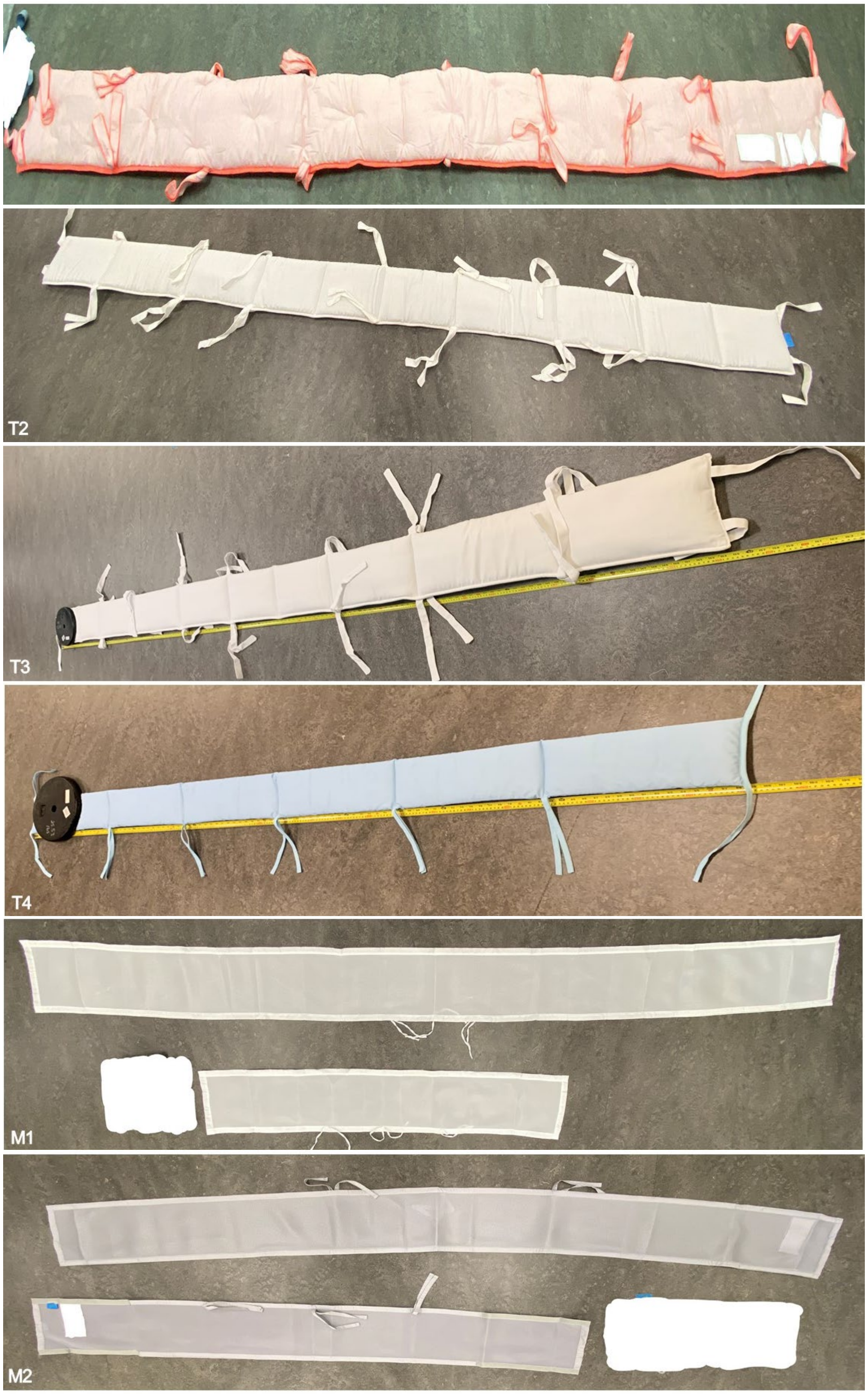

Figure 4 Photos of the Chosen Product Samples: T1, T2, T3, T4, M1, and M2.

Table 2 Measurements and characteristics with procedures and photos of a representative product.

Measurement	Procedure	Representative Photos
Length	Tape measure used to measure overall length of each representative piece of product. Product intially stretched out and returned to rest for measurement.	
Width	Width of product measured with tape measure	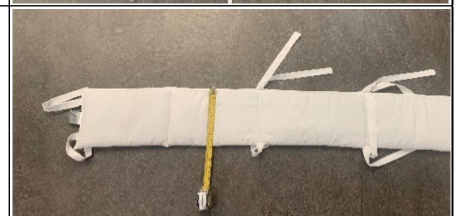
Thickness	Thickness of each product measured with analog calipers under zero force application	
Attachment Method	Crib attachment method	
Attachment Instructions (Y/N)	Were attachment instructions included with product packaging	
Material	Product materials recorded from all available sources (labels, packaging, listing)	
Number of Pieces	Total number of pieces in product set	
Cross-Sectional Photo	Approximately 10-inches in length piece of product cut and photo taken. Photos included in Appendix I	

New Probe Designs and Materials

To further expand on the CPSC staff's guided modification to BS 4578:1970 to make it more physiologically representative, we designed several different probes with increasing complexity featuring differing probe shapes, nare sizes, and 3D geometry.

To find a simple probe design that remains biofidelic, we made increasingly complex alterations to the original probe. This involved decreasing the air channel diameter, improving upon the overall probe geometry, increasing the number of channels, and including the presence of a flexible ridge. For the first step towards improving the biofidelity of the probes, we changed the diameter of the channel that air is drawn through from 36-mm to 4.5-mm, which is represented in Probe 2 (Table 3). This size is much more representative of the general nare size for infants (Mazmanyan et al., 2020; Haase et al., 2021; Sivieri et al., 2013). While this probe altered the air channel size, it still maintained the overall dimensions of the original probe's flange at 100-mm diameter. In the next step of increased complexity, we changed the overall geometry from a flat surface to hemispheric. This hemisphere had a diameter of 5-inches to be representative of the average infant head size and maintained a single 4.5-mm diameter air channel (Table 3 – Probe 3). This size was calculated (Appendix F) from the average measurement of head circumference for 0–6-month-old infants (Centers, 2001). Following this step, we went from a single air channel to two (Table 3 – Probe 4). These channels were spaced approximately 7-mm apart by centerline. After this step, we examined two different paths. For the first path, we looked at the inclusion of a flexible ridge 3.125-mm thick located between the nares (Table 3 – Probe 5). This was to represent the soft tissue of the nose. The second path looked at minimizing all dimensions within the probe and is shown in Table 3 as probe 6. The air channels were decreased to be 3.125-mm in diameter to represent the smallest nare sizes reported and remaining easy to manufacture (Mazmanyan et al., 2020; Haase et al., 2021; Sivieri et al., 2013). Furthermore, the overall size of the hemisphere was decreased to be 3-inches in diameter to represent the bizygomatic length of an infant's face (Brandt et al., 1990).

While the probe designs listed above represent the increasing biofidelity of a simple design, we also wanted to compare them to a standardized model. This came from the creation of our two idealized models of the airway system, for both a newborn (~1-month-old) and a 9-month-old. These models were obtained from the University of Alberta (Tavernini et al., 2018) and were created using computerized tomography scans of 10 infants (Storey-Bishoff et al., 2008). These scans were used to find 24 cross sections, which were then connected using splines. This led to an airway model that begins at the nostril entrance and ends distal to the larynx (Tavernini et al., 2018; Javaheri et al., 2013). This model also contain geometry to represent different portions of the nasal airway, such as a constriction leading to an offset axis to represent the laryngopharynx (Tavernini et al., 2018). The two models used in the project have the same geometry, except for isotropic scaling (Figure 5). Both model sizes have previously been used as physiological geometry to filter "the correct proportion of specifically sized inertial particles at realistic inhalation flow rates" (Tavernini et al., 2018). In the research done by the team at the University of Alberta, both models were shown to serve as a simplified and representative geometry for the actual airway system. As the models received represented the negative space of the airway system, an outer casing was formed around the model to create a useable probe (Table 3 – Probes 7 and 8). The nare sizes on these openings also matched the literature and other designs, with openings of approximately 3.1 mm and 4.5 mm diameters for the idealized newborn and idealized 9-month-old respectively. We also examined the inclusion of flexible ridges similar to that used in probe 5 to create probes 9 and 10.

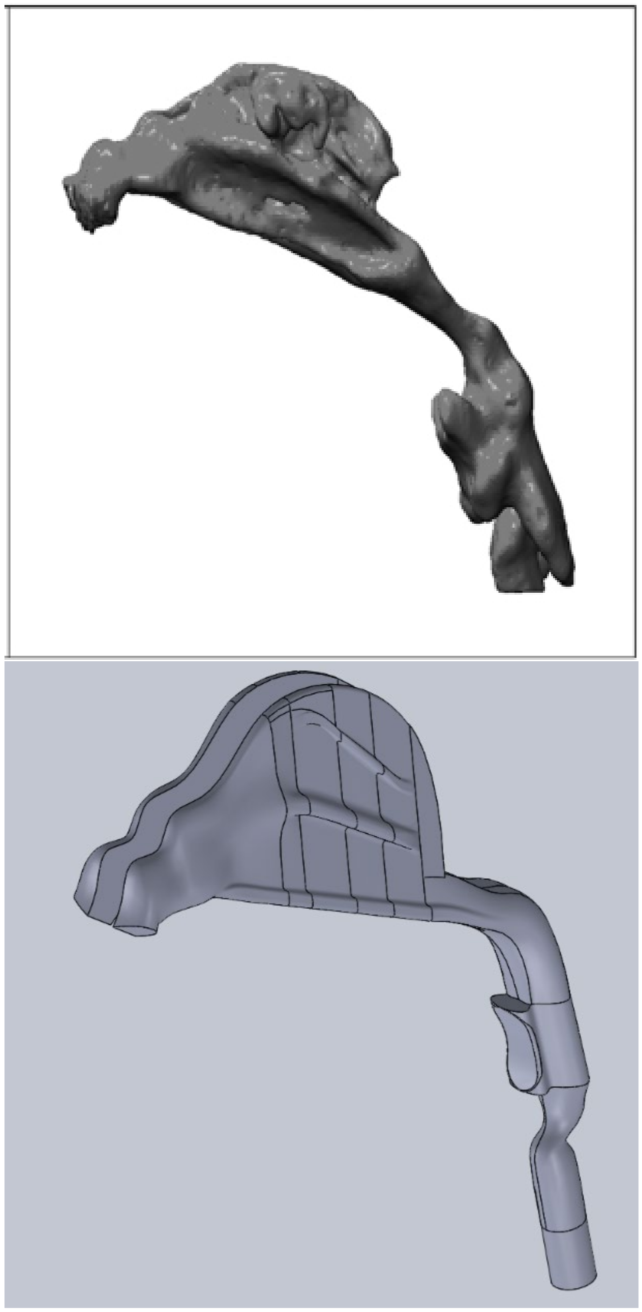

Figure 5 Real Airway (Javaheri et al., 2013) (Top) and Idealized Model Negative Space Geometry (Bottom).

During the creation of these new probes, a variety of materials were used. To prevent leakage as air is drawn through the different probes, all air channels for the probes, except for probe 6, were created using an LCD UV-Curing Resin (Elegoo, Inc., Shenzhen, China) in combination with an Elegoo Mars 2 Pro Mono LCD MSLA Resing 3D Printer (Elegoo, Inc., Shenzhen, China). This resulted in the idealized models, as well as 3 cylindrical pieces meant to be interchangeable in conjunction with the overall probe shape. These pieces possess a flat surface on one side and the curvature of a 5-inch diameter sphere on the other side to match the 5-inch diameter hemisphere. The overall outer shapes of the new probes consist of a 1.75-mm polylactic acid (PLA) filament (Hatchbox, Pomona, CA) and were created by Prusa i3 MK3S+ printers (Prusa Research a.s., Prague, Czech Republic). Lastly, probe 6 was created with a 3-inch diameter wood hemisphere with two 3.125-mm diameter channels placed approximately 7-mm apart by centerline. These channels were formed with brass tubing to allow for attachment to the airflow testing setup. All of these new probes and their descriptions can be seen in Table 3.

Table 3 Novel probe design descriptions and photos.

Probe	Description	Photo
Probe 1	Original apparatus described in current BS 4578:1970	
Probe 2	Flat surface with a single 4.5-mm diameter opening.	
Probe 3	5-inch diameter curvature with a single 4.5-mm diameter opening.	
Probe 4	5-inch diameter hemisphere with two 4.5-mm diameter openings spaced ~7-mm between centerlines.	
Probe 5	5-inch diameter hemisphere with two 4.5-mm diameter openings spaced ~7-mm between centerlines and a 3.175-mm thick flexible ridge.	

Probe	Description	Photo
Probe 6	3-inch diameter hemisphere with two 3.175-mm diameter openings spaced ~7-mm between centerlines.	
Probe 7	Idealized newborn airway	
Probe 8	Idealized 9-month-old airway	
Probe 9	Idealized newborn airway with a 3.175-mm thick flexible ridge.	
Probe 10	Idealized 9-month-old airway with a 3.175-mm thick flexible ridge.	

Airflow Testing

With the new probes produced, airflow testing was conducted following the previously described method in the initial modification of BS 4578:1970. That is, the pressure differential was recorded during an airflow rate of 2 L/min and a thrust of 10 ± 0.2 N into the product. For all trials, the product was held down in place with the use of weights on either side of the testing setup to limit movement. In order to achieve the required thrust, the probes were initially lowered as far into the product as possible before being raised back to the correct thrust. The maximum value during this process was approximately 25 N. This was repeated 3 times for each product and probe combination, with a resetting of the product occurring between tests. The probes were connected to the tubing system one of two ways, depending on the attachment method to the lifter. For probes 2 to 5, each probe was attached to the original metal apparatus by a PLA disk (Figure 6). A 100-mm inner diameter O-ring (McMaster-Carr, Santa Fe Springs, CA) was used to prevent leakage from this setup. For these probes, the digital manometer remained connected to the original apparatus.

Figure 6 Attachment of 5-inch Diameter Hemisphere to Original Probe with Additional Weight to Achieve 10 N of Thrust.

For probes 6 to 10, which includes the idealized models and the 3-inch hemisphere, direct attachment to the lifter was feasible. In these cases, the digital manometer was connected to tubing near the probe by a T-branch (Figure 7).

Figure 7 Example of Connection of Airflow Setup Directly to Probe 6. Branch of T-fitting Connects to the Digital Barometer. Run Section of T-fitting Connects to Flowmeter.

Firmness

<u>Force vs. Displacement</u>

To develop a better understanding of the firmness of each of these products, the applied force at different displacement was recorded. Specifically, the force was recorded at every 0.05-inches until the force was greater than 14 N. For the mesh products, this was continued until the force gauge overloaded at 50 N, as that only required an extra recording and the data was already limited. Each product was held in place with weights on either side of the testing area to prevent movement. As each product has varied thickness, the displacement and force were zeroed at a preload of 0.1 N. All testing was done using the 3-inch hemisphere probe (probe 6) attached to a separate vertical lifter mechanism (APH Test Stand, Boshi Electronic Instrument, Yueqing City, Zhejiang Province, China) and the use of a ZP-50 N digital force gauge (Boshi Electronic

Instrument, Yueqing City, Zhejiang Province, China). During this process, pressure values were also recorded at each displacement point. To analyze these results, the stress-strain relationship was calculated using MATLAB (Appendix G). To calculate the stress acting on the product from the axial load, it was necessary to determine the cross-sectional area over which the force was being applied. This was done by calculating the chord length by equations 2 and 3:

$$c = 2 * \sqrt{r^2 - h^2} \tag{2}$$

$$h = r - displacement \tag{3}$$

where ‘c’ is the chord length, ‘r’ is the radius of the hemisphere, and ‘h’ is the perpendicular distance from the chord to the center of the sphere. Using the calculated chord length as the cross-sectional diameter, the cross-sectional area can then be calculated and utilized for a stress calculation. Similarly, strain can be calculated using the displacement and the thickness of the product measured during product characterization.

<u>Stress Relaxation</u>

As these products experience stress relaxation, we sought to determine how long a probe should be applied before the applied force stabilizes, as well as the average percent of the peak force that was retained. The stress relaxation properties of each product were examined using the separate lifter mechanism and the new force gauge, which is able to store recorded values at a sampling rate of 10 Hz. For each product, 3 trials were conducted and involved the use of the 3-inch hemisphere probe. Each product was held in place through the use of weights on either side of the testing space. Once recording began, the probe was applied to the product at approximately 10 N for 1-2 minutes. After the test was complete, the stored values were exported from the recording software to Microsoft Excel. These excel sheets were then imported into MATLAB for further analysis (Appendix H).

RESULTS

Product Characterization

The measurements and notes of each product are listed in the tables below.

Table 4 Product Measurements and Characteristics. M1 and M2 have Two Separate Pieces of Variable Length.

Products	Length (cm)	Width (cm)	Thickness (cm)	Attachment Method	Attachment Instructions	Material	No of pieces
T1	402	25	3.7	Ties	N	100% Cotton, Filling: 100% Polyester	1
T2	379	25	3.5	Ties	N	100% Cotton, Filling: 100% Polyester Fiber	1
T3	394	25	3.7	Ties	N	Cover Fabric: 100% Cotton; Filling: 100% Polyester Fiber	1
T4	252	16	2.3	Ties	N	Cover Fabric: 100% Cotton; Filling: Resin treated polyester fiber batting	1
M1	340 (long); 161 (short)	30	0.4	Ties and Hook and loop system	Y	Soft 3D Mesh Fabric	2
M2	279 (long); 205 (short)	28	0.4	Ties and Hook and loop system	Y	100% Polyester	2

Table 5 Notes of Pertinent Product Details

Samples	Notes
T1	Product has variable thickness due to intermittent quilting
T2	Product has variable thickness due to intermittent quilting
T3	Product has variable thickness due to intermittent quilting
T4	Product has variable thickness due to intermittent quilting
M1	Product has 2 pieces of different lengths. The long piece covers 3 of the 4 sides in a crib (Both short sides and 1 long). Shorter piece covers last long side/unused with solid back crib. There are no warning/identifying labels. The material is not listed, only described as "soft, 3D mesh fabric" on packaging. Combines use of hook and loop attachment on the end with ties along the length.
M2	Product has 2 pieces of different lengths. The long piece covers 3 of the 4 sides in a crib (Both short sides and 1 long). Shorter piece covers last long side/unused with solid back crib. Combines use of hook and loop attachment on the end with ties along the length.

Airflow Testing

The values found for each probe varied significantly but are summarized by product category in Table 6. More detailed box plots for each probe can be found in Appendix A.

Table 6 Mean and Standard Deviation Values for Traditional and Mesh Categories when Tested with Different Probe Designs. Probe 6 is Highlighted as it was chosen to be the Preferred Model.

Probe	Category	Mean	Standard deviation
Probe 1	Traditional	0.053	0.011
	Mesh	0.000	0.000
Probe 2	Traditional	0.672	0.094
	Mesh	0.028	0.004
Probe 3	Traditional	0.379	0.051
	Mesh	0.178	0.068
Probe 4	Traditional	0.348	0.042
	Mesh	0.082	0.018
Probe 5	Traditional	0.138	0.019
	Mesh	0.017	0.001
Probe 6	Traditional	2.038	0.417
	Mesh	0.254	0.019
Probe 7	Traditional	2.191	0.201
	Mesh	0.435	0.019
Probe 8	Traditional	0.976	0.094
	Mesh	0.087	0.008
Probe 9	Traditional	0.294	0.066
	Mesh	0.047	0.008
Probe 10	Traditional	0.127	0.009
	Mesh	0.014	0.001

While all of these probes were able to be tested, five of them are worth taking a more in-depth look at. These are the original apparatus, the two idealized models (probes 7 and 8), the 5-inch diameter hemisphere with two 4.5-mm openings (probe 4), and the 3-inch diameter hemisphere with the two 3.175-mm openings (probe 6). The results for these four probes are shown in Figure 8.

Two tailed t-tests with equal variance were used to compare pressure measurements between the product categories for different probes. All probes were able to significantly differentiate between the two product categories, with various levels of significance. This was also true for the original probe (probe 1). However, no results were able to be measured for the mesh products, limiting the functionality of this probe.

With the goal of achieving a physiologically representative model, it was decided that the idealized newborn airway model would serve as our ideal model, and the values recorded for each probe were recorded to its values. In this comparison, the desired outcome was to show the values were not significantly different, which was only achieved by the 3-inch hemisphere (probe 6) with a p-value of 0.59. While probe 6 was the only probe capable of matching the idealized newborn model (probe 7), a few probes were comparable to the idealized 9-month-old model (probe 8). This included probe 2 ($p > 0.05$), probe 3 ($p > 0.001$), and probe 6 ($p > 0.001$).

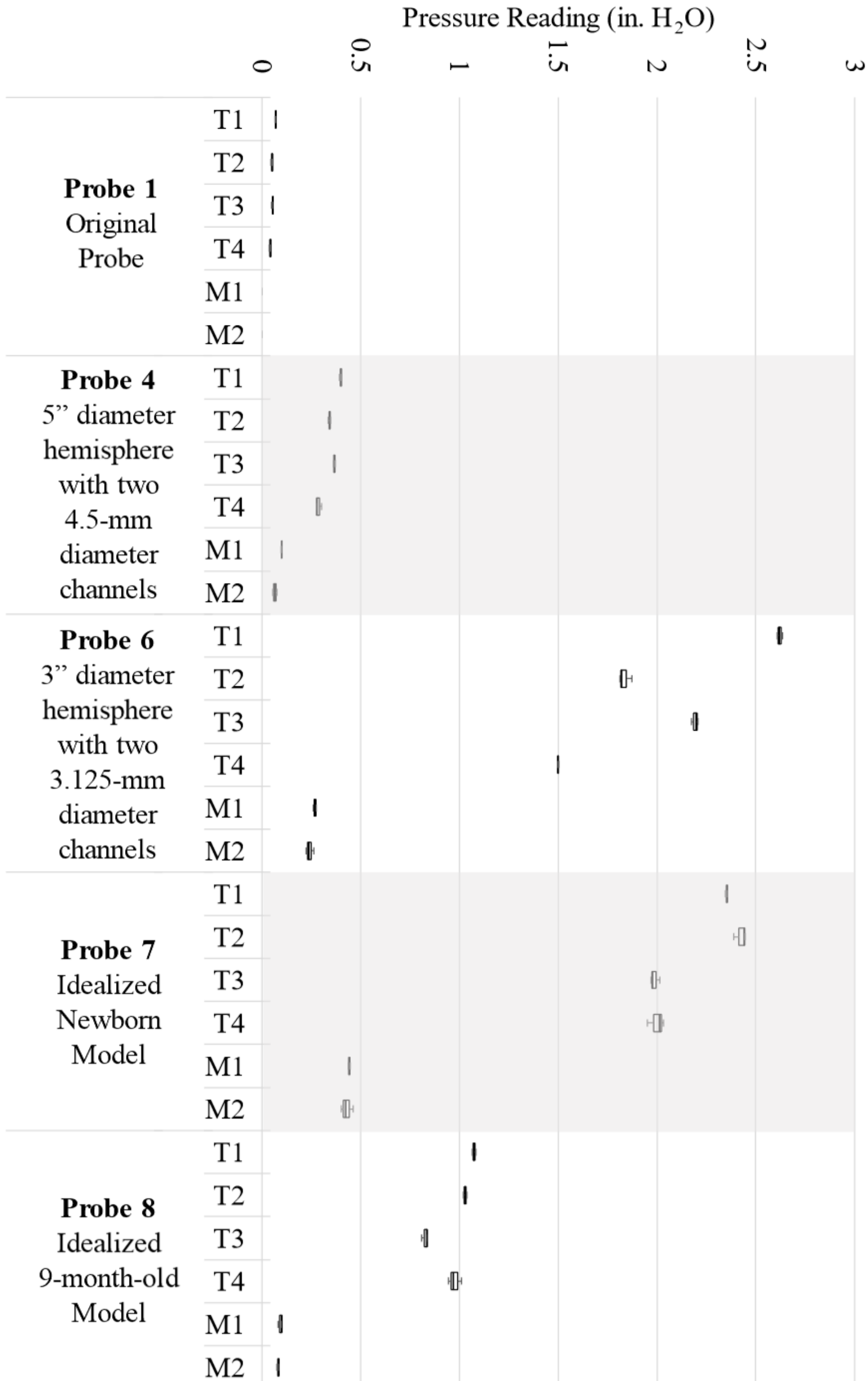

Figure 8 Box Plots of the Pressure Readings Recorded for Various Probes of Note at 10 N of Thrust. Error Bars Represent the Maximum and Minimum Values Recorded.

Threshold Development

During the creation of a new testing standard for product safety, it is vital to determine the threshold that defines the failure or passage of a product. In this case, the threshold will come from the results of airflow testing, as the primary concern is the suffocation risk for infants. It is our recommendation that this **threshold be set at a pressure reading of 0.311 in. H_2O** while using the recommended probe 6 and a flowrate of 2 L/min, with failure occurring above this value. This threshold lies 3 standard deviations above the mean reading for the mesh bumpers tested, meaning that 99.7% of mesh liners will fall within the safe region.

Validation of Threshold

To validate the recommended threshold, 18 products (16 Traditional, 2 Mesh) not used for developing the threshold were tested a single time under the same airflow conditions. The results of this testing are shown in Figure 9.

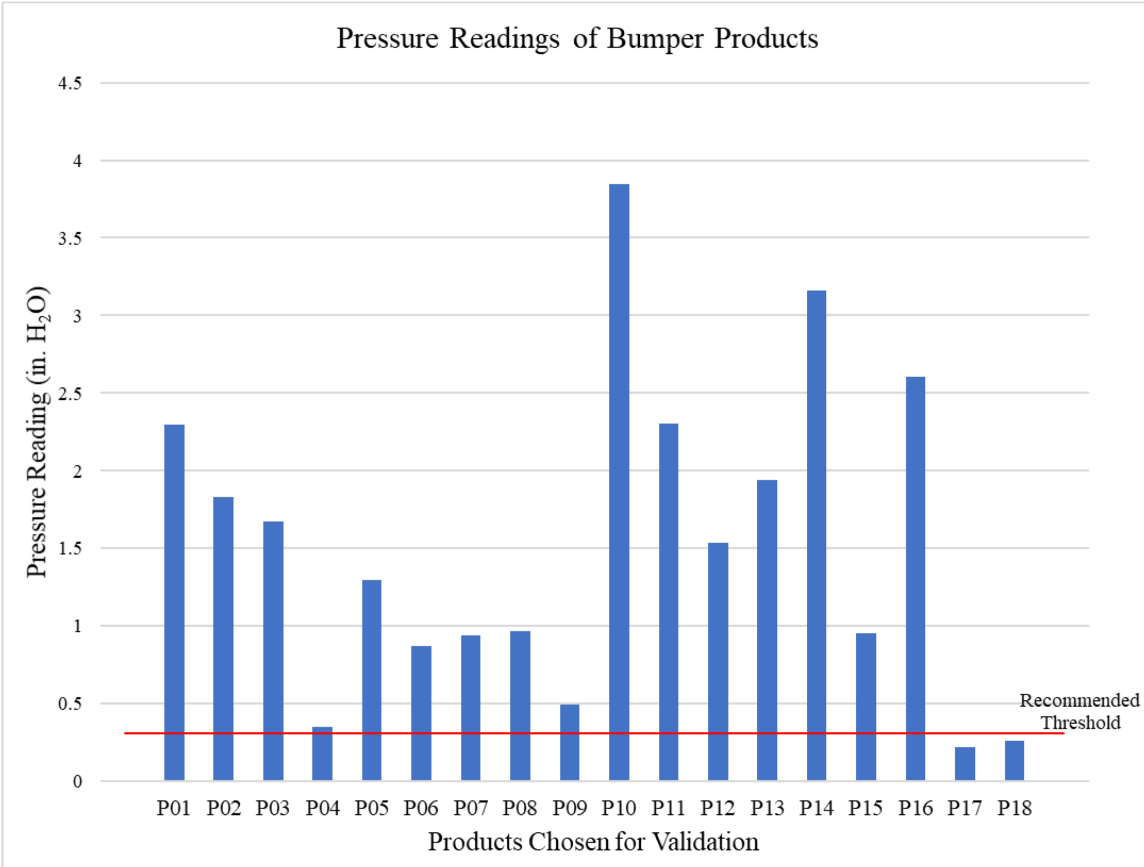

Figure 9 Results of Airflow Testing on 18 Different Products

In this testing, only P17 and P18 were able to meet the threshold. Both of these products were categorized as mesh liners and are considered to be safe from a suffocation perspective. For the other products, P04 was very close to meeting the threshold with a pressure reading of 0.348 in. H_2O. This product is categorized as a traditional bumper but is marketed as “breathable” and has a unique design among the product used. The outward facing side of this product is a 100% Polyester solid cover and the inward facing side has a mesh pattern. Testing was conducted on the mesh pattern, as that is the intended surface that an infant would be in contact with.

Firmness

Force vs. Displacement

This method of testing provided further insight between the two product categories and the results can be found in Appendix B. Representative photos of this test can also be found in Appendix D. Using these results, it is possible to analyze the stress-strain relationship in these products using MATLAB and equations 2 and 3 (Appendix G). Graphs showing the relationship between these two values in traditional bumpers can be seen in Figure 10. Due to the mesh products being extremely thin, only a limited number of measurements were made within the desired force range. However, they both have stress values an order of magnitude higher than any of the traditional products. One limitation of this method is the limited values that can be recorded for the mesh products. While we can apply levels of force that are greater than our area of interest, this data is not relevant to the inherent risk of these products to infants. Furthermore, it introduces potential sources of strain in the lifter setup above 15 N. Another limitation is that these tests were conducted on a solid, firm surface with the products lying horizontally and flat. However, in reality, these products will be attached to crib slats vertically. This means they will have areas that can experience greater deformation under less force due to the lack of solid backing in spaces between slats. Similarly, the applied force will be likely be directed into the product at an angle due to the infant's head both pushing into the product horizontally and being pulled down by gravity, whereas this test examined applied force normal to the surface of the product.

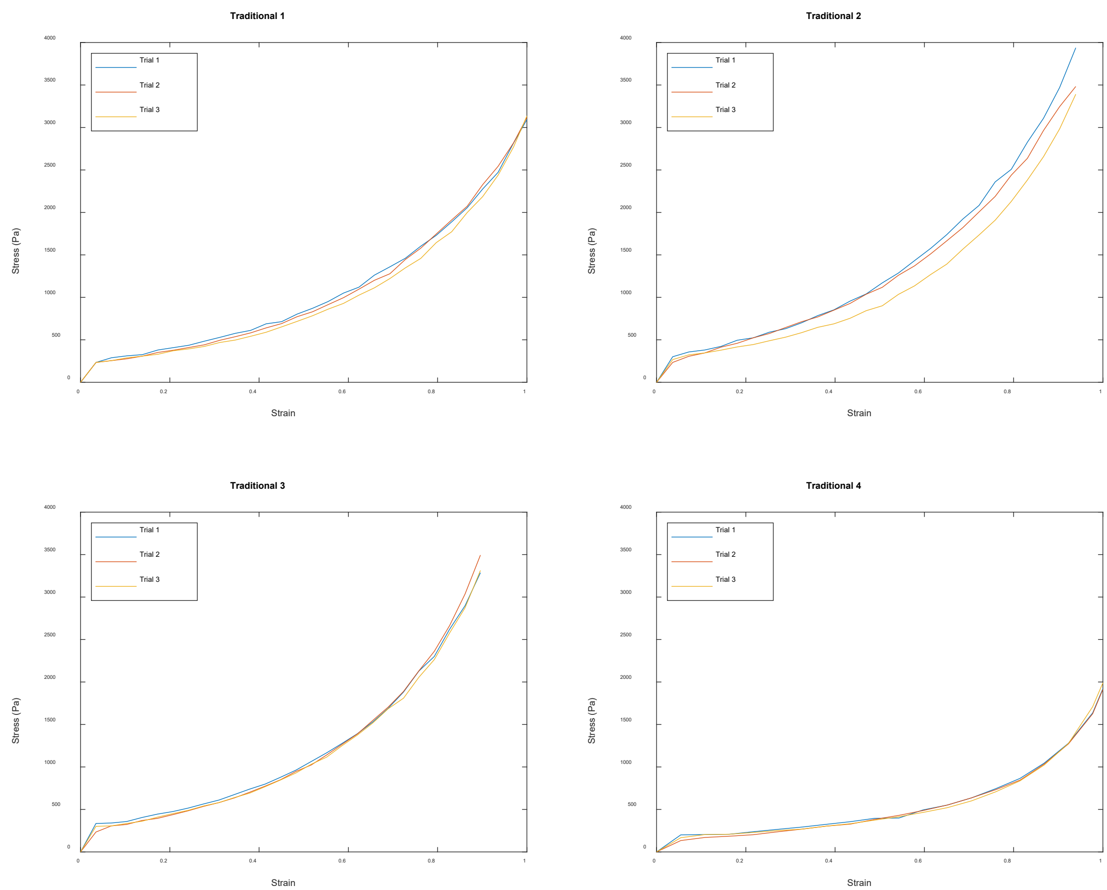

Figure 10 Stress-strain curves for only Traditional Bumpers.

Stress Relaxation

During the stress relaxation testing, probe 6 was applied to each product at approximately 10 N. However, this was a difficult value to achieve, especially with the mesh products, as once the probe was applied, it was not lifted any until the recording was done. Representative photos of the testing process can be found in Appendix E. The resulting data was imported into MATLAB (Appendix H). Stress was calculated following the method listed above, with the displacement used being the average value at which 10 N was reached. The data was then filtered to exclude any sudden spikes that caused a difference of over 50 Pa after the peak stress was reached and the values were then normalized to the peak force recorded, as shown in Figure 11. In each of these plots, the results of the 3 trials conducted are shown for each product and each data set appears almost identical to the others for the same product, although offset by the time at which the peak force was reached. As one can see, the stress values have settled by the time 60 seconds have passed, meaning this is an appropriate time to let the probe settle into the product before recording any pressure or force values. The average percentage of the initial force was calculated at the end for each product and each product category. For traditional bumpers, after approximately one minute passed, $90.66 \pm 0.02\%$ of the original force remained acting on the force gauge. This testing method faced similar limitations to that of the force-displacement testing, primarily that the applied force was directed normal to the product and the testing was conducted on a solid surface.

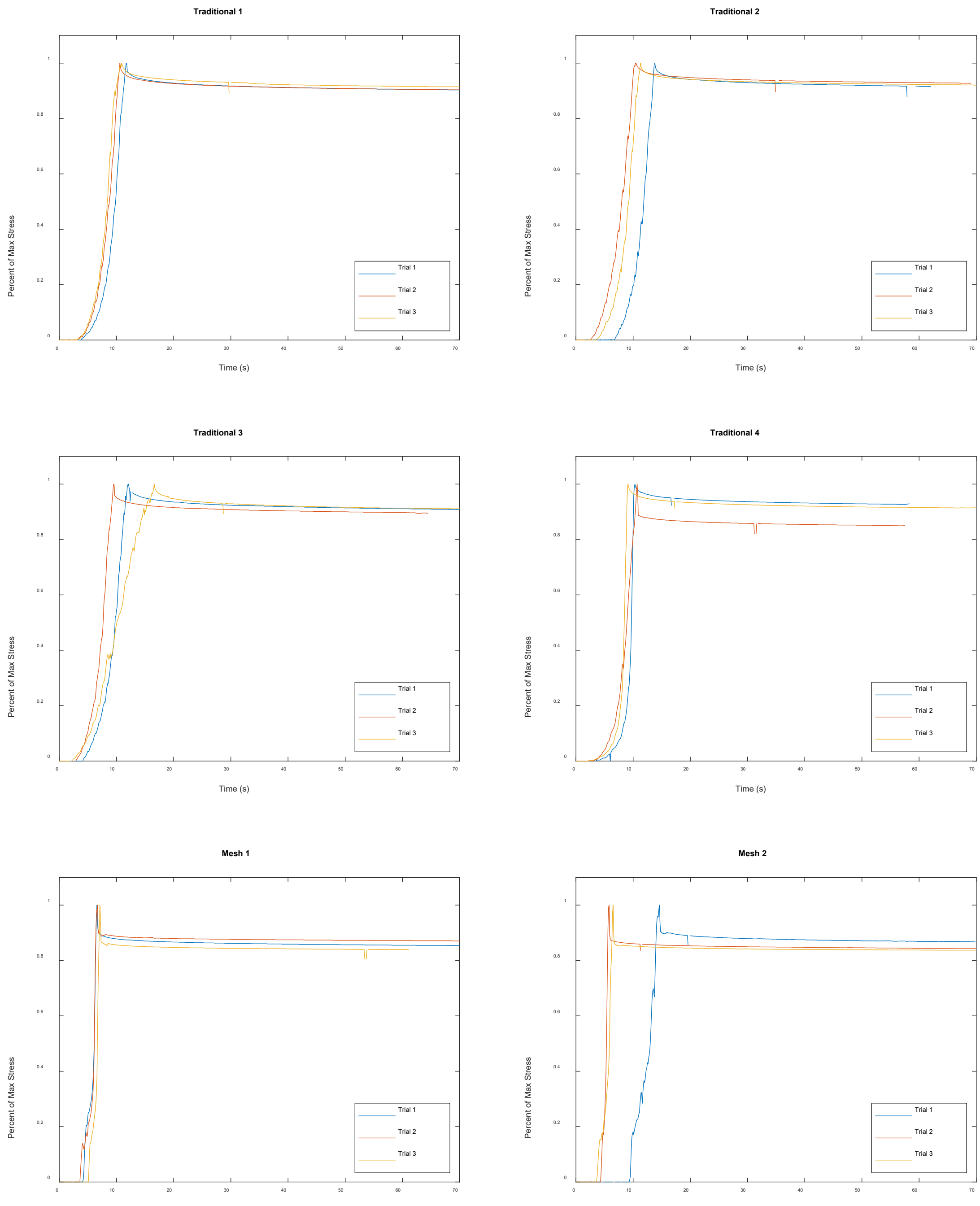

Figure 11 Stress-relaxation of 6 different crib bumper products

Airflow and Firmness Combined

Beyond looking at the stress-strain relationships for each of these products, it is also worth looking at the relationship between applied force and measured pressure through the probe. These pressure readings were taken using the same setup as the airflow testing, but at different displacements rather than a single force. The results of this comparison can be found in Figure 12. The average values for force and measured pressure at each displacement were used for this plot and the average standard deviations for both force and pressure recordings are listed in Table 7 for each product.

Table 7 Average Standard Deviations of Pressure and Force Measurements for 6 Different Bumper Products.

		Product					
		T1	**T2**	**T3**	**T4**	**M1**	**M2**
Standard Deviation	Pressure Values	0.05	0.08	0.09	0.07	0.02	0.02
	Force Values	0.16	0.45	0.09	0.09	0.86	1.1

For the traditional products, the pressure readings have a drastic increase in value before they begin to plateau as the force increases. As the slope plateaus, the average measured pressure and average applied force develop an almost linear relationship, particularly after 2.5 N of force is applied. This is likely due to a more prominent seal being formed between the probe and the product as more force is applied. Similarly, as the interior material of the traditional bumpers is fibrous, any air that is present between the fibers will be forced out as the probe continue to compress the product. A linear interpolation was found for all data points above 2.5 N and the R-squared values of the fit were calculated. For traditional products, all of the R-squared values were above 0.93. On the other hand, the mesh products varied, with R-squared values of 0.78 and 0.90 respectively. This interpolation process was repeated for recordings occurring at less than

1 N of force but resulted in worse fits for the traditional bumpers, ranging from 0.77 to 0.93, but showed an increase in the fit for mesh liners, which had values of 0.88 and 0.95 respectively. All of these R-squared values are summarized in Table 8. The interpolated lines for each region of interest were also plotted with the applied force vs. measured pressure data and can be found in Appendix G.

Table 8 R-Squared Values for Linear Interpolations of the Force-Pressure Relationship in Different Products for Different Force Ranges.

		Product					
		T1	**T2**	**T3**	**T4**	**M1**	**M2**
R^2 Values	Force > 2.5 N	0.94	0.93	0.98	0.99	0.78	0.90
	Force < 1 N	0.89	0.85	0.77	0.93	0.88	0.95

With this in mind, it is reasonable to maintain the current standard's requirement of a 10 N thrust, as it allows the pressure readings to increase and level out even more. The mesh products were able to be measured up to 50 N, as both products experienced overloading of the force gauge at the 0.30-inch and 0.25-inch displacement mark respectively. However, the plot was limited to only 20 N of force, as our area of interest remains below that level of force.

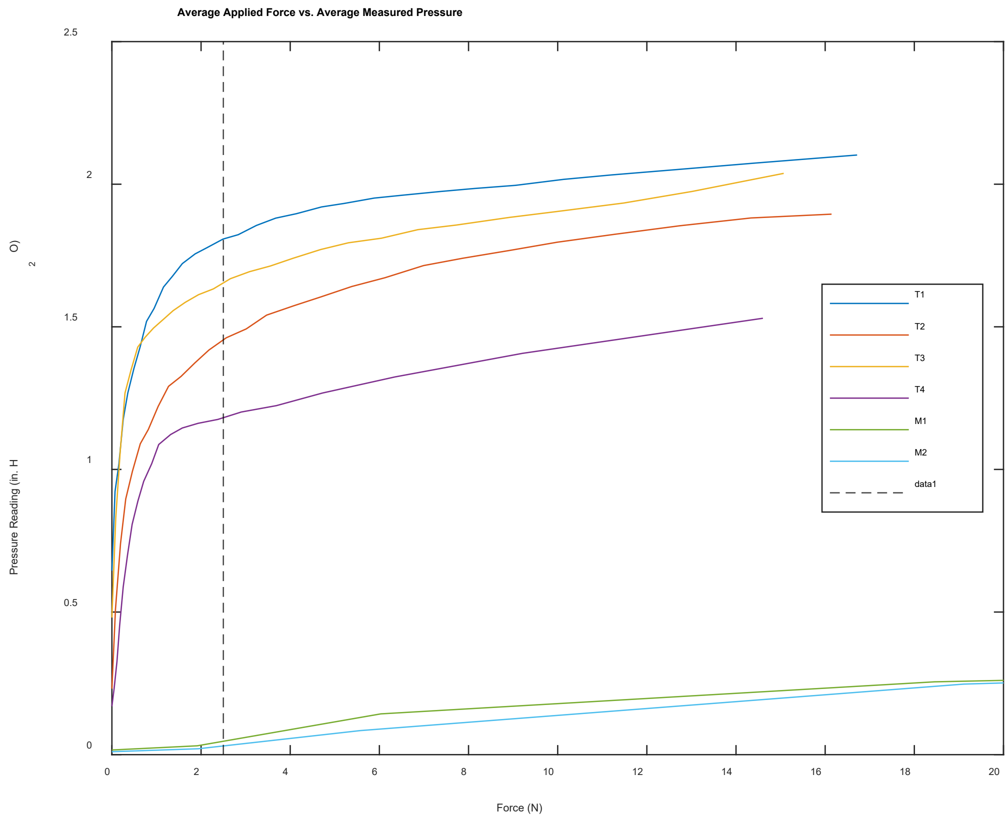

Figure 12 Mean Force vs. Mean Pressure Plots for each Crib Bumper Product. Values Recorded at every 0.05-inches of Displacement over 3 Trials.

DISCUSSION

Overview

This document serves to provide a report to the United States Consumer Product Safety Commission regarding biofidelic improvements made to existing testing standards that can distinguish between safe and unsafe products. The primary goal of this research was to establish a threshold which can be used to judge the safety of product by use of a simple probe that adheres to a physiological model for use in airflow testing. A secondary objective was to establish a method for the characterization of different product categories based on firmness testing. We hypothesized that:

(1) increased complexity of the probe geometry in airflow testing will result in more physiologically accurate results and allow the establishment of a threshold value that distinguishes between safe and unsafe products, and

(2) improvements to the static firmness testing will enable us to better characterize different product categories and provide greater insight into the relationship between the applied force and relative pressure created during the creation of a seal.

Airflow

In our airflow testing, we used a variety of probes of increasing complexity to find the pressure required to draw air through a set of products at 2 L/min. The recorded values for each probe were then compared to an idealized model of an infant's upper airway system to determine the simplest design that remained comparable to the idealized model. While we found that probe 6, the 3-inch diameter hemisphere, was the best fit for our criteria, it is still not a perfect test for modeling reality. When an occlusion to an infant's nares initially occurs, the esophageal pressure has been measured to be 9.5 ± 5.0 cm H_2O (3.74 ± 1.96 in. H_2O) (Cohen and Henderson-Smart, 1986). Our recorded pressures for traditional bumper products (2.038 ± 0.417 in. H_2O) falls into that range, indicating a similar situation to full occlusion has occurred. However, in reality, infant's will alter their breathing pattern in an attempt to counteract the lower oxygen levels by both increasing the rate of breathings and the tidal volume of each breath. After this response occurs, a maximum drop of 23.5 ± 9.0 cm H_2O (9.25 ± 3.54 in. H_2O) has been recorded (Cohen and Henderson-Smart, 1986). In its current form, our methods utilize a normal breathing rate to model an infant at rest. While breathing rates under duress vary between individuals, future studies may consider altering the utilized flowrate to 3 or 4 L/min to a mimic this altered breathing rate.

Currently, our recommended threshold value is solely based on data from crib bumper products. This product category is relatively simple to test with, as the products are generally uniform and have relatively flat surfaces. With other infant product categories featuring soft goods, such as pillows or bouncers, the shape changes throughout the product and generally exhibits some curvature. Studies should be performed to discover if this change in shape affects the creation of a seal around the probe to determine if this method is effective for other product categories.

Firmness

The firmness of a material characterizes the deformation that occurs under loading of that material. In the field of infant sleep products featuring soft goods, this firmness characteristic relates to how well a product may conform to an infant's face, which can lead to the creation of a seal around the airway system creating a suffocation hazard. The current edition of BS 4578:1970 characterizes firmness by measuring the displacement a product experiences under a specific load. However, it currently does not provide any insight into what displacement indicates a firm or soft product. Furthermore, as firmness fits on a scale, it can be beneficial to examine the deformation under different loads. This project explored the benefits of characterizing firmness under different loads by conducting force versus displacement testing. Beyond that, this project also sought to characterize different products based on the levels of stress relaxation that occur. During both forms of testing, probe 6 was used to apply force to the products in order to limit to complexity of test setup for future implementation into a testing standard. Probe 6 is a hemisphere, meaning the cross-sectional area that the force is being applied across was changing as more force was applied, creating some difficulty in data analysis and interpretation. However, there are still some insights to be gained from these tests.

In the force versus displacement testing, pressure was also recorded at each point. For each traditional product, the relationship between force and pressure created a bilinear curve that became linear after 2.5 N of force was applied. Furthermore, the interpolated lines above this 2.5 N could be used for approximating the pressure readings at higher levels of force than those recorded. This could be useful for approximating the pressure readings that occur while an infant is experiencing entrapment or enclosure with these products, as the experienced forces will likely be higher than just the weight of an infant's head.

For the stress relaxation characterization, there was a clear level of retained force within the traditional products. It also showed that allowing the probe to settle into the product for 1 minute is sufficient to account for any stress relaxation that occurs. However, during this testing, all products were placed on a hard surface for the duration of the tests, which may have affected the results. The mesh products were particularly defined by this, as the resultant force against the probe came from the hard surface rather than the mesh itself after for limited displacement. This led to sharp increases in the applied force that was recorded. On the other hand, T1-T4 were able to fully exhibit a reactant force of 10 N from the material of the product itself, meaning the product was still deforming at 10 N.

While these different tests were useful for characterizing these specific products, they still do not account for the density of the filling material in the product. This density could be an important feature of these products, especially in the traditional bumper category. As T4 had a very low density of filling material, it was unable to exhibit a reaction force of 10 N on the probe with just its material. The mesh liners faced a similar condition, which makes characterizing the firmness of just these products more difficult.

Limitations

While these recommendations improve the current BS 4578:1970 standard, there are still some limitations. During the airflow testing, each product was placed on a hard surface and the probe was lowered perpendicular to the product's surface. While this is ideal for testing a variety of products, it does not represent the true usage of crib bumpers. For these products, they will be aligned vertically, with the applied force occurring in the horizontal direction. Depending on the attachment to the crib, any specific bumper can slightly give way between slats, which may lead to a tighter seal and suffocation risk. Currently, both forms of firmness testing are exploratory and serve to characterize specific products. These were both limited by the shape of the probe used. As it was a hemisphere, the area of which the force was applied was changing. However, it was also needed to examine the relationship between measured pressure vs. applied force. Similarly, it was impossible to tell how much strain occurred within the force gauge itself, leading to unrealistic strain values.

Besides limitations from the testing setup, this project primarily looked at products containing either cotton or polyester fiber, with the exception of M1, which only had a vague material listing of a "soft, 3D mesh fabric." Products consisting of cotton and polyester fiber are able to return to a similar overall shape fairly easily, but some products and other product categories utilize memory foam, among other materials. It is currently unclear how these materials will affect the results of continued testing.

Future Considerations and Directions

One of the main goals of this project was to find the most simplistic model that is remains consistent with a physiological scenario. This was achieved with probe 6, the 3-inch diameter hemisphere. With this method, we can recommend a threshold value of 0.311 in. H_2O, which is based on the standard deviation found for mesh liners. However, we only conducted testing on two representative mesh products and this threshold may slightly change as more products are examined. Furthermore, this threshold is defined by determining safe products, but an argument can be made for setting the threshold to determine hazardous products. By using the standard deviation found for traditional bumpers, thresholds of 0.368 and 0.787 can be argued for. These values represent limits that are 4 standard deviations and 3 standard deviations away from the mean pressure reading of traditional bumpers respectively. By defining a threshold based on products meeting hazardous readings, the regulation will allow more flexibility for manufacturers. While we are recommending our threshold to be conservative, the final decision of threshold will be decided by the Consumer Product Safety Commission and ASTM International upon creation of a formal testing standard. While we were able to find a threshold value for crib bumpers, there are still several directions to expand this testing into. These include looking at other materials, new product designs, and new product categories.

As previously mentioned, this report focused on products made with cotton and polyester. These are currently two of the most common materials used in infant sleep products, but they are not the only ones. Several products can utilize memory foam, microfibers, or a combination of a foam and polymer base. Future testing is required to validate this new probe and threshold for these materials and any others that may become popular in the future. Furthermore, as these different materials undergo characterization during firmness testing, it may be possible to distinguish between these materials. Currently, there is a clear difference between the traditional bumpers and mesh liners, due to how thin the mesh liners are. To become more marketable, some products are designed to be a combination of a mesh liner and a traditional bumper. These products do not possess the general thickness that is associated with traditional bumpers but are still thicker than mesh liners. One such product was used in our validation of our recommended threshold. With the current threshold, this product would need minimal design changes to occur in to be considered safe.

Lastly, the intent of updating the BS 4578:1970 standard is to make the test applicable for several product categories. This project strayed from the original standard by focusing on crib bumpers for testing, whereas the original standard was designed for infant pillows. Similar testing will be conducted with infant pillows to determine if there is any difference in safe thresholds. Beyond pillows, this testing may be applicable to other product categories in which infants can be found sleeping in proximity to soft goods, such as car seats and carriers. In all of these products, there is a risk of an infant suffering from an occlusion of the nares.

CONCLUSIONS

With the number of infant fatalities and other incidents related to crib bumpers that occur each year, it is clear that there is some suffocation risk with using these products. As the market is now, there is almost no regulation or testing standard that regulates the manufacturing of crib bumpers from a suffocation perspective, outside of stipulations on attachment tie strength. This leaves a large space that we have sought to fill by updating the British Standard, BS 4578:1970*, Test for Hardness of, and for Air Flow Through Infant Pillows*, to be more applicable to a variety of products and to make the testing results more physiologically representative of infants. In the current market, it is common to find these products on 3rd-party websites, such as Etsy.com and Amazon.com. Several available products are marketed as homemade by a single individual, which leads to a variety of quality. However, one of the goals of this project was to make the testing methods simple, while remaining meaningful to a physiological scenario. A simple test will allow a greater number of manufacturers to adhere to this standard, allowing manufacturers to develop safer products. To make the testing methods for the finalized version as simple, but meaningful as possible, our novel probes were compared to 2 idealized models of infants of different ages. In this case, the 3-inch diameter hemisphere with two 3.125-mm channels (probe 6) was the best match for the newborn model without showing any significant difference in pressure readings, which led to the development of a threshold of 0.311 in. H_2O during airflow testing. This threshold was validated with the testing of 18 other products, including 2 mesh liners which were the only two to meet the criteria. When solely looking at the firmness of products, some insight in the characteristics of the product may be gained. However, this is still exploratory. As other product categories and different materials are examined, this data may gain meaning for differentiating between product categories. Furthermore, a threshold for firmness regarding the displacement that occurs under a particular force may preclude the need for airflow testing, as extremely firm objects will limit the creation of a seal even if the material is impermeable. By combining the firmness and airflow test to examine the relationship between force and pressure, an even better understanding of these products is formed. All of the traditional bumpers formed a very linear relationship between these two variables once the applied force was greater than 2 N. This will allow for approximation of pressure values at higher levels of force than is typically applied, which can occur during situations such as entrapment.

REFERENCES

All Information (Except Text) for S.1259 – Safe Cribs Act. (n.d.) Congress.gov. https://www.congress.gov/bill/117th-congress/senate-bill/1259/all-info.

ASTM International. (n.d.). How Standards are Developed. ASTM International. https://www.astm.org/media/files/get-involved/How%20Standards%20are%20Developed.pdf

Brandt, J. M., Allen, G. A., Haynes, J. L., & Butler, M. G. (1990). NORMATIVE STANDARDS AND COMPARISON OF ANTHROPOMETRIC DATA OF WHITE AND BLACK NEWBORN INFANTS. *Dysmorphology and clinical genetics : official publication of the Center for Birth Defects Information Services, Inc*, *4*(4), 121–137.

British Standards Institution. (1970). *BS 4578:1970 Specification for Methods of Test for Hardness of, and for Air Flow Through Infant Pillows.* London: BSI.

Carleton, J. N., Donoghue, A. M., & Porter, W. K. (1998). Mechanical model testing of rebreathing potential in infant bedding materials. *Archives of Disease in Childhood*, *78*(4), 323–328. https://doi.org/10.1136/adc.78.4.323

Centers for Disease Control and Prevention. (2001, August 23). Growth charts - data table of infant head circumference-for-age charts. Centers for Disease Control and Prevention. https://www.cdc.gov/growthcharts/html_charts/hcageinf.htm

Coats, Brittany & Margulies, Susan. (2008). Potential for head injuries in infants from low-height falls: Laboratory investigation. Journal of neurosurgery. Pediatrics. 2. 321-30. 10.3171/PED.2008.2.11.321.

Cohen, G., & Henderson-Smart, D. J. (1986). Upper airway stability and apnea during nasal occlusion in newborn infants. *Journal of Applied Physiology*, *60*(5), 1511–1517. https://doi.org/10.1152/jappl.1986.60.5.1511

Consumer Product Safety Commission. (2013). Staff Briefing Package: Crib Bumpers Petition. https://www.cpsc.gov/s3fs-public/pdfs/foia_CribBumpersBriefingPackage.pdf

Lambert, A. B. E., Parks, S. E., Cottengim, C., Faulkner, M., Hauck, F. R., & Shapiro-Mendoza, C. K. (2019). Sleep-Related Infant Suffocation Deaths Attributable to Soft Bedding, Overlay, and Wedging. *Pediatrics*, *143*(5). https://doi.org/10.1542/peds.2018-3408

Haase, B., Badinska, A.-M., Maiwald, C. A., Poets, C. F., & Springer, L. (2021). Comparison of nostril sizes of newborn infants with outer diameter of endotracheal tubes. *BMC Pediatrics*, *21*(1). https://doi.org/10.1186/s12887-021-02889-5

Javaheri, E., Golshahi, L., & Finlay, W. H. (2013). An idealized geometry that mimics average infant nasal airway deposition. Journal of Aerosol Science, 55, 137–148

Maltese, M. R., & Leshner, M. (2019). Carbon dioxide rebreathing induced by crib bumpers and mesh liners using an infant manikin. *BMJ Paediatrics Open*, *3*(1), e000374. https://doi.org/10.1136/bmjpo-2018-000374

Mazmanyan P, Darakchyan M, Pinkham M.I., Tatkov S. (2020). Mechanisms of nasal high flow therapy in newborns. Journal of Applied Physiology. 128(4), 822-829. https://doi.org/10.1152/japplphysiol.00871.2019.

Safety Standard for Crib Bumpers/Liners: A Proposed Rule by the Consumer Product Safety Commission on 04/03/2020. 85 FR 18878. (proposed April 03, 2020).

Scheers, N., Woodard, D. W., & Thach, B. T. (2016). Crib Bumpers Continue to Cause Infant Deaths: A Need for a New Preventive Approach. *The Journal of Pediatrics*, *169*, 93-97.e1. https://doi.org/10.1016/j.jpeds.2015.10.050

Sivieri, E.M., Gerdes, J.S. and Abbasi, S. (2013), Effect of HFNC flow rate, cannula size, and nares diameter on generated airway pressures: An in vitro study. Pediatr. Pulmonol., 48: 506-514. https://doi.org/10.1002/ppul.22636.

Storey-Bishoff, J., Noga, M., & Finlay, W.H. (2008). Deposition of micrometer-sized aerosol particles in infant nasal airway replicas. Journal of Aerosol Science, 39, 1055–1065.

Tavernini S, Church T.K., Lewis D.A., Martin, A.R., Finlay W.H. (2018). Scaling an idealized infant nasal airway geometry to mimic inertial filtration of neonatal nasal airways. *Journal of Aerosol Science*, *118*, 14–21. https://doi.org/10.1016/j.jaerosci.2017.12.004

U.S. EPA. Metabolically Derived Human Ventilation Rates: A Revised Approach Based Upon Oxygen Consumption Rates (Final Report, 2009). U.S. Environmental Protection Agency, Washington, DC, EPA/600/R-06/129F, 2009.

APPENDIX A

Airflow Testing Results for Each Probe

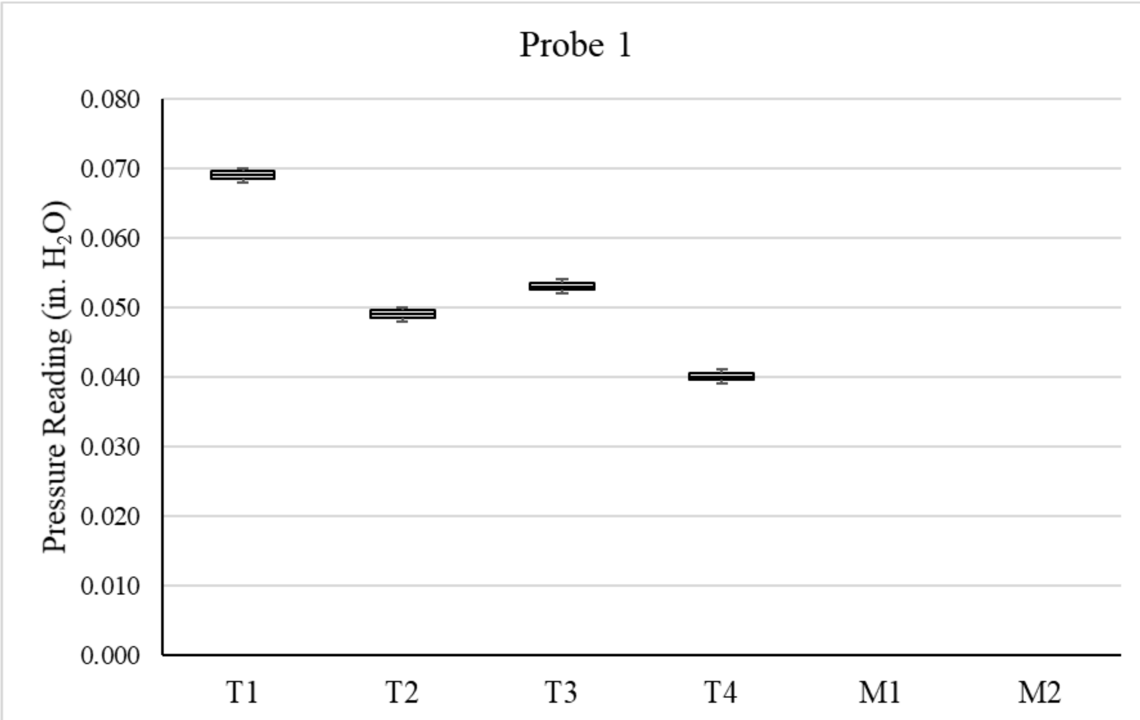

Figure A.1 Plot of Airflow Testing Results for Probe 1.

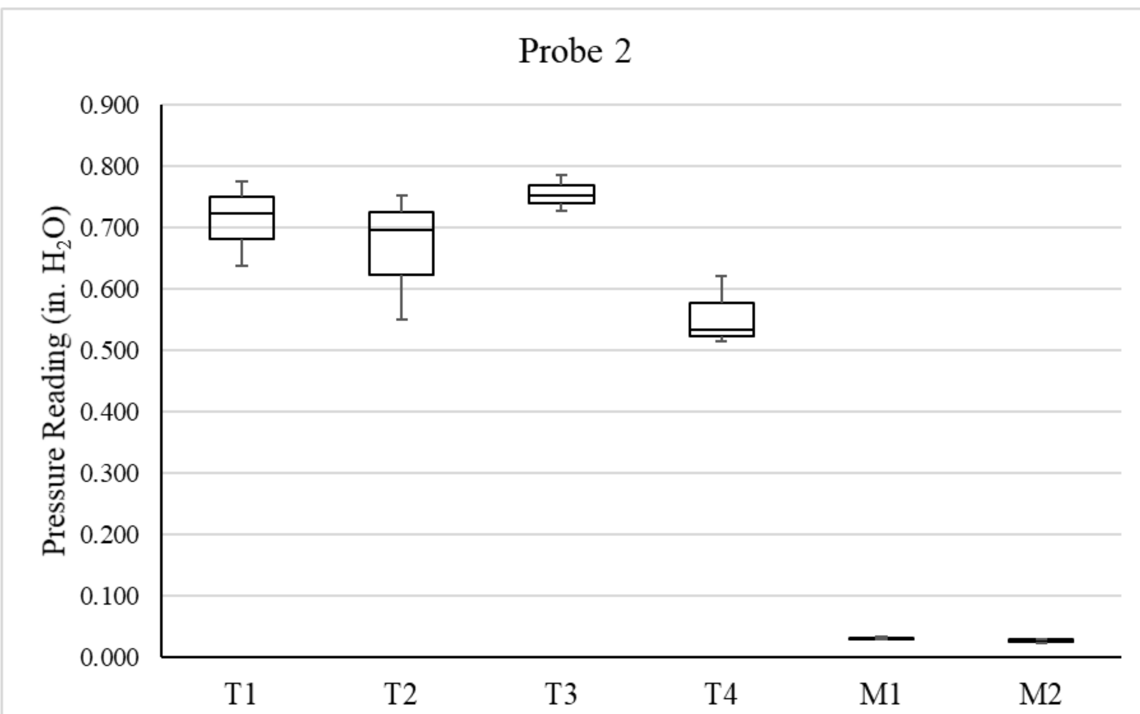

Figure A.2 Plot of Airflow Testing Results for Probe 2.

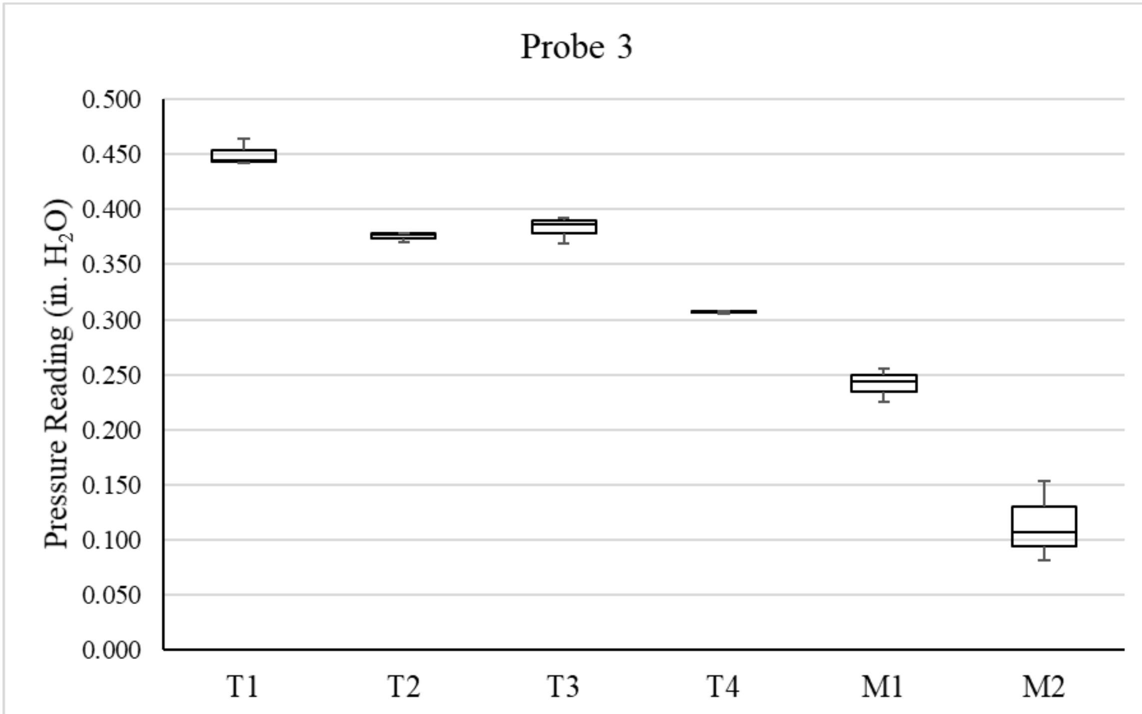

Figure A.3 Plot of Airflow Testing Results for Probe 3.

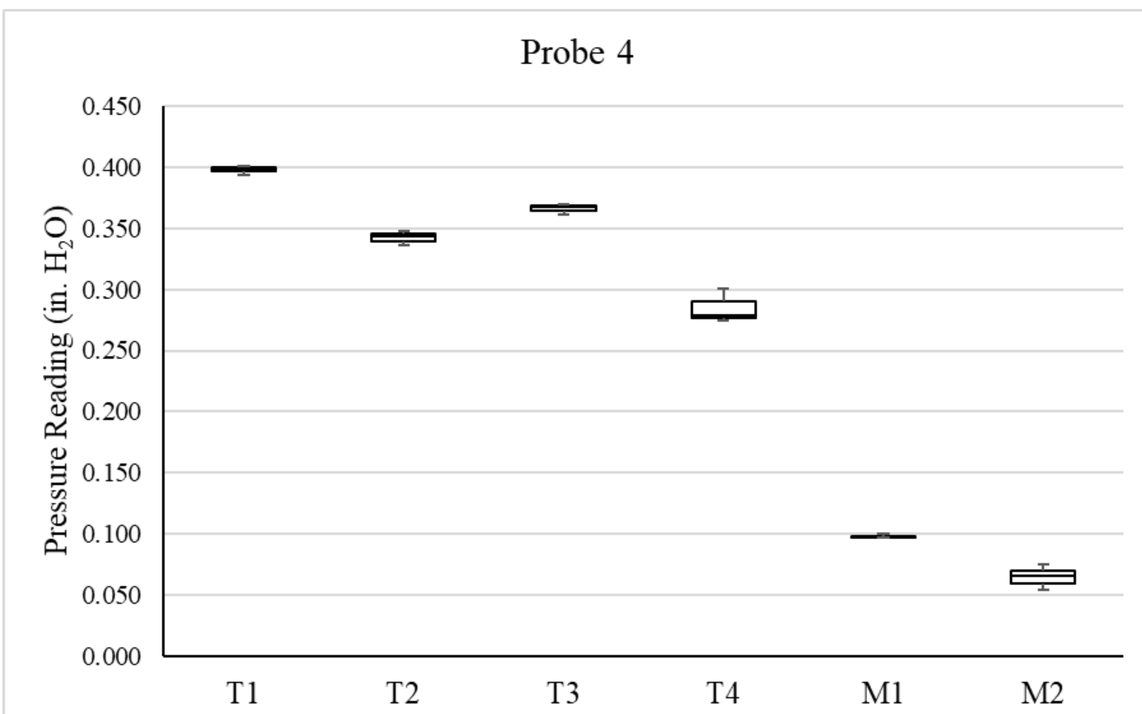

Figure A.4 Plot of Airflow Testing Results for Probe 4.

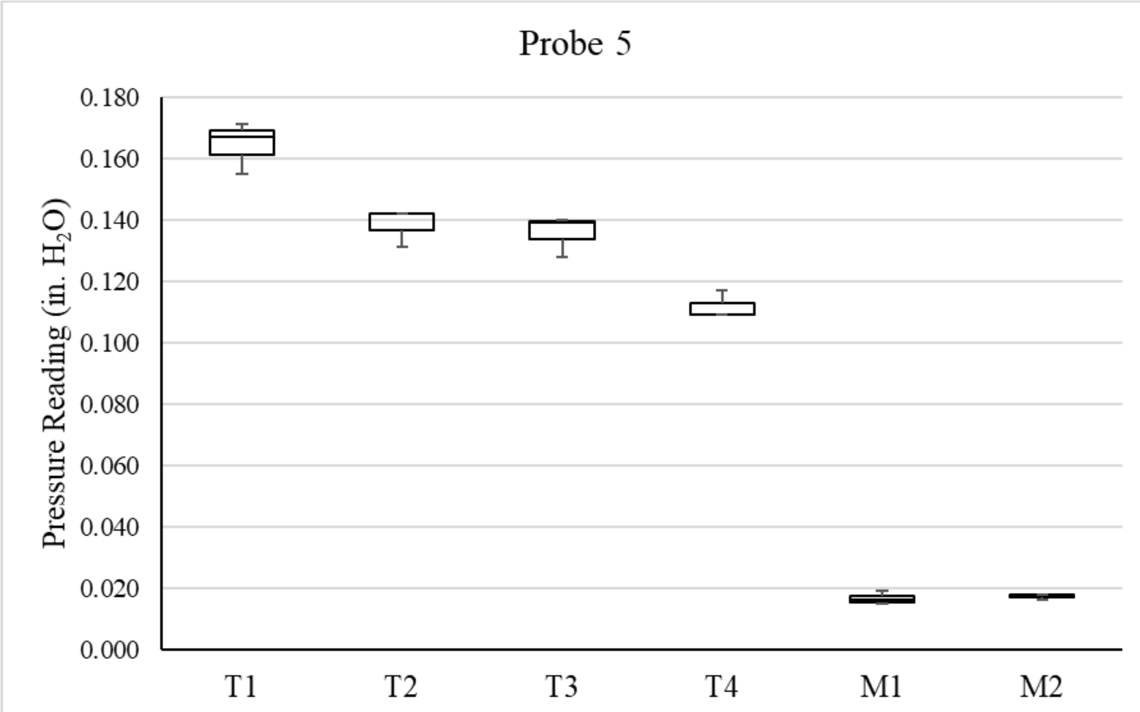

Figure A.5 Plot of Airflow Testing Results for Probe 5.

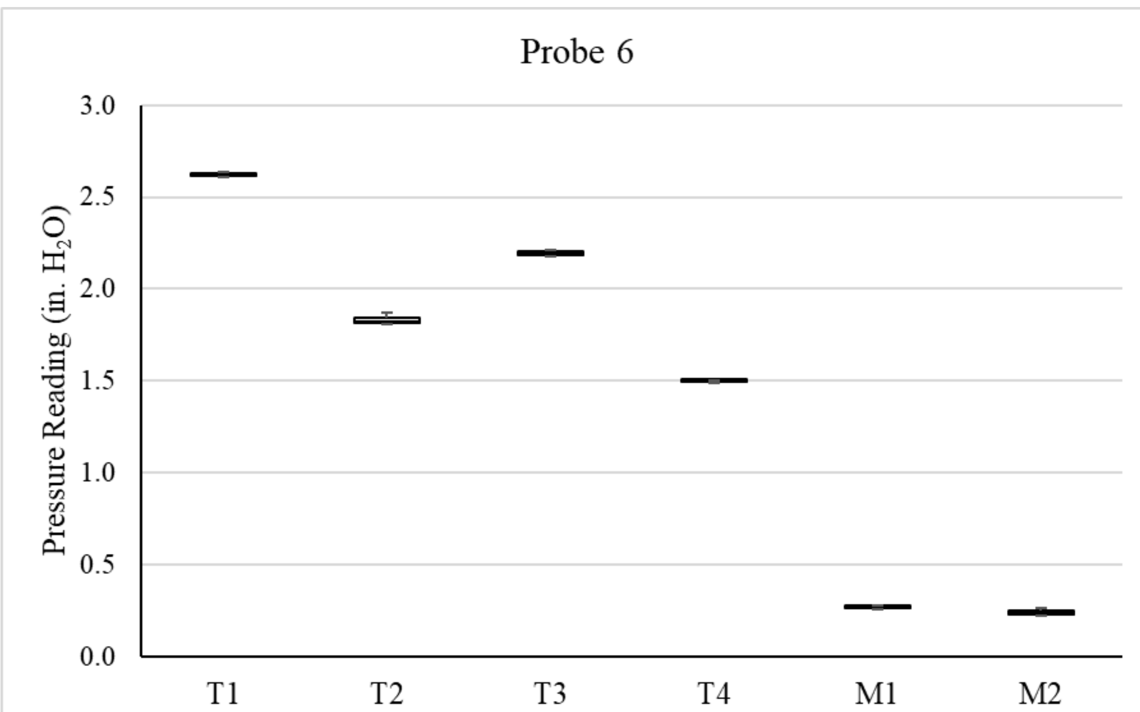

Figure A.6 Plot of Airflow Testing Results for Probe 6.

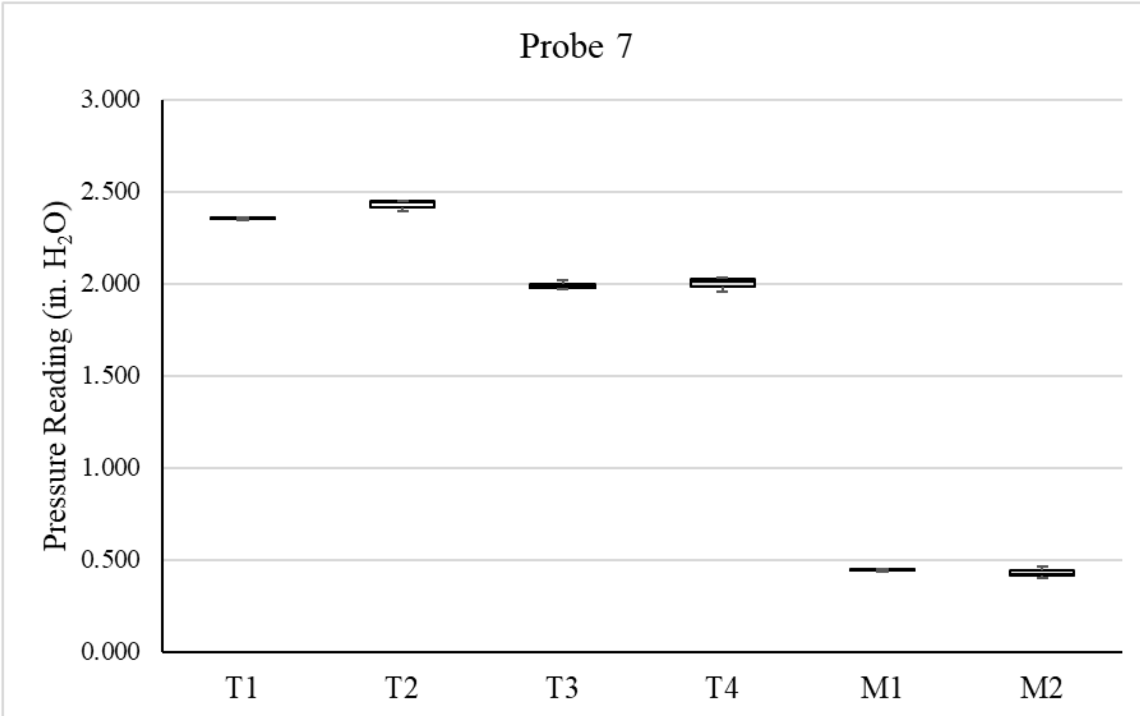

Figure A.7 Plot of Airflow Testing Results for Probe 7.

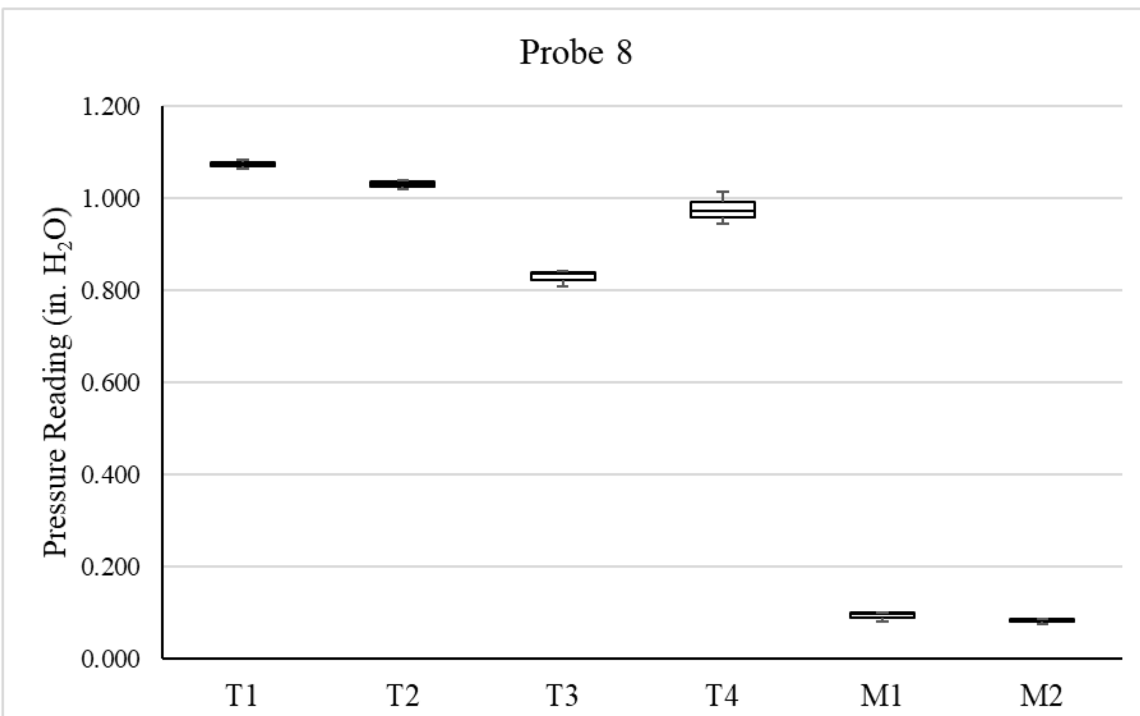

Figure A.8 Plot of Airflow Testing Results for Probe 8.

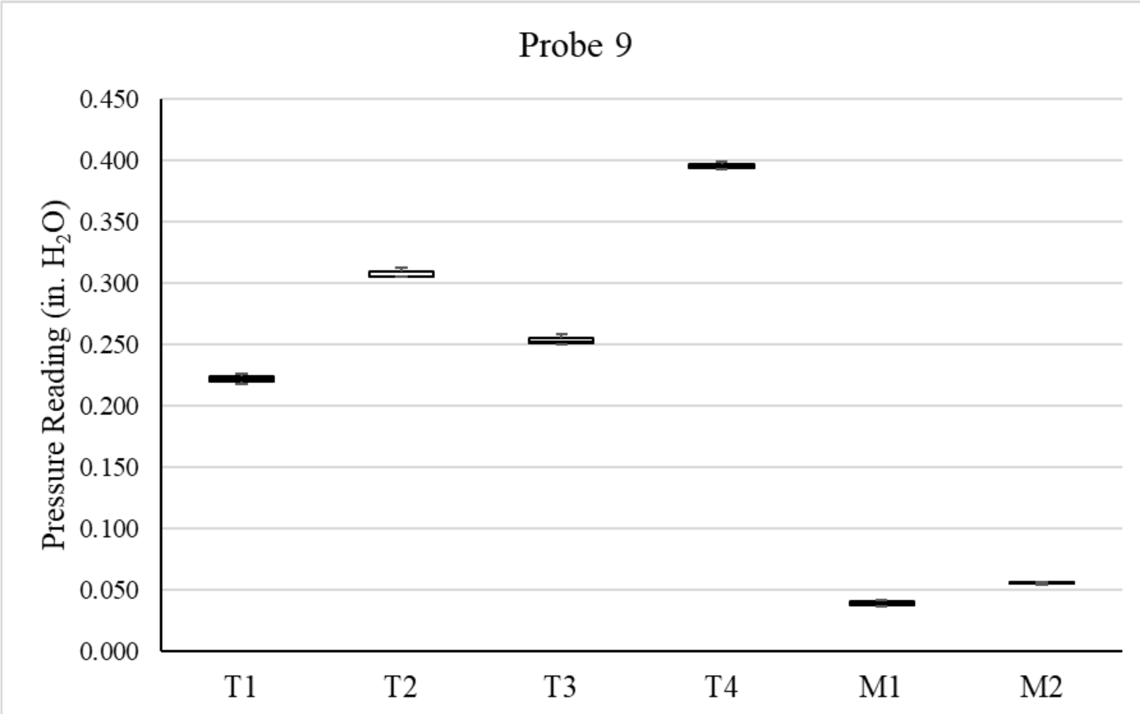

Figure A.9 Plot of Airflow Testing Results for Probe 9.

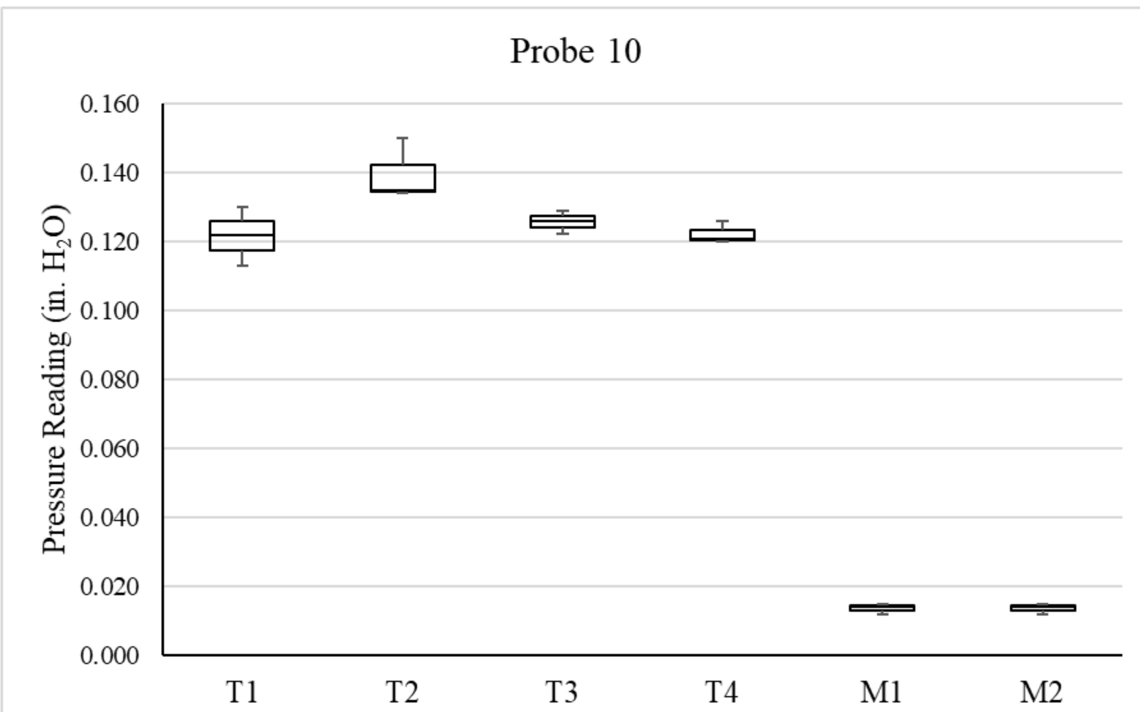

Figure A.10 Plot of Airflow Testing Results for Probe 10.

APPENDIX B

Force Vs. Displacement Data

Table B.1 Force and Pressure Recordings at Every 0.05-inches of Displacement (0.00 – 0.35 inches Displacement).

		Displacement (in)	**0.00**	**0.05**	**0.10**	**0.15**	**0.20**	**0.25**	**0.30**	**0.35**
Traditional 01	Trial 1	Force (N)	0.00	0.07	0.17	0.27	0.37	0.53	0.67	0.82
		Pressure (in. H2O)	0.556	0.866	0.863	0.978	1.094	1.206	1.286	1.485
	Trial 2	Force (N)	0.00	0.07	0.15	0.24	0.35	0.49	0.62	0.77
		Pressure (in. H2O)	0.679	0.985	1.111	1.320	1.382	1.433	1.492	1.522
	Trial 3	Force (N)	0.00	0.07	0.15	0.25	0.35	0.46	0.61	0.74
		Pressure (in. H2O)	0.700	0.917	1.083	1.227	1.328	1.422	1.511	1.550
Traditional 02	Trial 1	Force (N)	0.00	0.09	0.21	0.33	0.48	0.69	0.86	1.11
		Pressure (in. H2O)	0.332	0.646	0.852	0.983	1.039	1.118	1.165	1.232
	Trial 2	Force (N)	0.00	0.07	0.18	0.30	0.47	0.64	0.86	1.08
		Pressure (in. H2O)	0.093	0.316	0.586	0.782	0.898	0.993	1.064	1.121
	Trial 3	Force (N)	0.00	0.08	0.19	0.30	0.43	0.58	0.73	0.92
		Pressure (in. H2O)	0.269	0.567	0.783	0.924	1.043	1.159	1.191	1.309
Traditional 03	Trial 1	Force (N)	0.00	0.10	0.20	0.31	0.46	0.62	0.78	0.97
		Pressure (in. H2O)	0.458	0.769	1.052	1.313	1.398	1.509	1.540	1.583
	Trial 2	Force (N)	0.00	0.07	0.18	0.28	0.42	0.55	0.72	0.91
		Pressure (in. H2O)	0.490	0.801	0.981	1.129	1.207	1.287	1.319	1.352
	Trial 3	Force (N)	0.00	0.09	0.18	0.29	0.41	0.57	0.74	0.92
		Pressure (in. H2O)	0.494	0.922	1.158	1.361	1.442	1.491	1.532	1.552
Traditional 04	Trial 1	Force (N)	0.00	0.06	0.12	0.18	0.27	0.37	0.48	0.61
		Pressure (in. H2O)	0.143	0.196	0.283	0.392	0.533	0.679	0.779	0.868
	Trial 2	Force (N)	0	0.04	0.1	0.16	0.23	0.33	0.44	0.57
		Pressure (in. H2O)	0.183	0.262	0.399	0.599	0.755	0.866	0.949	1.002
	Trial 3	Force (N)	0.00	0.05	0.12	0.18	0.26	0.35	0.44	0.57
		Pressure (in. H2O)	0.183	0.238	0.297	0.366	0.475	0.554	0.693	0.798
Mesh 01	Trial 1	Force (N)	0.00	2.18	5.64	17.38	33.20	47.39	**Overload @ .258**	
		Pressure (in. H2O)	0.015	0.028	0.124	0.242	0.289	0.324	0.324	
	Trial 2	Force (N)	0	1.9	6.72	20.15	35.3	48.1	**Overload @ .252**	
		Pressure (in. H2O)	0.018	0.036	0.173	0.283	0.332	0.366	0.368	
	Trial 3	Force (N)	0.00	1.66	5.74	17.83	36.06	48.26	**Overload @ .255**	
		Pressure (in. H2O)	0.016	0.029	0.132	0.241	0.307	0.348	0.351	
Mesh 02	Trial 1	Force (N)	0.00	2.18	5.64	18.86	36.78	**Overload @ .238**		
		Pressure (in. H2O)	0.000	0.013	0.052	0.251	0.365	0.402		
	Trial 2	Force (N)	0	1.88	5.12	17.23	36.5	**Overload @ .241**		
		Pressure (in. H2O)	0.016	0.020	0.075	0.233	0.316	0.344		
	Trial 3	Force (N)	0.00	1.75	5.95	21.23	39.67	**Overload @ .229**		
		Pressure (in. H2O)	0.015	0.029	0.126	0.258	0.318	0.336		

Table B.2 Force and Pressure Recordings at Every 0.05-inches of Displacement (0.40 – 0.75 inches displacement).

		Displacement (in)	0.40	0.45	0.50	0.55	0.60	0.65	0.70	0.75
Traditional 01	Trial 1	Force (N)	1.02	1.23	1.46	1.67	2.01	2.21	2.62	2.98
		Pressure (in. H2O)	1.520	1.661	1.706	1.738	1.783	1.806	1.850	1.864
	Trial 2	Force (N)	0.93	1.15	1.36	1.59	1.87	2.14	2.52	2.84
		Pressure (in. H2O)	1.571	1.622	1.652	1.721	1.756	1.773	1.806	1.822
	Trial 3	Force (N)	0.89	1.09	1.26	1.48	1.72	2.02	2.34	2.68
		Pressure (in. H2O)	1.603	1.635	1.675	1.706	1.728	1.751	1.767	1.783
Traditional 02	Trial 1	Force (N)	1.33	1.63	1.99	2.33	2.79	3.22	3.82	4.40
		Pressure (in. H2O)	1.277	1.308	1.341	1.374	1.407	1.444	1.478	1.514
	Trial 2	Force (N)	1.36	1.66	1.95	2.32	2.71	3.21	3.65	4.31
		Pressure (in. H2O)	1.205	1.258	1.318	1.371	1.422	1.453	1.513	1.541
	Trial 3	Force (N)	1.12	1.36	1.64	1.88	2.20	2.61	2.94	3.54
		Pressure (in. H2O)	1.392	1.412	1.461	1.511	1.556	1.581	1.632	1.667
Traditional 03	Trial 1	Force (N)	1.19	1.42	1.71	2.02	2.33	2.72	3.14	3.64
		Pressure (in. H2O)	1.617	1.637	1.663	1.679	1.694	1.732	1.757	1.778
	Trial 2	Force (N)	1.13	1.35	1.61	1.92	2.26	2.63	3.09	3.50
		Pressure (in. H2O)	1.386	1.427	1.458	1.495	1.524	1.572	1.601	1.632
	Trial 3	Force (N)	1.14	1.35	1.62	1.89	2.24	2.62	3.03	3.53
		Pressure (in. H2O)	1.575	1.606	1.637	1.664	1.681	1.702	1.722	1.730
Traditional 04	Trial 1	Force (N)	0.75	0.92	1.01	1.35	1.61	1.97	2.43	2.96
		Pressure (in. H2O)	0.928	0.992	1.090	1.096	1.103	1.109	1.126	1.147
	Trial 2	Force (N)	0.69	0.89	1.09	1.33	1.61	1.97	2.39	2.89
		Pressure (in. H2O)	1.068	1.106	1.119	1.147	1.168	1.173	1.186	1.212
	Trial 3	Force (N)	0.70	0.87	1.05	1.27	1.52	1.86	2.31	2.86
		Pressure (in. H2O)	0.879	0.963	1.053	1.124	1.165	1.203	1.214	1.245
Mesh 01	Trial 1	Force (N)								
		Pressure (in. H2O)								
	Trial 2	Force (N)								
		Pressure (in. H2O)								
	Trial 3	Force (N)								
		Pressure (in. H2O)								
Mesh 02	Trial 1	Force (N)								
		Pressure (in. H2O)								
	Trial 2	Force (N)								
		Pressure (in. H2O)								
	Trial 3	Force (N)								
		Pressure (in. H2O)								

Table B.3 Force and Pressure Recordings at Every 0.05-inches of Displacement (0.80 – 1.15 inches displacement).

		Displacement (in)	0.80	0.85	0.90	0.95	1.00	1.05	1.10	1.15
Traditional 01	Trial 1	Force (N)	3.39	3.89	4.29	4.98	5.51	6.06	6.79	7.46
		Pressure (in. H2O)	1.883	1.911	1.916	1.932	1.934	1.946	1.952	1.959
	Trial 2	Force (N)	3.26	3.69	4.20	4.74	5.18	6.00	6.69	7.53
		Pressure (in. H2O)	1.852	1.884	1.902	1.923	1.936	1.954	1.969	1.98
	Trial 3	Force (N)	3.07	3.44	3.93	4.39	4.95	5.59	6.18	7.09
		Pressure (in. H2O)	1.831	1.848	1.872	1.906	1.928	1.954	1.965	1.985
Traditional 02	Trial 1	Force (N)	5.11	5.84	6.66	7.59	8.44	9.79	10.62	12.19
		Pressure (in. H2O)	1.548	1.589	1.622	1.685	1.705	1.734	1.761	1.791
	Trial 2	Force (N)	4.89	5.60	6.38	7.19	8.13	9.08	10.33	11.37
		Pressure (in. H2O)	1.576	1.613	1.643	1.679	1.718	1.744	1.775	1.803
	Trial 3	Force (N)	4.05	4.70	5.33	6.19	7.03	7.92	9.02	10.27
		Pressure (in. H2O)	1.690	1.722	1.751	1.780	1.798	1.826	1.854	1.879
Traditional 03	Trial 1	Force (N)	4.16	4.73	5.33	6.04	6.85	7.81	9.02	9.92
		Pressure (in. H2O)	1.798	1.827	1.852	1.867	1.906	1.927	1.953	1.985
	Trial 2	Force (N)	4.07	4.69	5.32	6.11	6.91	7.84	9.03	10.18
		Pressure (in. H2O)	1.649	1.687	1.721	1.747	1.782	1.798	1.838	1.852
	Trial 3	Force (N)	3.98	4.63	5.27	5.99	6.83	7.51	8.71	9.76
		Pressure (in. H2O)	1.775	1.799	1.811	1.818	1.834	1.845	1.860	1.874
Traditional 04	Trial 1	Force (N)	3.73	4.74	6.27	9.14	14.21			
		Pressure (in. H2O)	1.170	1.211	1.263	1.354	1.446			
	Trial 2	Force (N)	3.69	4.71	6.23	9.11	13.82			
		Pressure (in. H2O)	1.233	1.281	1.332	1.404	1.549			
	Trial 3	Force (N)	3.65	4.73	6.55	9.38	15.78			
		Pressure (in. H2O)	1.268	1.312	1.378	1.463	1.595			
Mesh 01	Trial 1	Force (N)								
		Pressure (in. H2O)								
	Trial 2	Force (N)								
		Pressure (in. H2O)								
	Trial 3	Force (N)								
		Pressure (in. H2O)								
Mesh 02	Trial 1	Force (N)								
		Pressure (in. H2O)								
	Trial 2	Force (N)								
		Pressure (in. H2O)								
	Trial 3	Force (N)								
		Pressure (in. H2O)								

Table B.4 Force and Pressure Recordings at Every 0.05-inches of Displacement (1.20 – 1.50 inches displacement).

		Displacement (in)	1.20	1.25	1.30	1.35	1.40	1.45	1.50
Traditional 01	Trial 1	Force (N)	8.27	9.11	10.19	11.16	12.79	14.29	16.03
		Pressure (in. H2O)	1.968	1.974	1.992	2.001	2.016	2.029	2.053
	Trial 2	Force (N)	8.37	9.19	10.42	11.48	12.80	14.42	16.78
		Pressure (in. H2O)	1.986	2.000	2.021	2.031	2.046	2.071	2.092
	Trial 3	Force (N)	7.76	8.86	9.79	11.01	12.58	14.55	17.34
		Pressure (in. H2O)	2.001	2.014	2.038	2.066	2.094	2.122	2.162
Traditional 02	Trial 1	Force (N)	13.61	15.39	17.64				
		Pressure (in. H2O)	1.824	1.854	1.877				
	Trial 2	Force (N)	12.98	14.39	15.60				
		Pressure (in. H2O)	1.836	1.864	1.887				
	Trial 3	Force (N)	11.63	13.23	15.19				
		Pressure (in. H2O)	1.903	1.927	1.921				
Traditional 03	Trial 1	Force (N)	11.48	12.85	14.72				
		Pressure (in. H2O)	2.003	2.039	2.097				
	Trial 2	Force (N)	11.67	13.46	15.65				
		Pressure (in. H2O)	1.897	1.957	2.030				
	Trial 3	Force (N)	11.29	12.74	14.84				
		Pressure (in. H2O)	1.902	1.928	1.987				
Traditional 04	Trial 1	Force (N)							
		Pressure (in. H2O)							
	Trial 2	Force (N)							
		Pressure (in. H2O)							
	Trial 3	Force (N)							
		Pressure (in. H2O)							
Mesh 01	Trial 1	Force (N)							
		Pressure (in. H2O)							
	Trial 2	Force (N)							
		Pressure (in. H2O)							
	Trial 3	Force (N)							
		Pressure (in. H2O)							
Mesh 02	Trial 1	Force (N)							
		Pressure (in. H2O)							
	Trial 2	Force (N)							
		Pressure (in. H2O)							
	Trial 3	Force (N)							
		Pressure (in. H2O)							

APPENDIX C

Representative Airflow Testing Photos

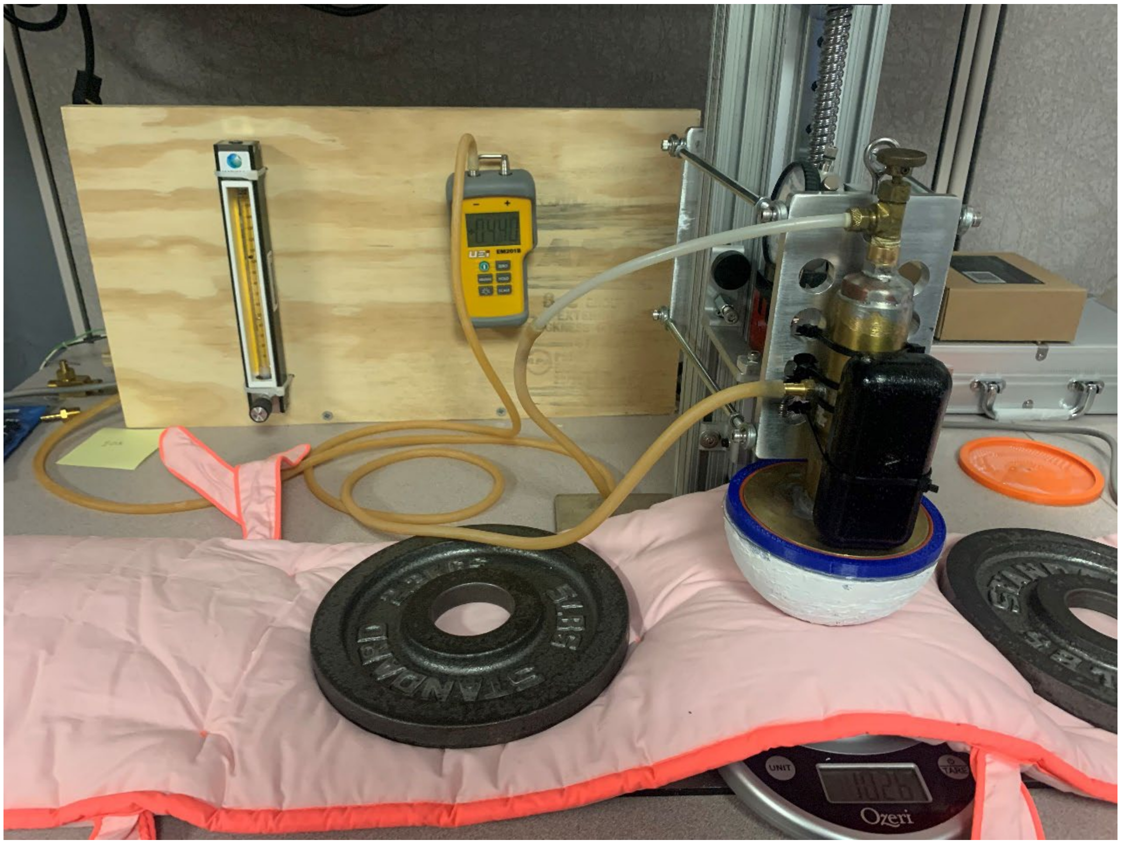

Figure C.1 Representative Photo of Traditional 1 during Airflow Testing.

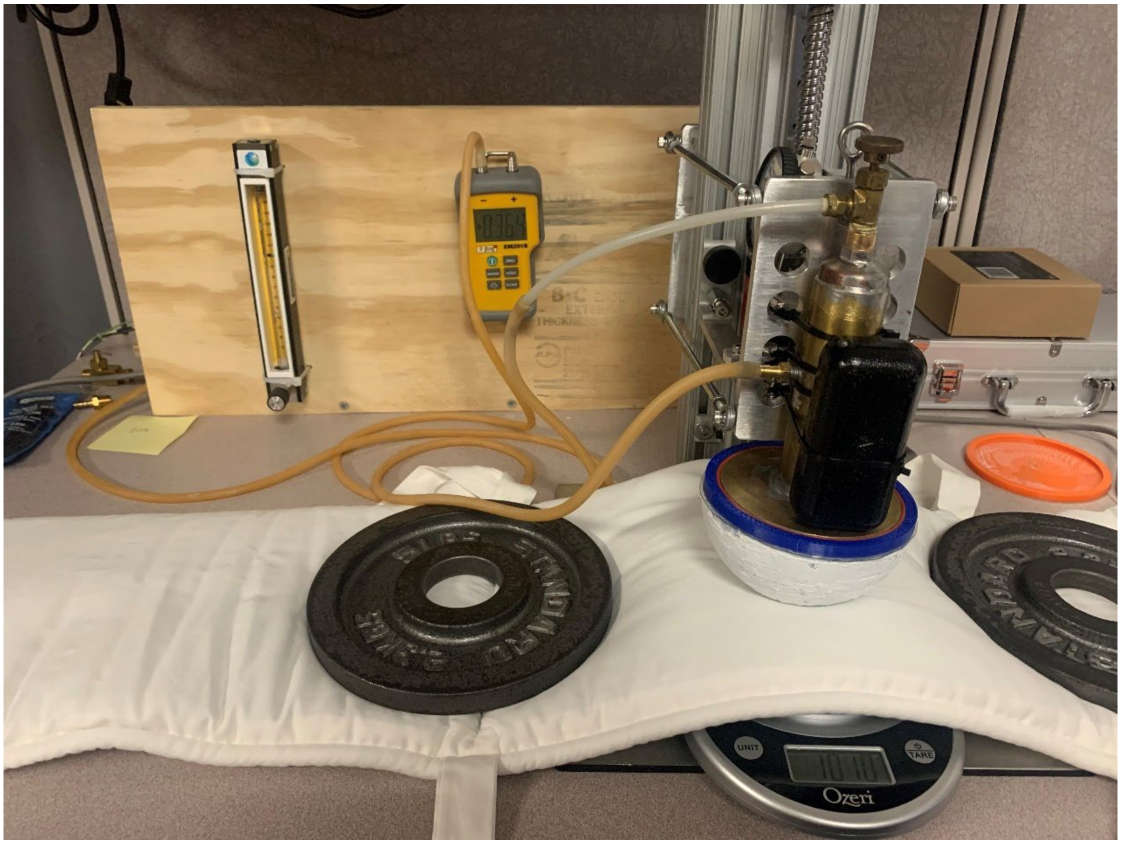

Figure C.2 Representative Photo of Traditional 2 during Airflow Testing.

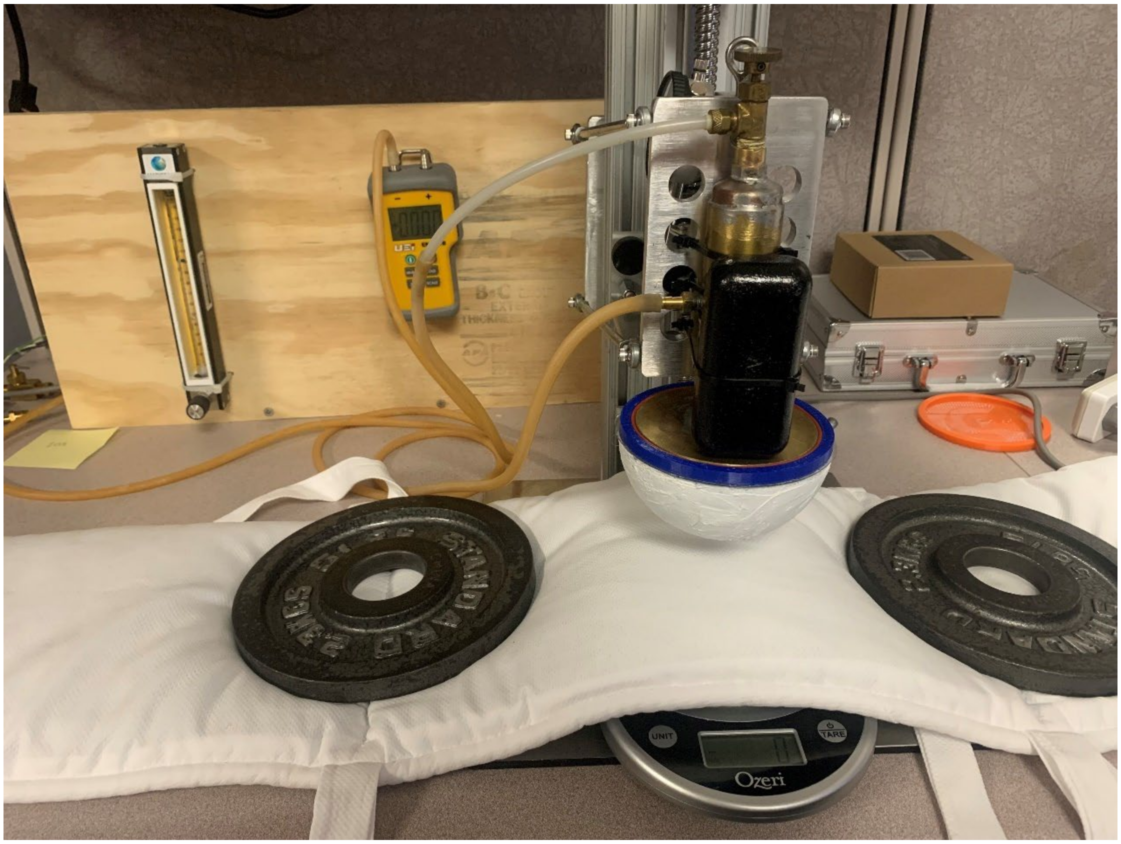

Figure C.3 Representative Photo of Traditional 3 during Airflow Testing.

Figure C.4 Representative Photo of Traditional 4 during Airflow Testing.

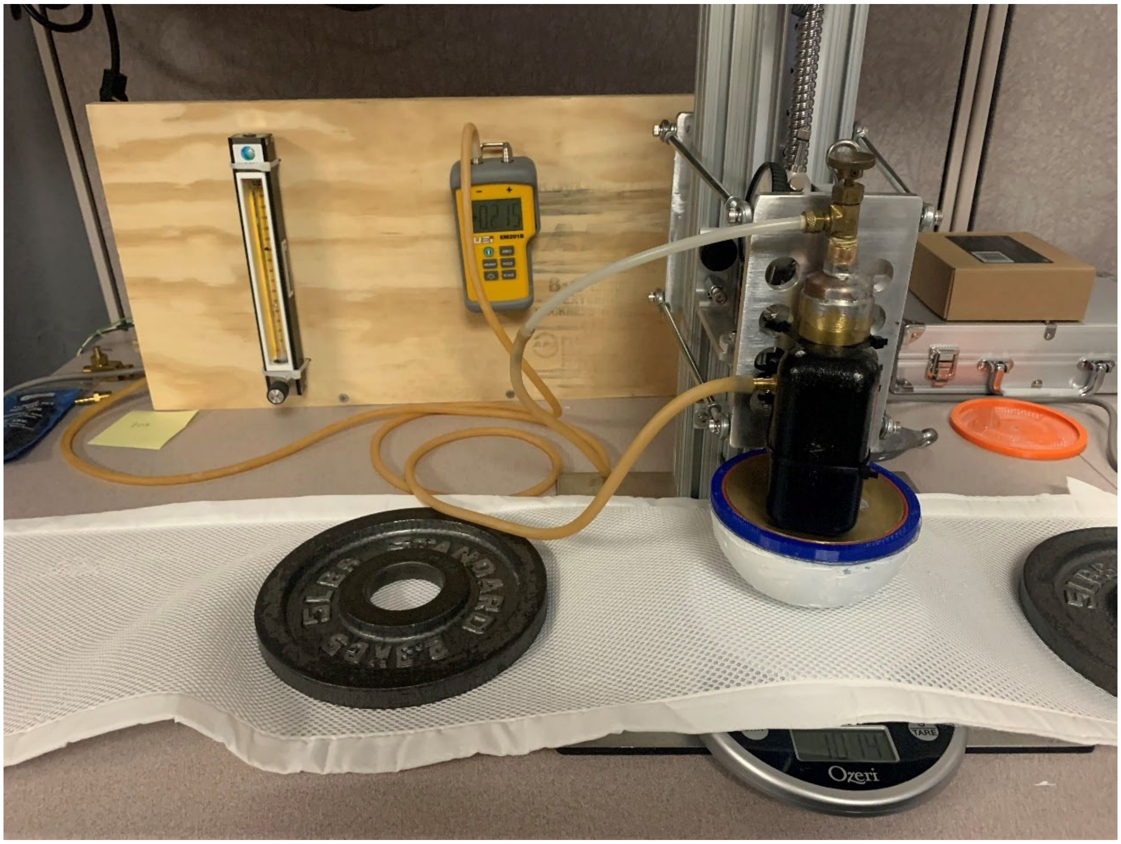

Figure C.5 Representative Photo of Mesh 1 during Airflow Testing.

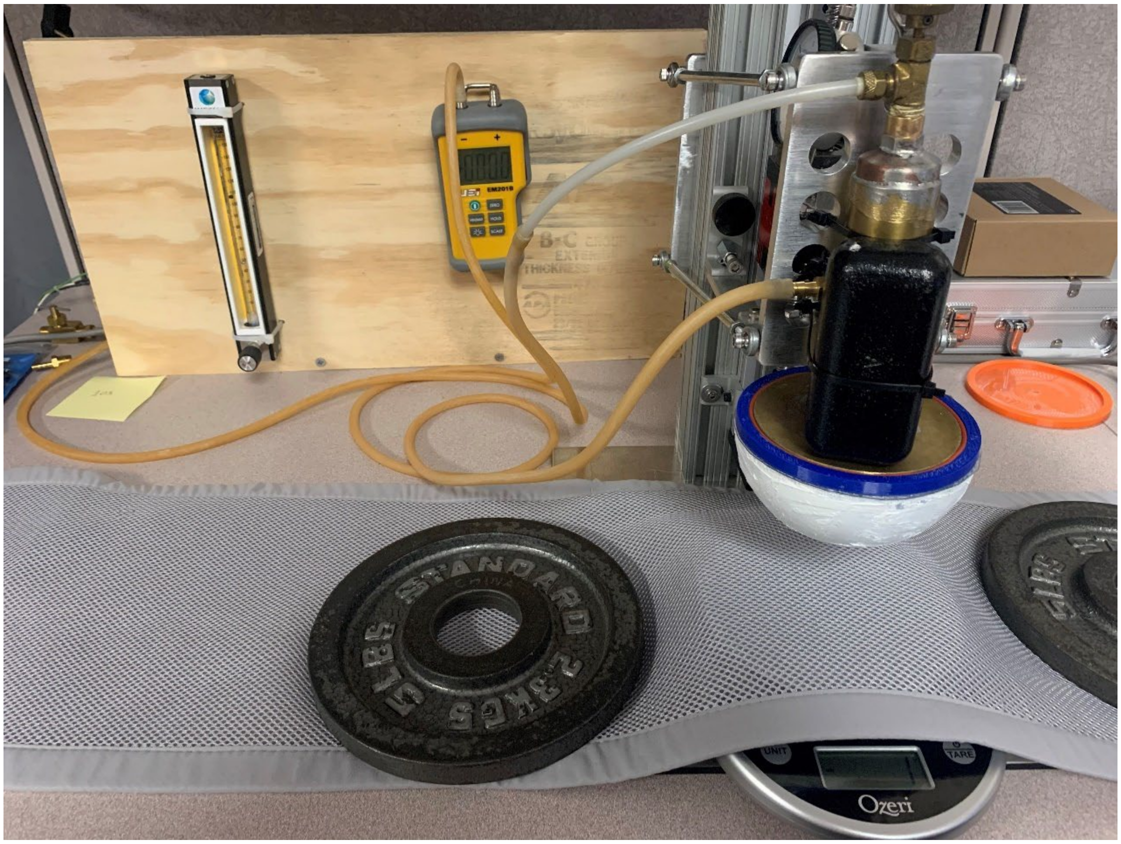

Figure C.6 Representative Photo of Mesh 2 during Airflow Testing.

APPENDIX D

Representative Force Vs. Displacement Testing Photos

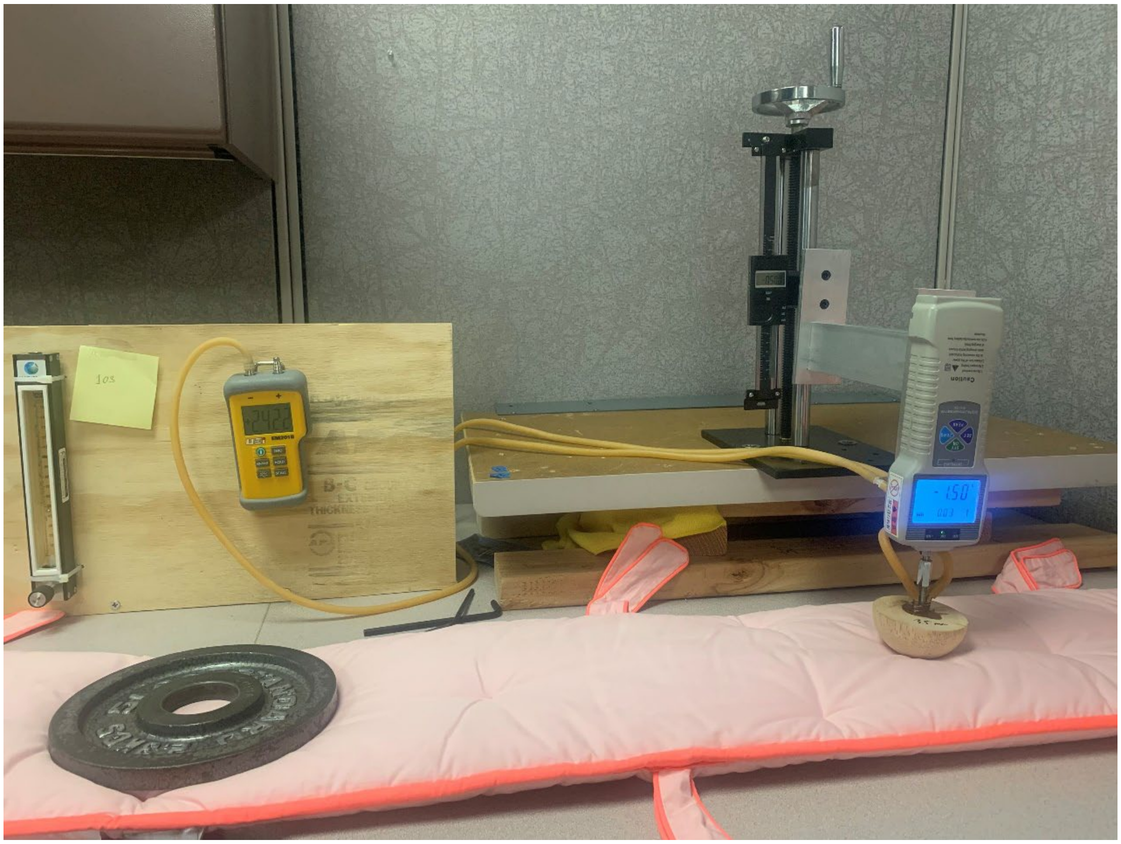

Figure D.1 Representative Photo of Traditional 1 during Force vs. Displacement Testing.

Figure D.2 Representative Photo of Traditional 2 during Force vs. Displacement Testing.

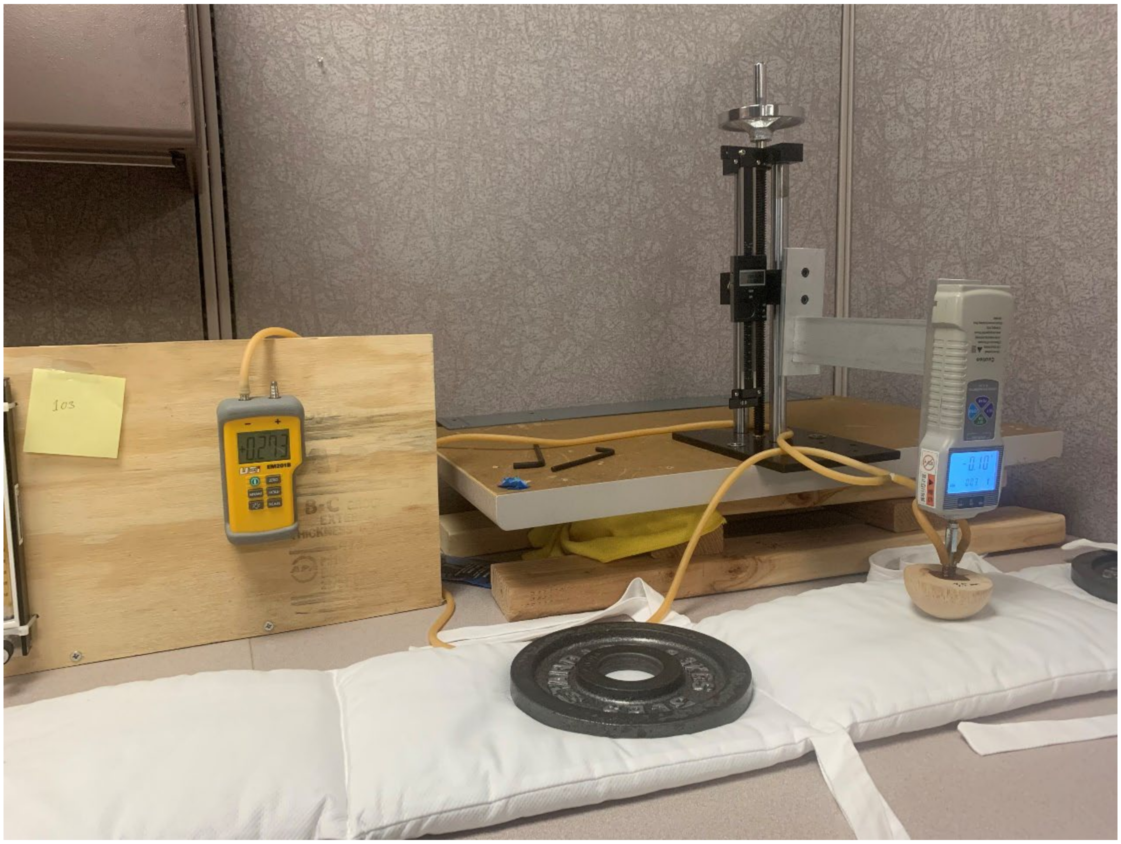

Figure D.3 Representative Photo of Traditional 3 during Force vs. Displacement Testing.

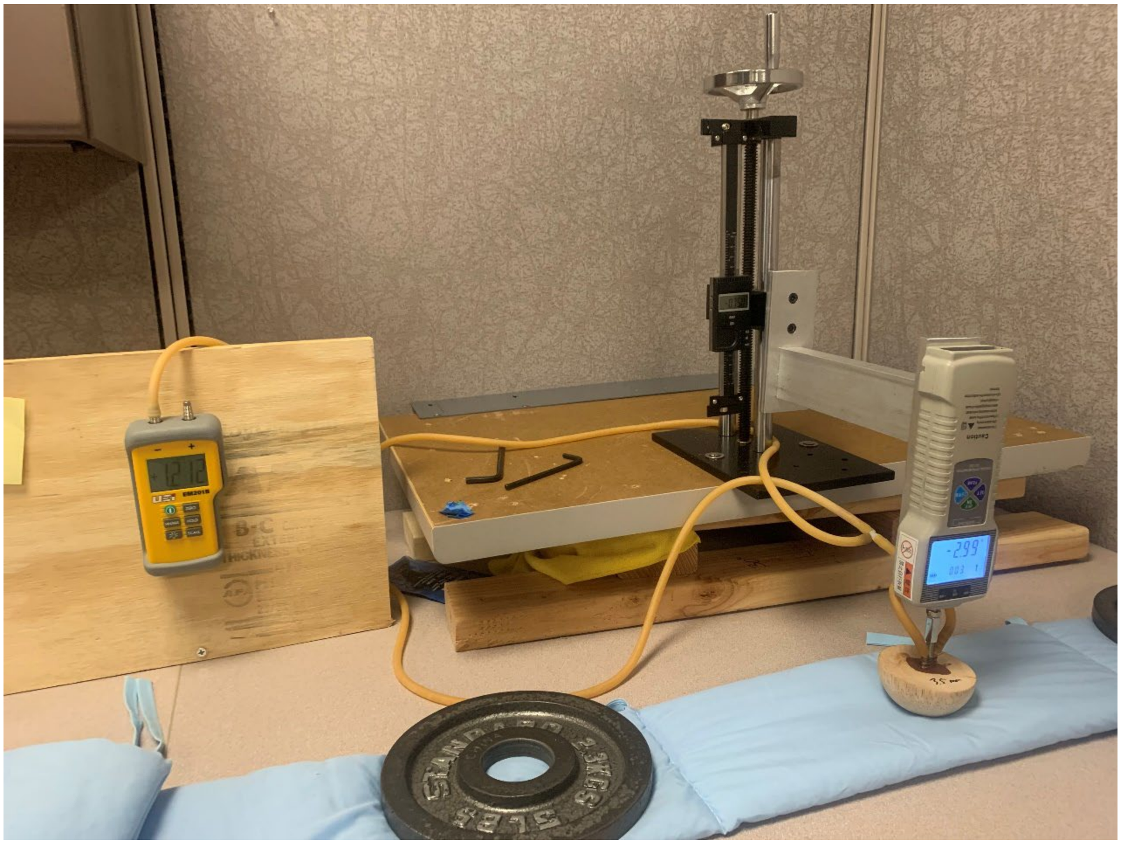

Figure D.4 Representative Photo of Traditional 4 during Force vs. Displacement Testing.

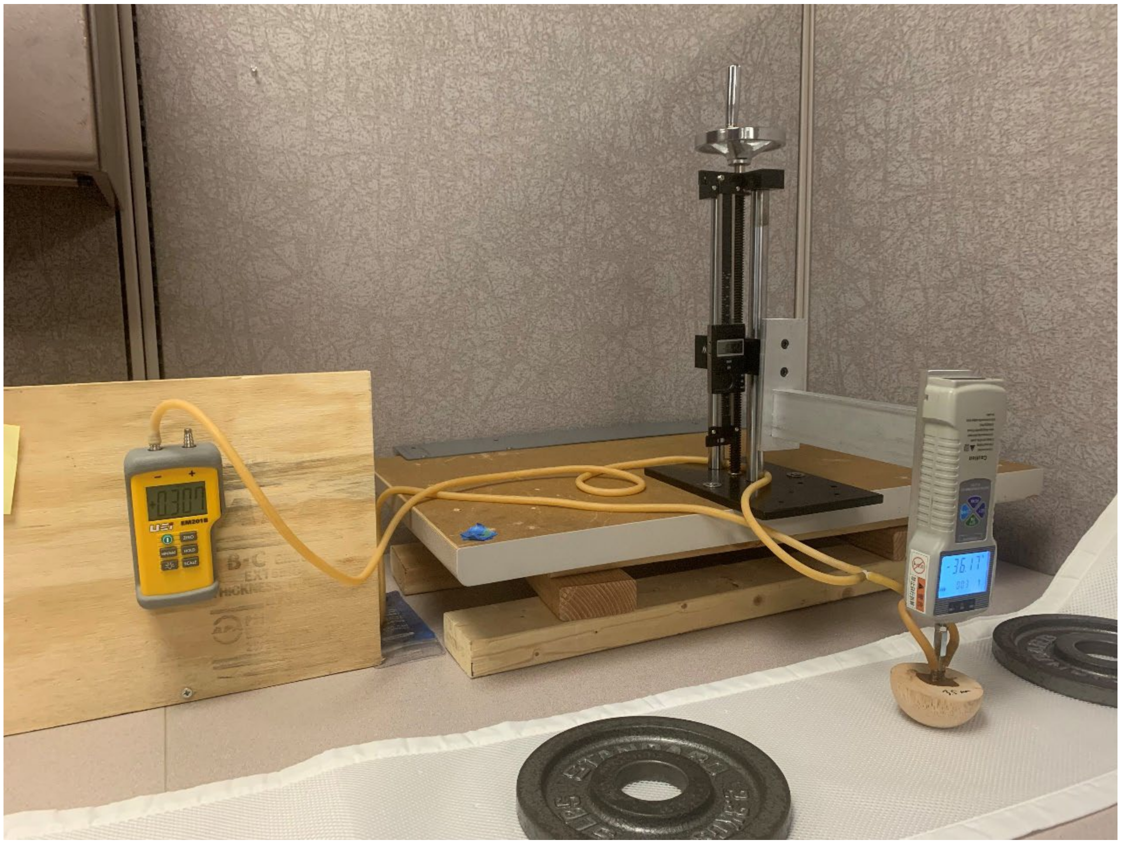

Figure D.5 Representative Photo of Mesh 1 during Force vs. Displacement Testing.

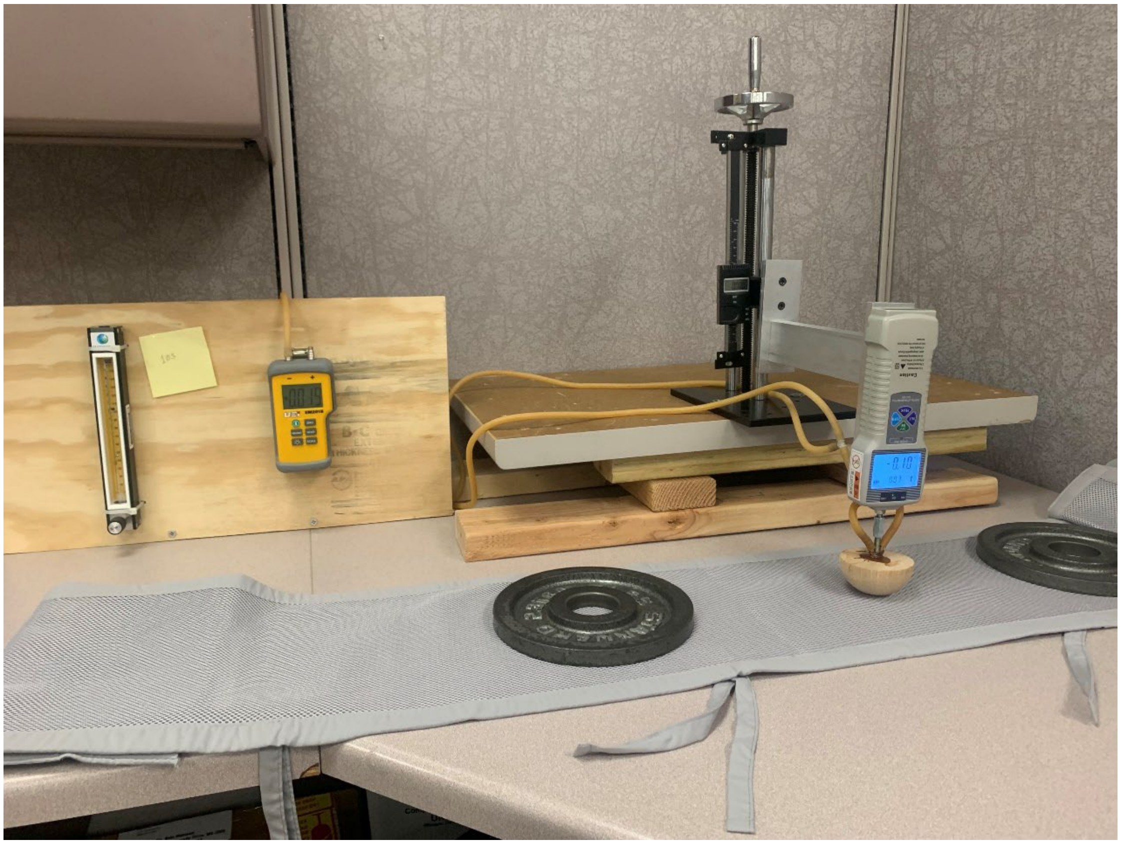

Figure D.6 Representative Photo of Mesh 2 during Force vs. Displacement Testing.

APPENDIX E

Representative Stress Relaxation Testing Photos

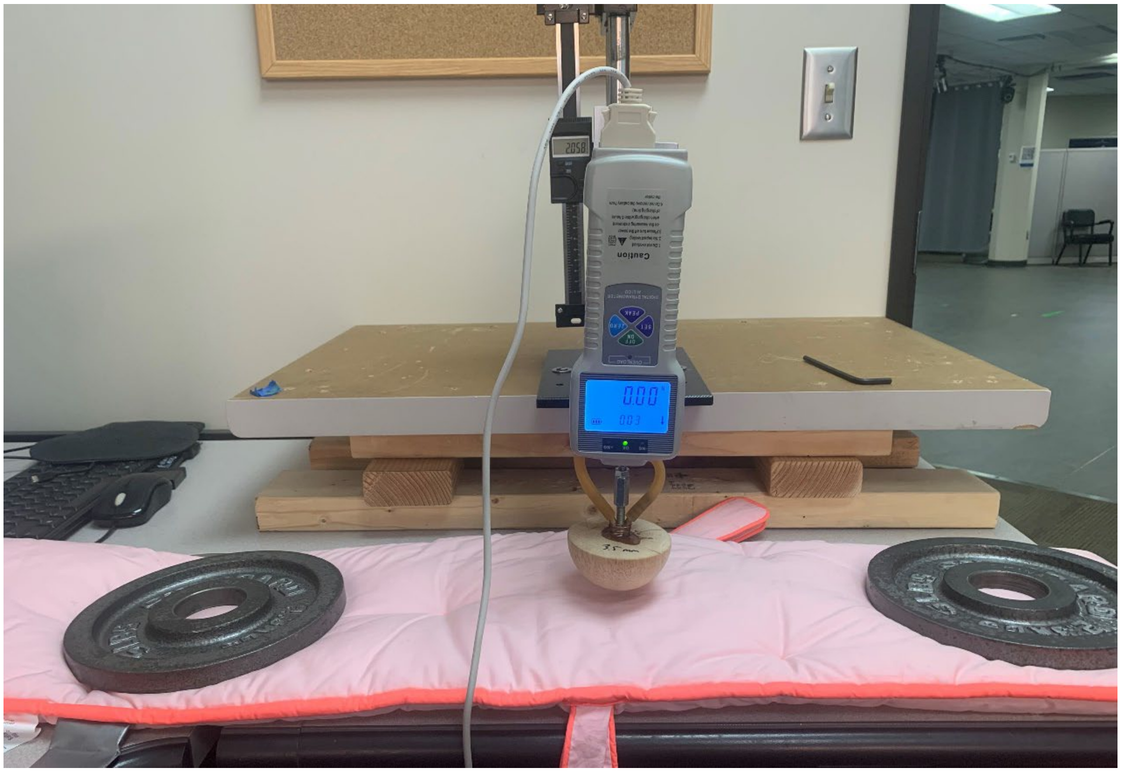

Figure E.1 Representative Photo of Traditional 1 during Stress Relaxation Testing.

Figure E.2 Representative Photo of Traditional 2 during Stress Relaxation Testing.

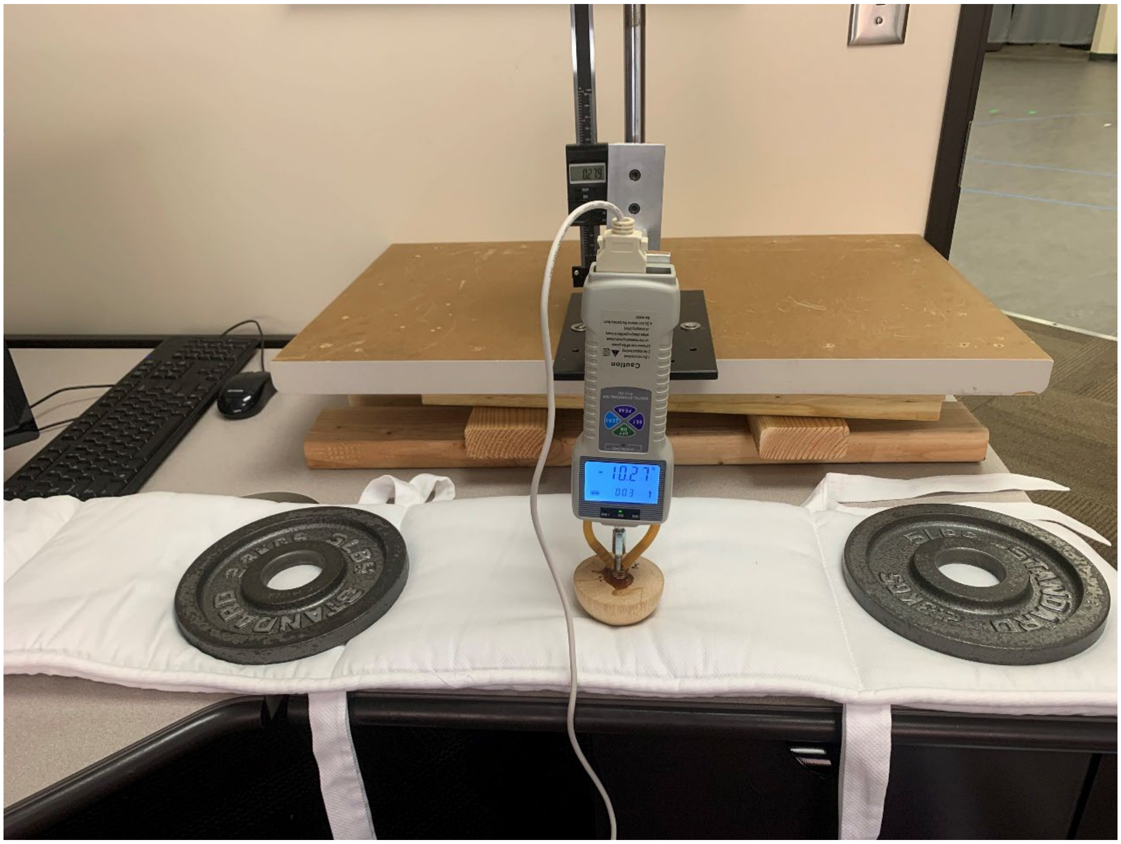

Figure E.3 Representative Photo of Traditional 3 during Stress Relaxation Testing.

Figure E.4 Representative Photo of Traditional 4 during Stress Relaxation Testing.

Figure E.5 Representative Photo of Mesh 1 during Stress Relaxation Testing.

Figure E.6 Representative Photo of Mesh 2 during Stress Relaxation Testing.

APPENDIX F

Head Circumference Calculation Code

Average Head Circumference Calculation

Created by Wyatt Davis

```
% Data taken from 50th percentile column in CDC Charts listed in references (Centers,
2001)
clc;clear;

% Average values for 0-9 months old

c_9mon = [35.81367 37.19361 39.20743 40.77713 41.71483 42.48889 43.14204
43.70245 44.18964 45.05761 ... % Male
    34.71156 36.03454 37.97672 39.38013 40.46774 41.34841 42.08335 42.71034
43.25429 43.7325];          % Female
cav_9mon = mean(c_9mon);
dcm_9mon = cav_9mon/(pi); % Circumference = d*pi
din_9mon = dcm_9mon/2.54 % Conversion from cm to in

% Average values for 0-6 months old

c_6mon = [35.81367 37.19361 39.20743 40.65233 41.76517 42.66116 43.40489
44.0361...                  % Male
    34.71156 36.03454 37.97672 39.38013 40.46774 41.34841 42.08335 42.71034];
% Female
cav_6mon = mean(c_6mon);
dcm_6mon = cav_6mon/(pi); % C = d*pi
din_6mon = dcm_6mon/2.54 % Conversion to in
```

```
din_9mon =
    5.1067
din_6mon =
    5.0084
```

Published with MATLAB® R2020a

APPENDIX G

Force Displacement Analysis Code

<u>Force Displacement Testing</u>

Created by Wyatt Davis

```
clc;clear;close all;

opts = spreadsheetImportOptions("NumVariables", 31);

% Specify sheet and range
opts.Sheet = "Sheet 1";
opts.DataRange = "D2:AH38";

opts.VariableTypes = ["double", "double", "double", "double", "double", "double",
"double", "double", "double", "double", "double", "double", "double", "double",
"double", "double", "double", "double", "double", "double", "double", "double",
"double", "double", "double", "double", "double", "double", "double", "double",
"string"];

data = readtable("C:\Users\davis\Documents\Thesis\Force Displacement
Testingv2.xlsx",opts);
data = str2double(table2array(data));

disp = data(1,:)*0.0254; %Displacement of testing probe into product, in meters
thick = [1.443 1.384 1.451 0.921 0.162 0.154]*0.0254; %Measured thickness of each
product, in meters

% Calculation of cross-sectional area applied to products based on
% displacements and chord length. Assuming initial value is size of openings

r = 1.5*0.0254; %radius of hemisphere, meters
d = r - disp;
for i = 1:length(d)
```

```
    if d(i) >= 0
        c(i) = 2*sqrt(r^2-d(i)^2); %calculated chord length + assumed original
        Ax(i) = pi*(c(i)/2)^2; % cross-sectional area applied to products
    else
        Ax(i) = pi*r^2; % Maximum cross-sectional area
    end
end

% Organization of data into force and pressure readings for each product,
% each row is a separate trial

T1_f = vertcat(data(2,:),data(4,:),data(6,:));
T1_p = vertcat(data(3,:),data(5,:),data(7,:));

T2_f = vertcat(data(8,:),data(10,:),data(12,:));
T2_p = vertcat(data(9,:),data(11,:),data(13,:));

T3_f = vertcat(data(14,:),data(16,:),data(18,:));
T3_p = vertcat(data(15,:),data(17,:),data(19,:));

T4_f = vertcat(data(20,:),data(22,:),data(24,:));
T4_p = vertcat(data(21,:),data(23,:),data(25,:));

M1_f = vertcat(data(26,:),data(28,:),data(30,:));
M1_p = vertcat(data(27,:),data(29,:),data(31,:));

M2_f = vertcat(data(32,:),data(34,:),data(36,:));
M2_p = vertcat(data(33,:),data(35,:),data(37,:));
```

Stress and Strain Calculations and Plotting

```
figure(1)
T1_s = T1_f./Ax; %Stress Calculation for T1
T1_s(:,1) = 0;
T1_ep = [1;1;1]*disp/thick(1); %Strain Calculation for T1
for i = 1:3
   plot(T1_ep(i,:),T1_s(i,:))
   hold on
end
xlabel('Strain','FontSize',18)
ylabel('Stress (Pa)','FontSize',18)
title('Traditional 1','FontSize',18)
legend('Trial 1','Trial 2','Trial 3','Location','NorthWest','FontSize',14)
ylim([200 40000])
xlim([0 1])

figure(2)
T2_s = T2_f./Ax; %Stress Calculation for T2
T2_s(:,1) = 0;
T2_ep = [1;1;1]*disp/thick(2); %Strain Calculation for T2
for i = 1:3
   plot(T2_ep(i,:),T2_s(i,:))
   hold on
end
xlabel('Strain','FontSize',18)
ylabel('Stress (Pa)','FontSize',18')
title('Traditional 2','FontSize',18)
legend('Trial 1','Trial 2','Trial 3','Location','NorthWest','FontSize',14)
ylim([200 40000])
xlim([0 1])
```

```
figure(3)
T3_s = T3_f./Ax; %Stress Calculation for T3
T3_s(:,1) = 0;
T3_ep = [1;1;1]*disp/thick(3); %Strain Calculation for T3
for i = 1:3
    plot(T3_ep(i,:),T3_s(i,:))
    hold on
end
xlabel('Strain','FontSize',18)
ylabel('Stress (Pa)','FontSize',18)
title('Traditional 3','FontSize',18)
legend('Trial 1','Trial 2','Trial 3','Location','NorthWest','FontSize',14)
ylim([200 40000])
xlim([0 1])


figure(4)
T4_s = T4_f./Ax;  %Stress Calculation for T4
T4_s(:,1) = 0;
T4_ep = [1;1;1]*disp/thick(4); %Strain Calculation for T4
for i = 1:3
    plot(T4_ep(i,:),T4_s(i,:))
    hold on
end
xlabel('Strain','FontSize',18)
ylabel('Stress (Pa)','FontSize',18)
title('Traditional 4','FontSize',18)
legend('Trial 1','Trial 2','Trial 3','Location','NorthWest','FontSize',14)
ylim([200 40000])
xlim([0 1])
```

```
for i = 1:3
    for j = 1:length(M1_f)
        if ~isnan(M1_f(i,j))
            M1_s(i,j) = M1_f(i,j)/Ax(j);  %Stress Calculation for M1
            M1_ep(i,j) = disp(j)/thick(5); %Strain Calculation for M1
        end

        if ~isnan(M2_f(i,j))
            M2_s(i,j) = M2_f(i,j)/Ax(j);  %Stress Calculation for M2
            M2_ep(i,j) = disp(j)/thick(6); %Strain Calculation for M2
        end
    end
end
M1_s(:,1) = 0;
M2_s(:,1) = 0;

figure(5)
for i = 1:3
    plot(M1_ep(i,:),M1_s(i,:))
    hold on
end
xlabel('Strain','FontSize',18)
ylabel('Stress (Pa)','FontSize',18)
title('Mesh 1','FontSize',18)
legend('Trial 1','Trial 2','Trial 3','Location','NorthWest','FontSize',14)
ylim([200 40000])
xlim([0 1])
```

```
figure(6)
for i = 1:3
    plot(M2_ep(i,:),M2_s(i,:))
    hold on
end
xlabel('Strain','FontSize',18)
ylabel('Stress (Pa)','FontSize',18)
title('Mesh 2','FontSize',18)
legend('Trial 1','Trial 2','Trial 3','Location','NorthWest','FontSize',14)
ylim([200 40000])
xlim([0 1])
```

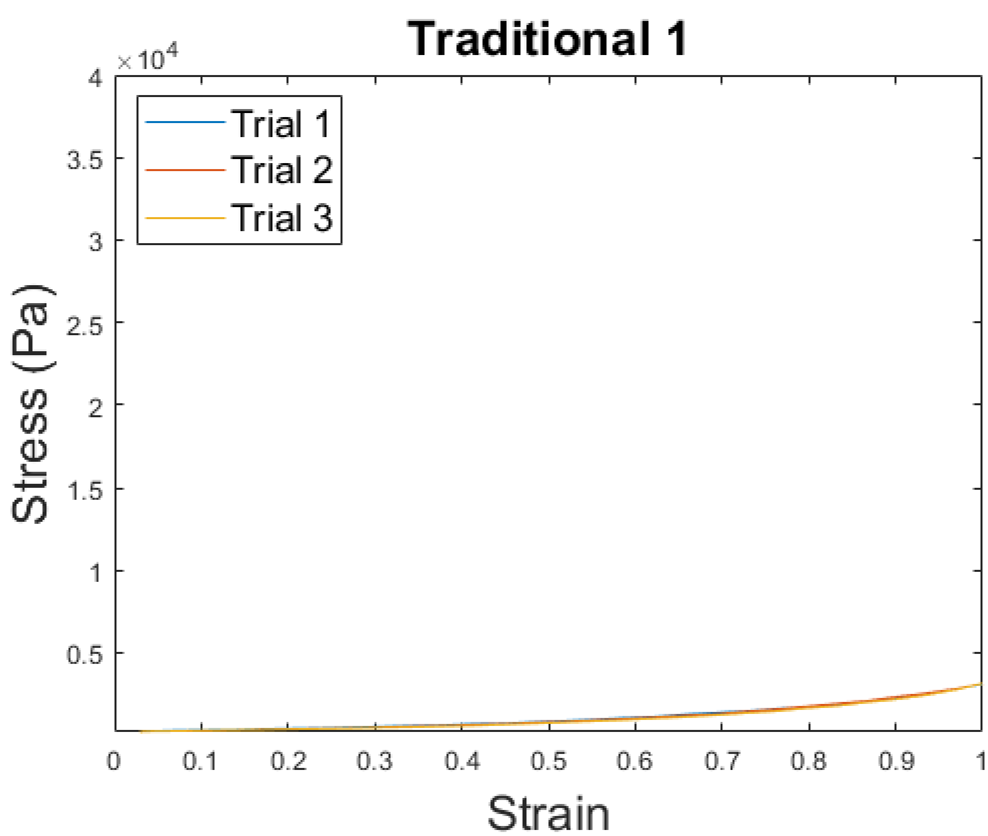

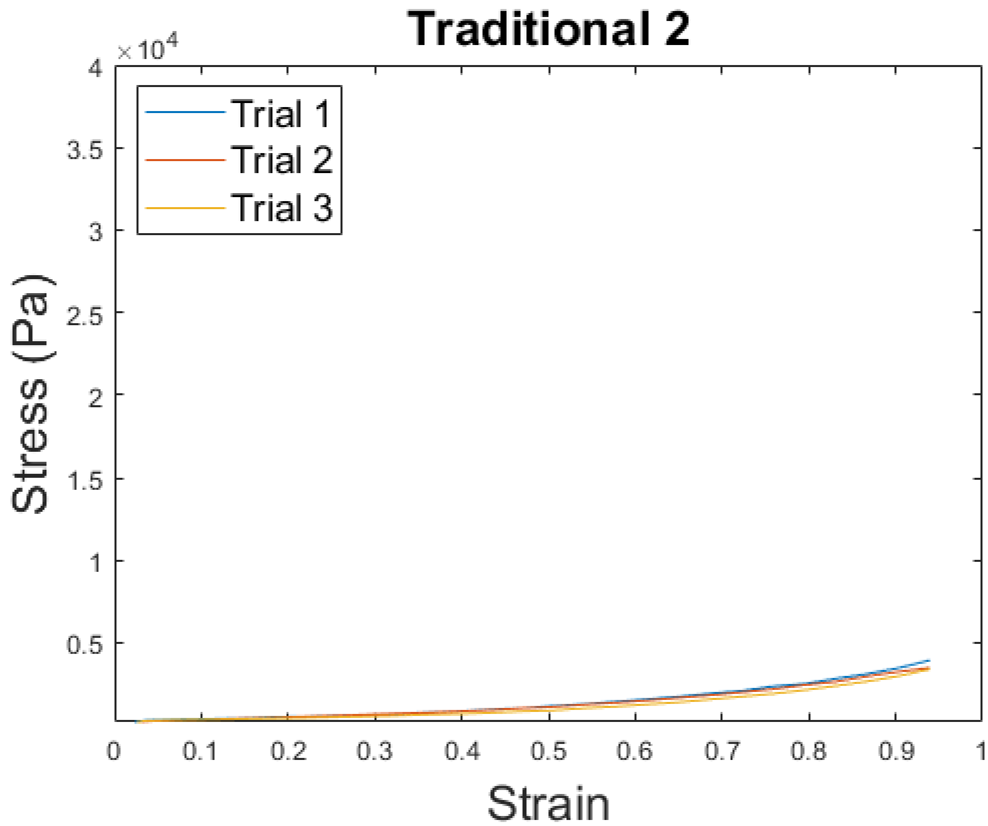
Traditional 2
×10^4
4
3.5
3
2.5
2
1.5
1
0.5
Stress (Pa)
Trial 1
Trial 2
Trial 3
0
0.1
0.2
0.3
0.4
0.5
0.6
0.7
0.8
0.9
1
Strain

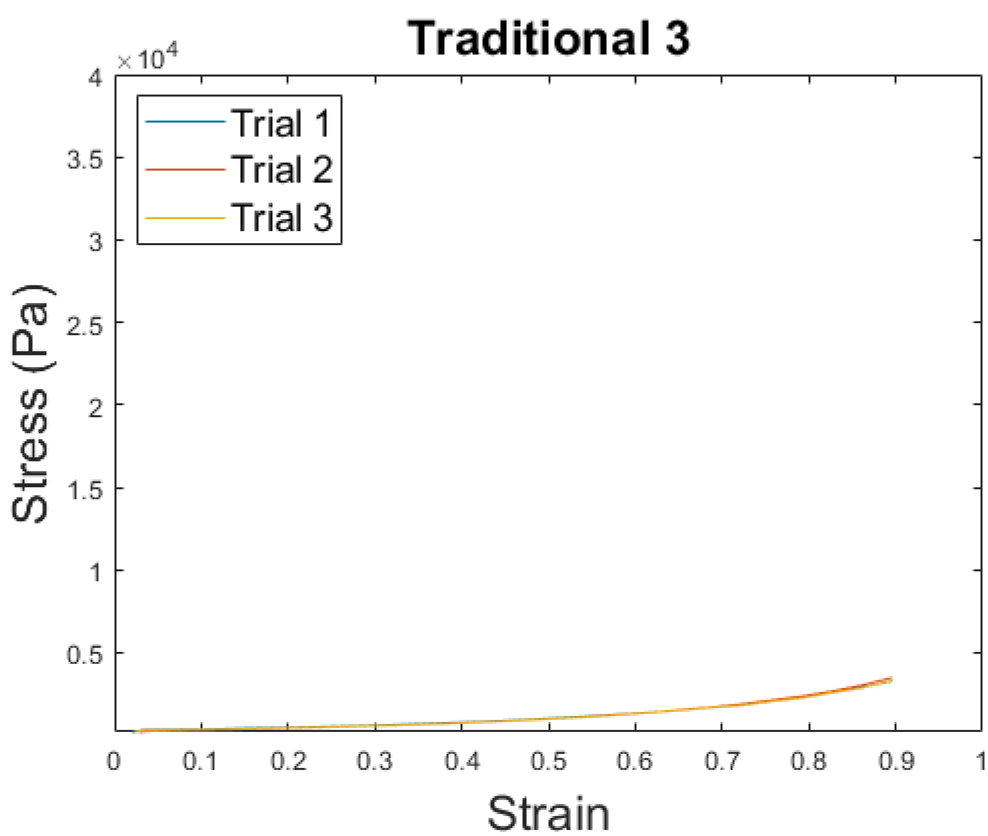
Traditional 3
×10^4
4
3.5
3
2.5
2
1.5
1
0.5
Stress (Pa)
Trial 1
Trial 2
Trial 3
0
0.1
0.2
0.3
0.4
0.5
0.6
0.7
0.8
0.9
1
Strain

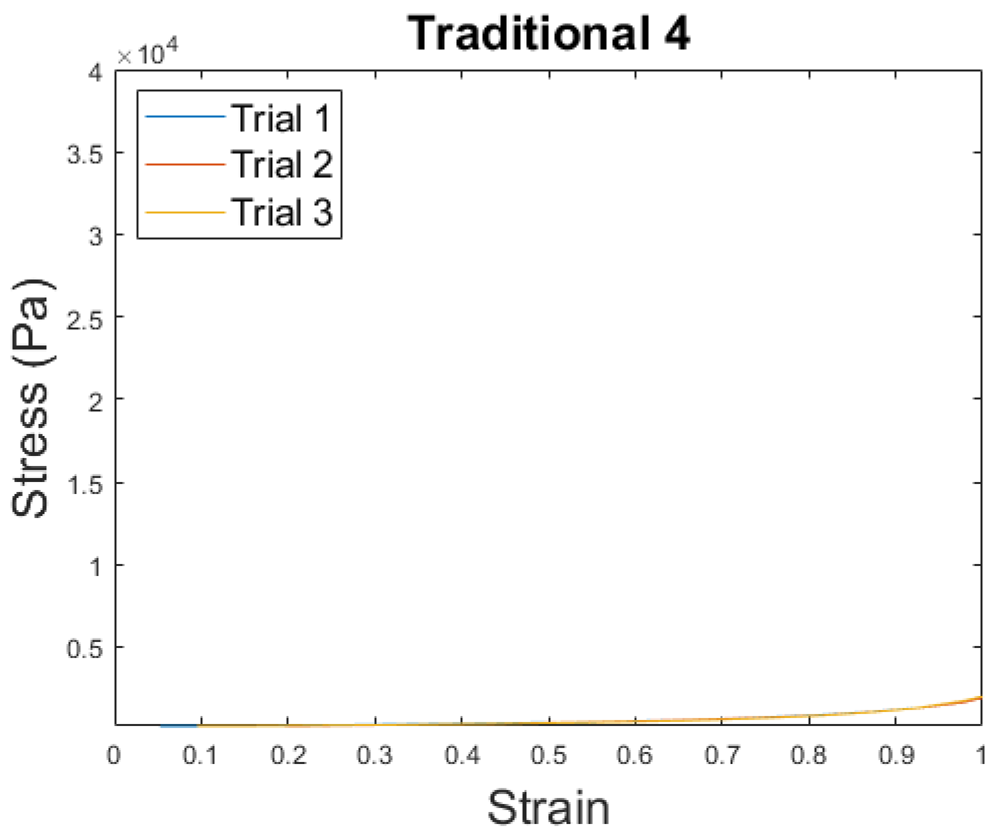
Traditional 4
×10^4
4
3.5
3
2.5
2
1.5
1
0.5
Stress (Pa)
Trial 1
Trial 2
Trial 3
0
0.1
0.2
0.3
0.4
0.5
0.6
0.7
0.8
0.9
1
Strain

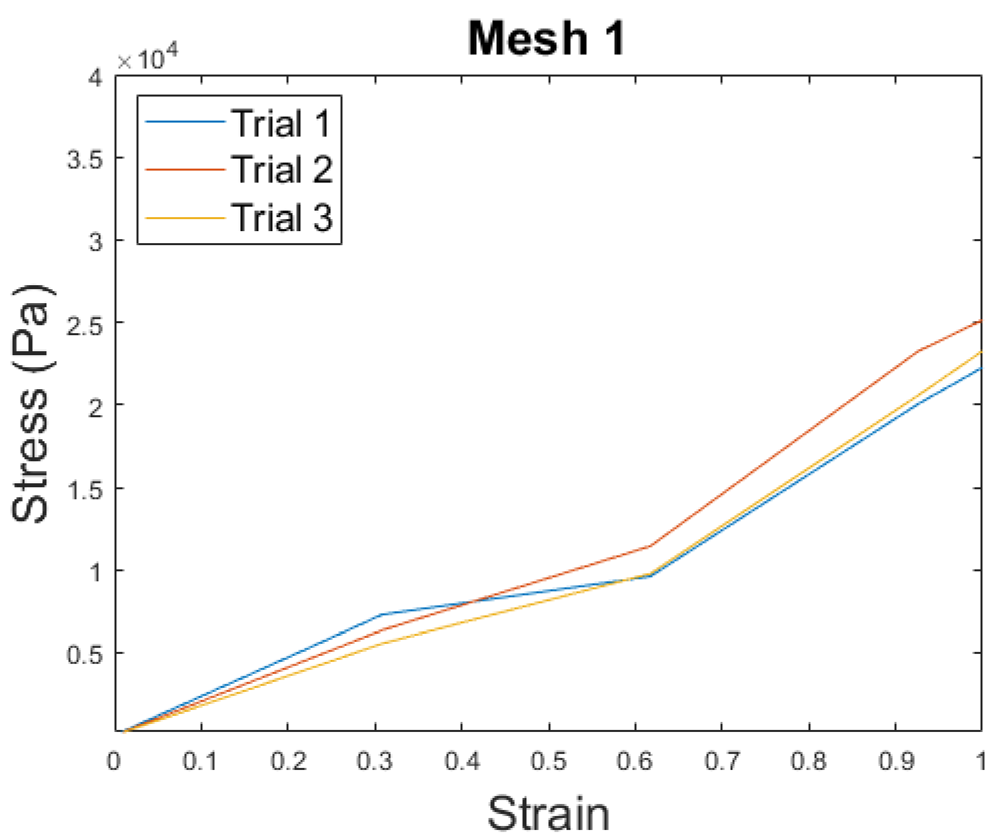
Mesh 1
×10^4
4
3.5
3
2.5
2
1.5
1
0.5
Stress (Pa)
Trial 1
Trial 2
Trial 3
0
0.1
0.2
0.3
0.4
0.5
0.6
0.7
0.8
0.9
1
Strain

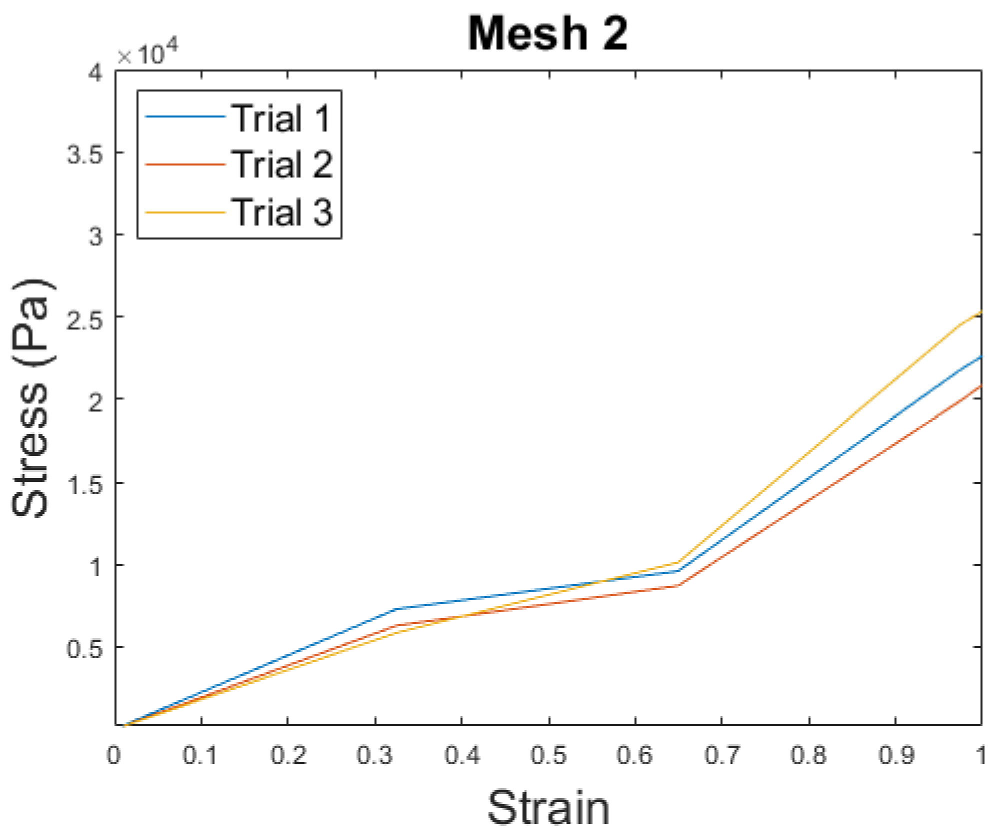

Stress-Strain Plots of Only Traditional Bumpers

```
figure(7)
for i = 1:3
   plot(T1_ep(i,:),T1_s(i,:))
   hold on
end
xlabel('Strain','FontSize',18)
ylabel('Stress (Pa)','FontSize',18)
title('Traditional 1','FontSize',18)
legend('Trial 1','Trial 2','Trial 3','Location','NorthWest','FontSize',14)
ylim([0 4000])
xlim([0 1])

% Stress Strain of Traditional
figure(8)
```

```
for i = 1:3
    plot(T2_ep(i,:),T2_s(i,:))
    hold on
end
xlabel('Strain','FontSize',18)
ylabel('Stress (Pa)','FontSize',18)
title('Traditional 2','FontSize',18)
legend('Trial 1','Trial 2','Trial 3','Location','NorthWest','FontSize',14)
ylim([0 4000])
xlim([0 1])

% Stress Strain of Traditional
figure(9)
for i = 1:3
    plot(T3_ep(i,:),T3_s(i,:))
    hold on
end
xlabel('Strain','FontSize',18)
ylabel('Stress (Pa)','FontSize',18)
title('Traditional 3','FontSize',18)
legend('Trial 1','Trial 2','Trial 3','Location','NorthWest','FontSize',14)
ylim([0 4000])
xlim([0 1])

% Stress Strain of Traditional
figure(10)
for i = 1:3
    plot(T4_ep(i,:),T4_s(i,:))
    hold on
end
xlabel('Strain','FontSize',18)
```

```
ylabel('Stress (Pa)','FontSize',18)
title('Traditional 4','FontSize',18)
legend('Trial 1','Trial 2','Trial 3','Location','NorthWest','FontSize',14)
ylim([0 4000])
xlim([0 1])
```

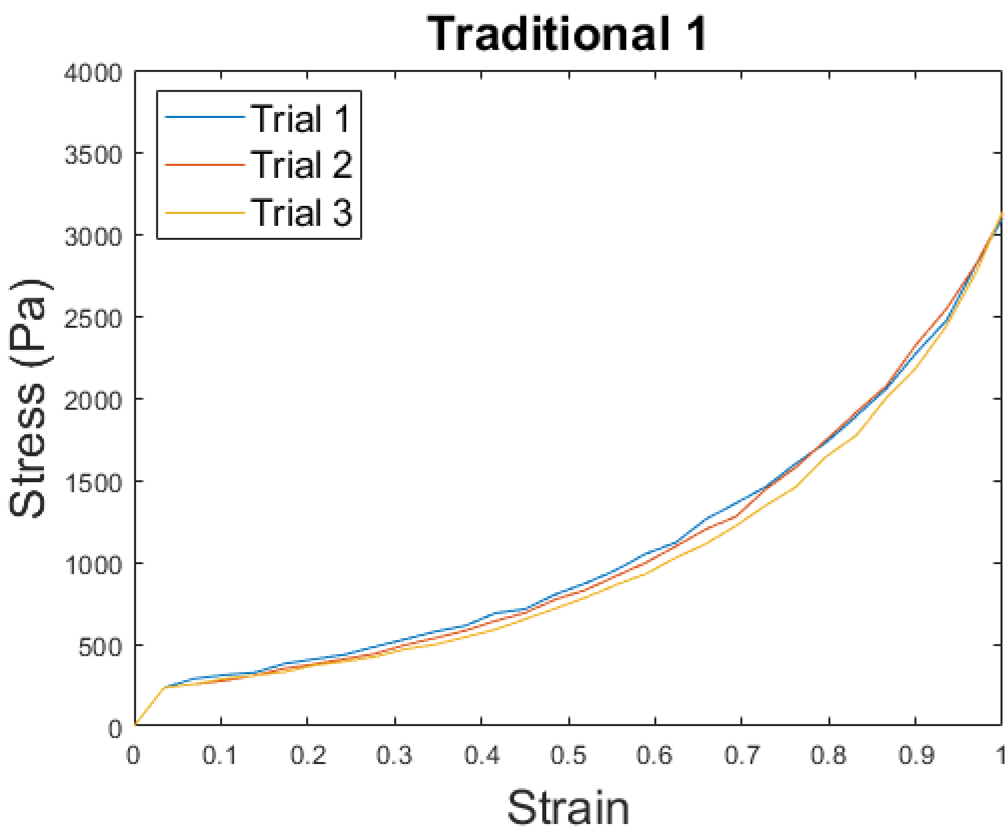

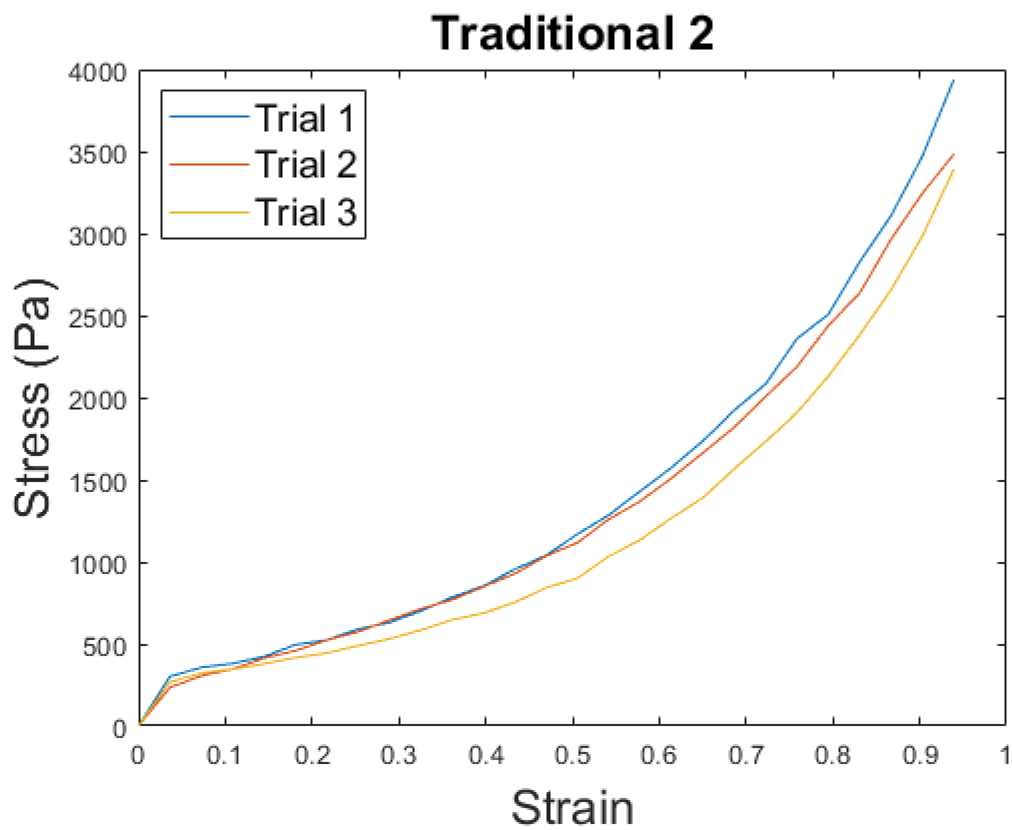
Traditional 2
Trial 1
Trial 2
Trial 3
Stress (Pa)
Strain
0
500
1000
1500
2000
2500
3000
3500
4000
0
0.1
0.2
0.3
0.4
0.5
0.6
0.7
0.8
0.9
1

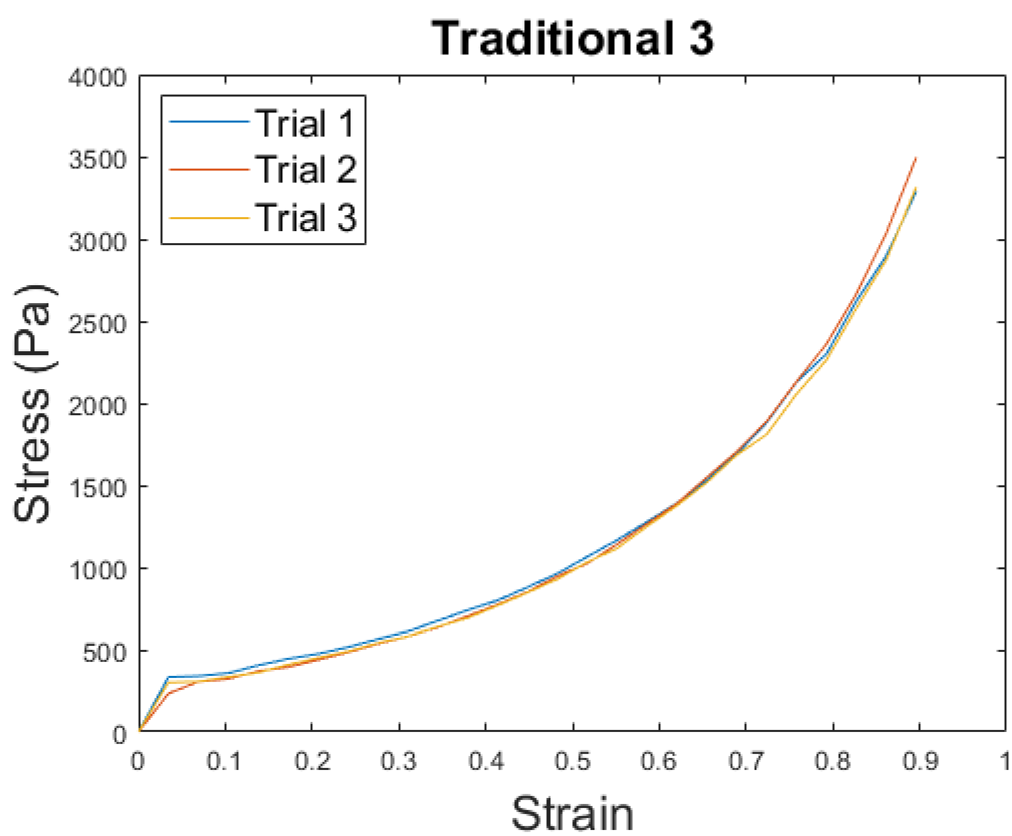
Traditional 3
Trial 1
Trial 2
Trial 3
Stress (Pa)
Strain
0
500
1000
1500
2000
2500
3000
3500
4000
0
0.1
0.2
0.3
0.4
0.5
0.6
0.7
0.8
0.9
1

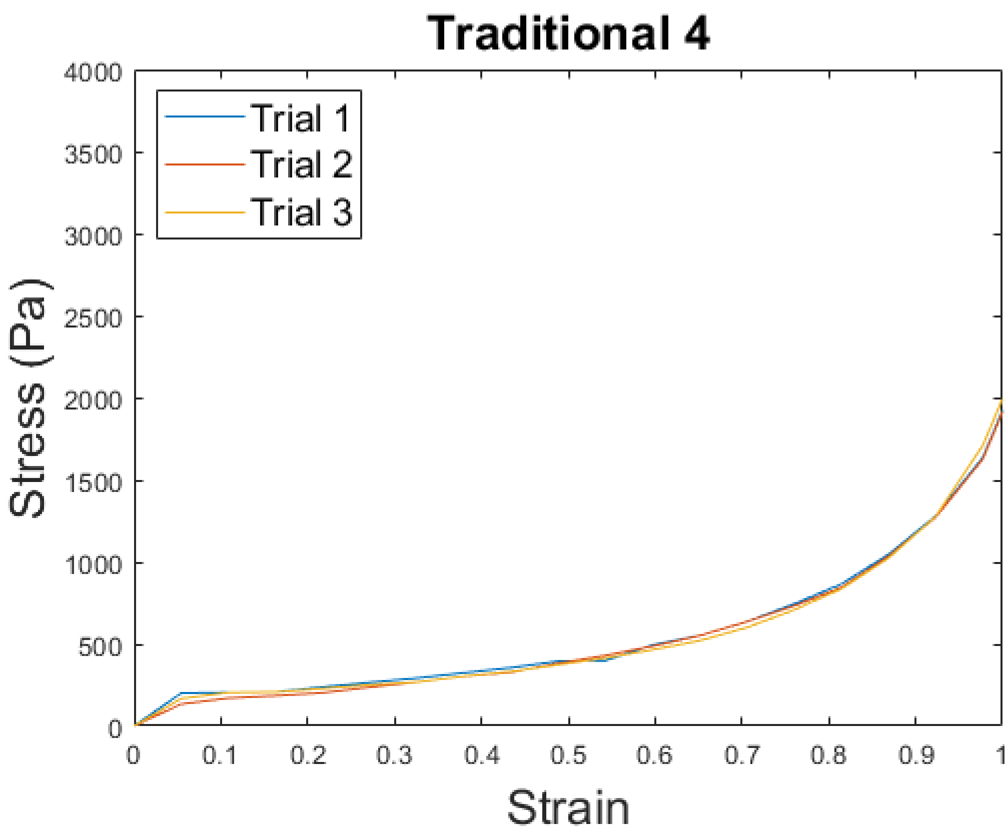

<u>Force vs. Pressure Graph</u>

```
figure(11)
plot(mean(T1_f),mean(T1_p));
hold on
plot(mean(T2_f),mean(T2_p));
hold on
plot(mean(T3_f),mean(T3_p));
hold on
plot(mean(T4_f),mean(T4_p));
hold on
plot(mean(M1_f),mean(M1_p));
hold on
plot(mean(M2_f),mean(M2_p));
xlabel('Force (N)')
ylabel('Pressure Reading (in. H_{2}O)')
```

```
title('Average Applied Force vs. Average Measured Pressure')


legend('T1','T2','T3','T4','M1','M2','Location','East')
xlim([0 20])
xline(2.5,'k--')
```

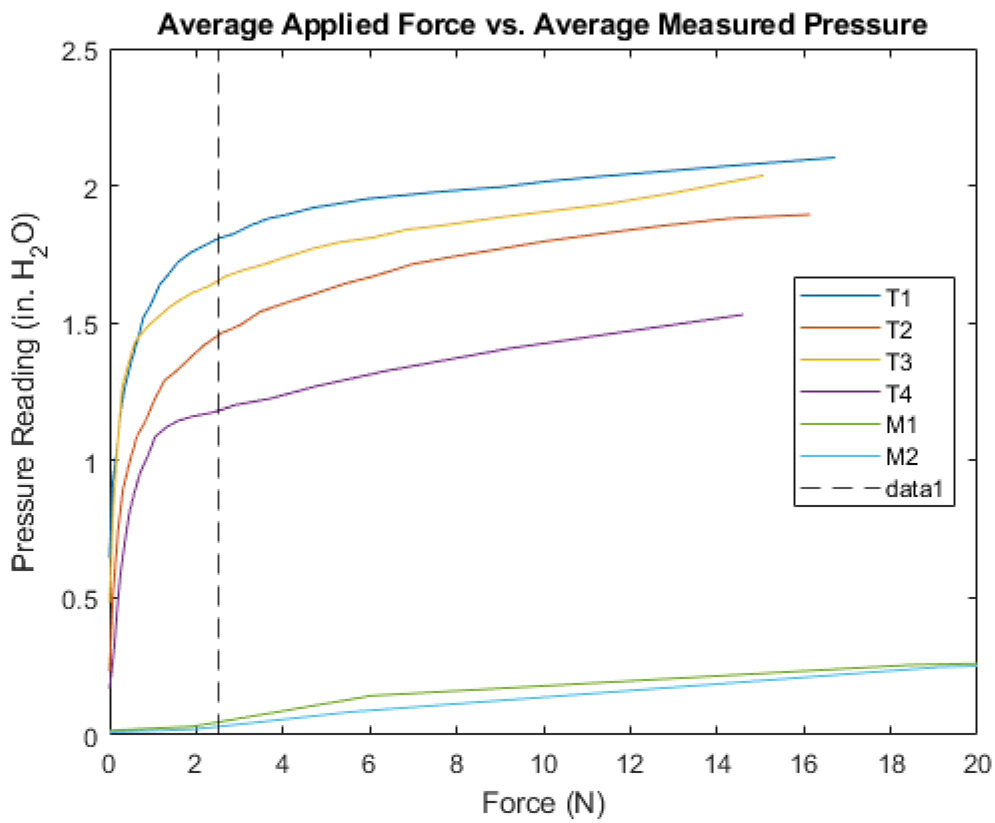

Linear Interpolation of Points on F v. P above 2.5 N of Force for Traditional Bumpers

```
% Average pressure and force over 3 trials


T1_pm = mean(T1_p); T1_fm = mean(T1_f);
T2_pm = mean(T2_p(:,1:27)); T2_fm = mean(T2_f(:,1:27));
T3_pm = mean(T3_p(:,1:27)); T3_fm = mean(T3_f(:,1:27));
T4_pm = mean(T4_p(:,1:21)); T4_fm = mean(T4_f(:,1:21));
```

```
M1_pm = mean(M1_p(:,2:6)); M1_fm = mean(M1_f(:,2:6)); %Range set based on data
recorded. Overload after 6 measurements. Excluding NaNs
M2_pm = mean(M2_p(:,2:5)); M2_fm = mean(M2_f(:,2:5)); %Overload after 5
measurements

%Standard deviations of pressure and force over 3 trials

T1_pst = std(T1_p); T1_fst = std(T1_f);
T2_pst= std(T2_p(:,1:27)); T2_fst = std(T2_f(:,1:27));
T3_pst = std(T3_p(:,1:27)); T3_fst = std(T3_f(:,1:27));
T4_pst = std(T4_p(:,1:21)); T4_fst = std(T4_f(:,1:21));
M1_pst = std(M1_p(:,2:6)); M1_fst = std(M1_f(:,2:6));
M2_pst = std(M2_p(:,2:5)); M2_fst = std(M2_f(:,2:5));

% Average st. dev. of pressure and force for each product

T1_p_av_st = mean(T1_pst); T1_f_av_st = mean(T1_fst);
T2_p_av_st = mean(T2_pst); T2_f_av_st = mean(T2_fst);
T3_p_av_st = mean(T3_pst); T3_f_av_st = mean(T3_fst);
T4_p_av_st = mean(T4_pst); T4_f_av_st = mean(T4_fst);
M1_p_av_st = mean(M1_pst); M1_f_av_st = mean(M1_fst);
M2_p_av_st = mean(M2_pst); M2_f_av_st = mean(M2_fst);

table(T1_p_av_st,T2_p_av_st,T3_p_av_st,T4_p_av_st,M1_p_av_st,M2_p_av_st)
table(T1_f_av_st,T2_f_av_st,T3_f_av_st,T4_f_av_st,M1_f_av_st,M2_f_av_st)

% Plotting linear interpolation

figure(12)
plot(mean(T1_f),mean(T1_p));
hold on
```

```
plot(mean(T2_f),mean(T2_p));
hold on
plot(mean(T3_f),mean(T3_p));
hold on
plot(mean(T4_f),mean(T4_p));
hold on
plot(mean(M1_f),mean(M1_p));
hold on
plot(mean(M2_f),mean(M2_p));
xlabel('Force (N)')
ylabel('Pressure Reading (in. H_{2}O)')
title('Applied Force vs. Measured Pressure')
legend('T1','T2','T3','T4','M1','M2','Location','NorthEast')
xlim([0 20])

% Linear interpolation of starting at 1st recorded force value >= 2 N

p1 = polyfit(T1_fm(find(T1_fm >= 2.5):end),T1_pm(find(T1_fm >= 2.5):end),1);
p2 = polyfit(T2_fm(find(T2_fm >= 2.5):end),T2_pm(find(T2_fm >= 2.5):end),1);
p3 = polyfit(T3_fm(find(T3_fm >= 2.5):end),T3_pm(find(T3_fm >= 2.5):end),1);
p4 = polyfit(T4_fm(find(T4_fm >= 2.5):end),T4_pm(find(T4_fm >= 2.5):end),1);
p5 = polyfit(M1_fm,M1_pm,1);
p6 = polyfit(M2_fm,M2_pm,1);

% Plotting interpolated lines

x1 = linspace(T1_fm(find(T1_fm>=2.5,1)),12);
x2 = linspace(T2_fm(find(T2_fm>=2.5,1)),12);
x3 = linspace(T3_fm(find(T3_fm>=2.5,1)),12);
x4 = linspace(T4_fm(find(T4_fm>=2.5,1)),12);
x5 = linspace(M1_fm(1),M2_fm(end));
```

```
x6 = linspace(M2_fm(1),M2_fm(end));

plot(x1,polyval(p1,x1))
plot(x2,polyval(p2,x2))
plot(x3,polyval(p3,x3))
plot(x4,polyval(p4,x4))
plot(x5,polyval(p5,x5))
plot(x6,polyval(p6,x6))
legend('T1','T2','T3','T4','M1','M2','Int T1 Line','Int T2 Line','Int T3 Line','Int T4 Line','Int
M1 Line','Int M2 Line','Location','East')

%R-squared Calculation

errors = T1_pm(find(T1_fm >= 2.5):end) - polyval(p1,T1_fm(find(T1_fm >= 2.5):end));
%difference between interpolation and
sq_errors = errors.*errors;
ssq = sum(sq_errors); %sum of squared errors
sst = (length(T1_pm(find(T1_fm >= 2.5):end))-1)*var(T1_pm(find(T1_fm >= 2.5):end));
% total sum of squares. The function var returns the variance in the vector y containing
our y data
rsq_T1 = 1 - ssq/sst; % R-squared = 1 - sum of squares/total sum of squares

errors = T2_pm(find(T2_fm >= 2.5):end) - polyval(p2,T2_fm(find(T2_fm >= 2.5):end));
%difference between interpolation and
sq_errors = errors.*errors;
ssq = sum(sq_errors); %sum of squared errors
sst = (length(T2_pm(find(T2_fm >= 2.5):end))-1)*var(T2_pm(find(T2_fm >= 2.5):end));
% total sum of squares. The function var returns the variance in the vector y containing
our y data
rsq_T2 = 1 - ssq/sst; % R-squared = 1 - sum of squares/total sum of squares
```

```
errors = T3_pm(find(T3_fm >= 2.5):end) - polyval(p3,T3_fm(find(T3_fm >= 2.5):end));
%difference between interpolation and
sq_errors = errors.*errors;
ssq = sum(sq_errors); %sum of squared errors
sst = (length(T3_pm(find(T3_fm >= 2.5):end))-1)*var(T3_pm(find(T3_fm >= 2.5):end));
% total sum of squares. The function var returns the variance in the vector y containing
our y data
rsq_T3 = 1 - ssq/sst; % R-squared = 1 - sum of squares/total sum of squares

errors = T4_pm(find(T4_fm >= 2.5):end) - polyval(p4,T4_fm(find(T4_fm >= 2.5):end));
%difference between interpolation and
sq_errors = errors.*errors;
ssq = sum(sq_errors); %sum of squared errors
sst = (length(T4_pm(find(T4_fm >= 2.5):end))-1)*var(T4_pm(find(T4_fm >= 2.5):end));
% total sum of squares. The function var returns the variance in the vector y containing
our y data
rsq_T4 = 1 - ssq/sst; % R-squared = 1 - sum of squares/total sum of squares

errors = M1_pm(find(M1_fm >= 2.5):end) - polyval(p5,M1_fm(find(M1_fm >=
2.5):end)); %difference between interpolation and
sq_errors = errors.*errors;
ssq = sum(sq_errors); %sum of squared errors
sst = (length(M1_pm(find(M1_fm >= 2.5):end))-1)*var(M1_pm(find(M1_fm >=
2.5):end)); % total sum of squares. The function var returns the variance in the vector y
containing our y data
rsq_M1 = 1 - ssq/sst; % R-squared = 1 - sum of squares/total sum of squares

errors = M2_pm(find(M2_fm >= 2.5):end) - polyval(p6,M2_fm(find(M2_fm >=
2.5):end)); %difference between interpolation and
sq_errors = errors.*errors;
ssq = sum(sq_errors); %sum of squared errors
```

```
sst = (length(M2_pm(find(M2_fm >= 2.5):end))-1)*var(M2_pm(find(M2_fm >=
2.5):end)); % total sum of squares. The function var returns the variance in the vector y
containing our y data
rsq_M2 = 1 - ssq/sst; % R-squared = 1 - sum of squares/total sum of squares

% R-squared values for each product

table(rsq_T1,rsq_T2,rsq_T3,rsq_T4,rsq_M1,rsq_M2)
```

```
ans =
  1×6 table
    T1_p_av_st    T2_p_av_st    T3_p_av_st    T4_p_av_st    M1_p_av_st    M2_p_av_st
    __________    __________    __________    __________    __________    __________
     0.048037      0.077585      0.085608      0.070867      0.019455      0.02163
ans =
  1×6 table
    T1_f_av_st    T2_f_av_st    T3_f_av_st    T4_f_av_st    M1_f_av_st    M2_f_av_st
    __________    __________    __________    __________    __________    __________
     0.15976       0.44974      0.093653      0.090574      0.85759       1.1016
ans =
  1×6 table
    rsq_T1     rsq_T2     rsq_T3     rsq_T4     rsq_M1     rsq_M2
    _______    _______    _______    _______    _______    _______
    0.93534    0.92799    0.97654    0.98828    0.77686    0.90343
```

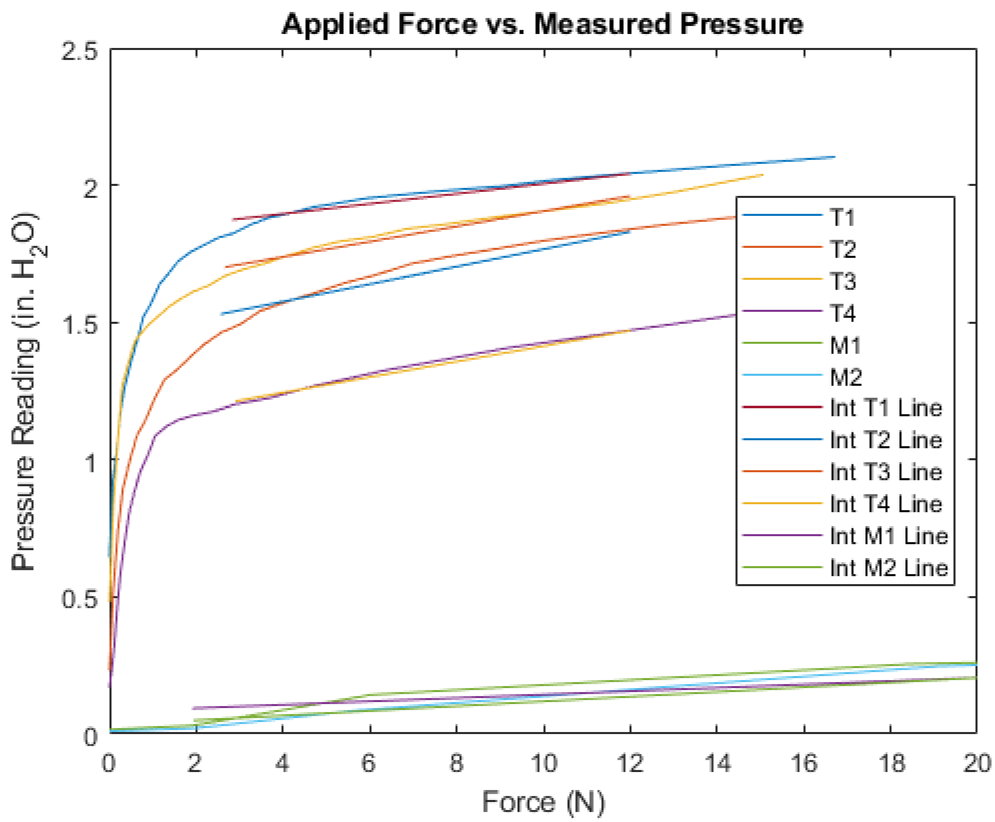

Linear Interpolation of Points on F v. P below 1 N of Force for Traditional Bumpers

```
% Force vs. Pressure Graph
figure(13)
plot(mean(T1_f),mean(T1_p));
hold on
plot(mean(T2_f),mean(T2_p));
hold on
plot(mean(T3_f),mean(T3_p));
hold on
plot(mean(T4_f),mean(T4_p));
hold on
plot(mean(M1_f),mean(M1_p));
hold on
```

```
plot(mean(M2_f),mean(M2_p));
xlabel('Force (N)')
ylabel('Pressure Reading (in. H_{2}O)')
title('Applied Force vs. Measured Pressure')
legend('T1','T2','T3','T4','M1','M2','Location','NorthEast')
xlim([0 20])

% Average pressure and force over 3 trials

T1_pm = mean(T1_p); T1_fm = mean(T1_f);
T2_pm = mean(T2_p); T2_fm = mean(T2_f);
T3_pm = mean(T3_p); T3_fm = mean(T3_f);
T4_pm = mean(T4_p); T4_fm = mean(T4_f);
M1_pm = mean(M1_p(:,1:6)); M1_fm = mean(M1_f(:,1:6)); %Range set based on data
recorded. Overload after 6 measurements. Excluding NaNs
M2_pm = mean(M2_p(:,1:5)); M2_fm = mean(M2_f(:,1:5)); %Overload after 5
measurements

% Linear interpolation of starting at 1st recorded force value <= 1 N

p1 = polyfit(T1_fm(find(T1_fm <= 1)),T1_pm(find(T1_fm <= 1)),1);
p2 = polyfit(T2_fm(find(T2_fm <= 1)),T2_pm(find(T2_fm <= 1)),1);
p3 = polyfit(T3_fm(find(T3_fm<= 1)),T3_pm(find(T3_fm <= 1)),1);
p4 = polyfit(T4_fm(find(T4_fm <= 1)),T4_pm(find(T4_fm <= 1)),1);
p5 = polyfit(M1_fm,M1_pm,1);
p6 = polyfit(M2_fm,M2_pm,1);

% Plotting interpolated lines

x1 = linspace(T1_fm(find(T1_fm<= 1,1)),1);
x2 = linspace(T2_fm(find(T2_fm<= 1,1)),1);
```

```
x3 = linspace(T3_fm(find(T3_fm<= 1,1)),1);
x4 = linspace(T4_fm(find(T4_fm<= 1,1)),1);
x5 = linspace(M1_fm(1),M2_fm(end));
x6 = linspace(M2_fm(1),M2_fm(end));

plot(x1,polyval(p1,x1))
plot(x2,polyval(p2,x2))
plot(x3,polyval(p3,x3))
plot(x4,polyval(p4,x4))
plot(x5,polyval(p5,x5))
plot(x6,polyval(p6,x6))
legend('T1','T2','T3','T4','M1','M2','Int T1 Line','Int T2 Line','Int T3 Line','Int T4 Line','Int
M1 Line','Int M2 Line')

%R-squared Calculation

errors = T1_pm(find(T1_fm <= 1)) - polyval(p1,T1_fm(find(T1_fm <= 1))); %difference
between interpolation and
sq_errors = errors.*errors;
ssq = sum(sq_errors); %sum of squared errors
sst = (length(T1_pm(find(T1_fm <= 1)))-1)*var(T1_pm(find(T1_fm <= 1))); % total sum
of squares. The function var returns the variance in the vector y containing our y data
rsq_T1 = 1 - ssq/sst; % R-squared = 1 - sum of squares/total sum of squares

errors = T2_pm(find(T2_fm <= 1)) - polyval(p2,T2_fm(find(T2_fm <= 1))); %difference
between interpolation and
sq_errors = errors.*errors;
ssq = sum(sq_errors); %sum of squared errors
sst = (length(T2_pm(find(T2_fm <= 1)))-1)*var(T2_pm(find(T2_fm <= 1))); % total sum
of squares. The function var returns the variance in the vector y containing our y data
rsq_T2 = 1 - ssq/sst; % R-squared = 1 - sum of squares/total sum of squares
```

```
errors = T3_pm(find(T3_fm <= 1)) - polyval(p3,T3_fm(find(T3_fm <= 1))); %difference
between interpolation and
sq_errors = errors.*errors;
ssq = sum(sq_errors); %sum of squared errors
sst = (length(T3_pm(find(T3_fm <= 1)))-1)*var(T3_pm(find(T3_fm <= 1))); % total sum
of squares. The function var returns the variance in the vector y containing our y data
rsq_T3 = 1 - ssq/sst; % R-squared = 1 - sum of squares/total sum of squares

errors = T4_pm(find(T4_fm <= 1)) - polyval(p4,T4_fm(find(T4_fm <= 1))); %difference
between interpolation and
sq_errors = errors.*errors;
ssq = sum(sq_errors); %sum of squared errors
sst = (length(T4_pm(find(T4_fm <= 1)))-1)*var(T4_pm(find(T4_fm <= 1))); % total sum
of squares. The function var returns the variance in the vector y containing our y data
rsq_T4 = 1 - ssq/sst; % R-squared = 1 - sum of squares/total sum of squares

errors = M1_pm - polyval(p5,M1_fm); %difference between interpolation and
sq_errors = errors.*errors;
ssq = sum(sq_errors); %sum of squared errors
sst = (length(M1_pm)-1)*var(M1_pm); % total sum of squares. The function var returns
the variance in the vector y containing our y data
rsq_M1 = 1 - ssq/sst; % R-squared = 1 - sum of squares/total sum of squares

errors = M2_pm - polyval(p6,M2_fm); %difference between interpolation and
sq_errors = errors.*errors;
ssq = sum(sq_errors); %sum of squared errors
sst = (length(M2_pm)-1)*var(M2_pm); % total sum of squares. The function var returns
the variance in the vector y containing our y data
rsq_M2 = 1 - ssq/sst; % R-squared = 1 - sum of squares/total sum of squares
```

```
% R-squared values for each product

table(rsq_T1,rsq_T2,rsq_T3,rsq_T4,rsq_M1,rsq_M2)
```

ans =

1×6 table

rsq_T1	rsq_T2	rsq_T3	rsq_T4	rsq_M1	rsq_M2
0.88557	0.85002	0.76674	0.93114	0.87978	0.94884

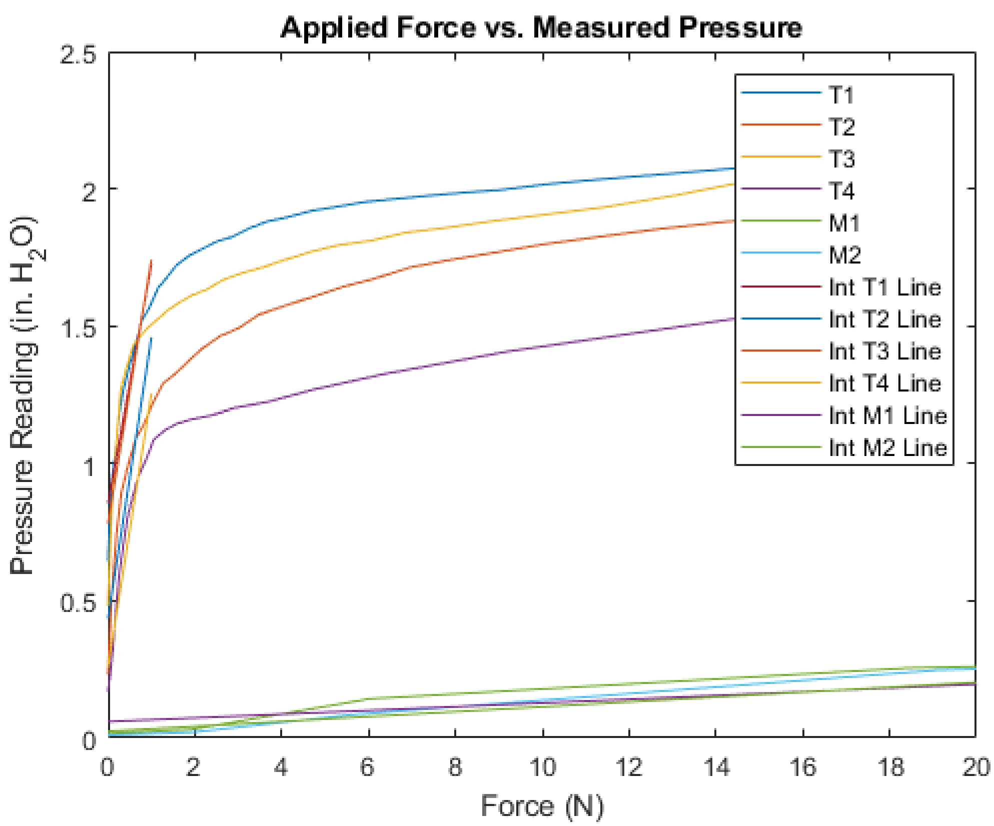

Published with MATLAB® R2020a

APPENDIX H

Stress Relaxation Calculation Code

Stress Relaxation Testing

Created by Wyatt Davis

```
clc;clear;
```

File Import

```
Sheet = ["Trad 1_1" "Trad 1_2" "Trad 1_3" ...
    "Trad 2_1" "Trad 2_2" "Trad 2_3"...
    "Trad 3_1" "Trad 3_2" "Trad 3_3" ...
    "Trad 4_1" "Trad 4_2" "Trad 4_3" ...
    "Mesh 1_1" "Mesh 1_2" "Mesh 1_3"...
    "Mesh 2_1" "Mesh 2_2" "Mesh 2_3"];

for i = 1:length(Sheet)
    opts = spreadsheetImportOptions("NumVariables", 6);

    % Specify sheet and range
    opts.Sheet = Sheet(i);
    opts.DataRange = "A7:F1000";

    % Specify column names and types
    opts.VariableNames = ["Recording", "Time", "Force", "Recording2", "Time2",
"Force2"];
    opts.VariableTypes = ["double", "double", "string", "double", "double", "string"];

    % Specify file level properties
    opts.ImportErrorRule = "error";

    % Specify variable properties
    opts = setvaropts(opts, ["Force", "Force2"], "WhitespaceRule", "preserve");
```

```
    opts = setvaropts(opts, ["Force", "Force2"], "EmptyFieldRule", "auto");
    opts = setvaropts(opts, ["Recording", "Time", "Recording2", "Time2"],
"TreatAsMissing", ");

    % Import the data
    TestData = readtable("C:\Users\davis\Downloads\TestData1.xlsx", opts, "UseExcel",
false);

    time = vertcat(TestData.Time,TestData.Time2);
    force = str2double(vertcat(TestData.Force,TestData.Force2));

    range = 0;
    for j = 1:length(time)
        if ~isnan(force(j))
            range = [range j];
        end
    end
    time = time(range(2:end));
    force = force(range(2:end));

    %start = find(force==min(force));
    %time = time(start:end)-time(start); force = -force(start:end);

    if Sheet(i) == "Trad 1_1"
        T11 = [time -force];
    elseif Sheet(i) == "Trad 1_2"
        T12 = [time -force];
    elseif Sheet(i) == "Trad 1_3"
        T13 = [time -force];
    elseif Sheet(i) == "Trad 2_1"
        T21 = [time -force];
```

```
    elseif Sheet(i) == "Trad 2_2"
        T22 = [time -force];
    elseif Sheet(i) == "Trad 2_3"
        T23 = [time -force];
    elseif Sheet(i) == "Trad 3_1"
        T31 = [time -force];
    elseif Sheet(i) == "Trad 3_2"
        T32 = [time -force];
    elseif Sheet(i) == "Trad 3_3"
        T33 = [time -force];
    elseif Sheet(i) == "Trad 4_1"
        T41 = [time -force];
    elseif Sheet(i) == "Trad 4_2"
        T42 = [time -force];
    elseif Sheet(i) == "Trad 4_3"
        T43 = [time -force];
    elseif Sheet(i) == "Mesh 1_1"
        M11 = [time -force];
    elseif Sheet(i) == "Mesh 1_2"
        M12 = [time -force];
    elseif Sheet(i) == "Mesh 1_3"
        M13 = [time -force];
    elseif Sheet(i) == "Mesh 2_1"
        M21 = [time -force];
    elseif Sheet(i) == "Mesh 2_2"
        M22 = [time -force];
    elseif Sheet(i) == "Mesh 2_3"
        M23 = [time -force];
    end

end
```

Percentage of Original Force at End of Test

```
T1_avg_end_force = mean([T11(end,2)/max(T11(:,2)),
T12(end,2)/max(T12(:,2)),T13(end,2)/max(T13(:,2))]);
T2_avg_end_force = mean([T21(end,2)/max(T21(:,2)),
T22(end,2)/max(T22(:,2)),T23(end,2)/max(T23(:,2))]);
T3_avg_end_force = mean([T31(end,2)/max(T31(:,2)),
T32(end,2)/max(T32(:,2)),T33(end,2)/max(T33(:,2))]);
T4_avg_end_force = mean([T41(end,2)/max(T41(:,2)),
T42(end,2)/max(T42(:,2)),T43(end,2)/max(T43(:,2))]);
M1_avg_end_force = mean([M11(end,2)/max(M11(:,2)),
M12(end,2)/max(M12(:,2)),M13(end,2)/max(M13(:,2))]);
M2_avg_end_force = mean([M21(end,2)/max(M21(:,2)),
M22(end,2)/max(M22(:,2)),M23(end,2)/max(M23(:,2))]);

table(T1_avg_end_force,T2_avg_end_force,T3_avg_end_force,T4_avg_end_force,M1_a
vg_end_force,M2_avg_end_force)

Average_Traditional_End_Force_Percent = mean([T11(end,2)/max(T11(:,2)),
T12(end,2)/max(T12(:,2)),T13(end,2)/max(T13(:,2)),...
    T21(end,2)/max(T21(:,2)), T22(end,2)/max(T22(:,2)),T23(end,2)/max(T23(:,2)),...
    T31(end,2)/max(T31(:,2)), T32(end,2)/max(T32(:,2)),T33(end,2)/max(T33(:,2)),...
    T41(end,2)/max(T41(:,2)), T42(end,2)/max(T42(:,2)),T43(end,2)/max(T43(:,2))]);

Traditional_StDev_End_Force_Percent = std([T11(end,2)/max(T11(:,2)),
T12(end,2)/max(T12(:,2)),T13(end,2)/max(T13(:,2)),...
    T21(end,2)/max(T21(:,2)), T22(end,2)/max(T22(:,2)),T23(end,2)/max(T23(:,2)),...
    T31(end,2)/max(T31(:,2)), T32(end,2)/max(T32(:,2)),T33(end,2)/max(T33(:,2)),...
    T41(end,2)/max(T41(:,2)), T42(end,2)/max(T42(:,2)),T43(end,2)/max(T43(:,2))]);

Average_Mesh_End_Force_Percent = mean([M11(end,2)/max(M11(:,2)),
```

```
M12(end,2)/max(M12(:,2)),M13(end,2)/max(M13(:,2)),...
   M21(end,2)/max(M21(:,2)), M22(end,2)/max(M22(:,2)),M23(end,2)/max(M23(:,2))]);

Mesh_StDev_End_Force_Percent = std([M11(end,2)/max(M11(:,2)),
M12(end,2)/max(M12(:,2)),M13(end,2)/max(M13(:,2)),...
   M21(end,2)/max(M21(:,2)), M22(end,2)/max(M22(:,2)),M23(end,2)/max(M23(:,2))]);

table(Average_Traditional_End_Force_Percent,Traditional_StDev_End_Force_Percent,
Average_Mesh_End_Force_Percent,Mesh_StDev_End_Force_Percent)
```

```
ans =
  1×6 table
   T1_avg_end_force    T2_avg_end_force    T3_avg_end_force    T4_avg_end_force
M1_avg_end_force    M2_avg_end_force
   ________________    ________________    ________________    ________________
________________    ________________
       0.90497          0.92118           0.9019          0.89815          0.85441
0.84269
ans =
  1×4 table
   Average_Traditional_End_Force_Percent    Traditional_StDev_End_Force_Percent
Average_Mesh_End_Force_Percent    Mesh_StDev_End_Force_Percent
   _____________________________________
___________________________________    ________________________________
______________________________
              0.90655                        0.020641                        0.84855
0.015838
```

Stress Relaxation Calculations and Filtering

```
disp = 0.0254*[mean([1.35,1.322,1.238]) mean([1.138,1.224,1.12])
mean([1.229,1.27,1.202]) mean([0.977,0.979,0.972]) .15 .15]; % Average displacements
```

```
for 10 N of force for traditional bumpers, mesh displacement ~.15in
r = 1.5*0.0254; %radius of hemisphere, meters
d = r - disp;
for i = 1:length(d)
    if d(i) >= 0
        c(i) = 2*sqrt(r^2-d(i)^2); %calculated chord length + assumed original
        Ax(i) = pi*(c(i)/2)^2; % cross-sectional area applied to products
    else
        Ax(i) = pi*r^2; % Maximum cross-sectional area
    end
end

T11_s = T11(:,2)/Ax(1); T12_s = T12(:,2)/Ax(1); T13_s = T13(:,2)/Ax(1);
T21_s = T21(:,2)/Ax(2); T22_s = T22(:,2)/Ax(2); T23_s = T23(:,2)/Ax(2);
T31_s = T31(:,2)/Ax(3); T32_s = T32(:,2)/Ax(3); T33_s = T33(:,2)/Ax(3);
T41_s = T41(:,2)/Ax(4); T42_s = T42(:,2)/Ax(4); T43_s = T43(:,2)/Ax(4);
M11_s = M11(:,2)/Ax(5); M12_s = M12(:,2)/Ax(5); M13_s = M13(:,2)/Ax(5);
M21_s = M21(:,2)/Ax(6); M22_s = M22(:,2)/Ax(6); M23_s = M23(:,2)/Ax(6);

%Filtering of data to exclude sudden spikes

df = diff(T11_s(find(T11_s==max(T11_s)):end));
k = 1;
for j = 4:length(df)
    if abs(df(j)) > 50
        T11_s(find(T11_s==max(T11_s))+j+1) = "NaN";
    end
end

df = diff(T12_s(find(T12_s==max(T12_s)):end));
k = 1;
```

```
for j = 4:length(df)
    if abs(df(j)) > 50
        T12_s(find(T12_s==max(T12_s))+j+1) = "NaN";
    end
end

df = diff(T13_s(find(T13_s==max(T13_s)):end));
k = 1;
for j = 4:length(df)
    if abs(df(j)) > 50
        T13_s(find(T13_s==max(T13_s))+j+1) = "NaN";
    end
end

df = diff(T21_s(find(T21_s==max(T21_s)):end));
k = 1;
for j = 4:length(df)
    if abs(df(j)) > 50
        T21_s(find(T21_s==max(T21_s))+j+1) = "NaN";
    end
end

df = diff(T22_s(find(T22_s==max(T22_s)):end));
k = 1;
for j = 4:length(df)
    if abs(df(j)) > 50
        T22_s(find(T22_s==max(T22_s))+j+1) = "NaN";
    end
end

df = diff(T23_s(find(T23_s==max(T23_s)):end));
```

```
k = 1;
for j = 4:length(df)
    if abs(df(j)) > 50
        T23_s(find(T23_s==max(T23_s))+j+1) = "NaN";
    end
end

df = diff(T31_s(find(T31_s==max(T31_s)):end));
k = 1;
for j = 4:length(df)
    if abs(df(j)) > 50
        T31_s(find(T31_s==max(T31_s))+j+1) = "NaN";
    end
end

df = diff(T32_s(find(T32_s==max(T32_s)):end));
k = 1;
for j = 4:length(df)
    if abs(df(j)) > 50
        T32_s(find(T32_s==max(T32_s))+j+1) = "NaN";
    end
end

df = diff(T33_s(find(T33_s==max(T33_s)):end));
k = 1;
for j = 4:length(df)
    if abs(df(j)) > 50
        T33_s(find(T33_s==max(T33_s))+j+1) = "NaN";
    end
end
```

```
df = diff(T41_s(find(T41_s==max(T41_s)):end));
k = 1;
for j = 4:length(df)
    if abs(df(j)) > 50
        T41_s(find(T41_s==max(T41_s))+j+1) = "NaN";
    end
end

df = diff(T42_s(find(T42_s==max(T42_s)):end));
k = 1;
for j = 4:length(df)
    if abs(df(j)) > 50
        T42_s(find(T42_s==max(T42_s))+j+1) = "NaN";
    end
end

df = diff(T43_s(find(T43_s==max(T43_s)):end));
k = 1;
for j = 4:length(df)
    if abs(df(j)) > 50
        T43_s(find(T43_s==max(T43_s))+j+1) = "NaN";
    end
end

df = diff(M11_s(find(M11_s==max(M11_s)):end));
k = 1;
for j = 4:length(df)
    if abs(df(j)) > 50
        M11_s(find(M11_s==max(M11_s))+j+1) = "NaN";
    end
end
```

```
df = diff(M12_s(find(M12_s==max(M12_s)):end));
k = 1;
for j = 4:length(df)
   if abs(df(j)) > 50
      M12_s(find(M12_s==max(M12_s))+j+1) = "NaN";
   end
end

df = diff(M13_s(find(M13_s==max(M13_s)):end));
k = 1;
for j = 4:length(df)
   if abs(df(j)) > 50
      M13_s(find(M13_s==max(M13_s))+j+1) = "NaN";
   end
end

df = diff(M21_s(find(M21_s==max(M21_s)):end));
k = 1;
for j = 4:length(df)
   if abs(df(j)) > 50
      M21_s(find(M21_s==max(M21_s))+j+1) = "NaN";
   end
end

df = diff(M22_s(find(M22_s==max(M22_s)):end));
k = 1;
for j = 4:length(df)
   if abs(df(j)) > 50
      M22_s(find(M22_s==max(M22_s))+j+1) = "NaN";
   end
```

```
end

df = diff(M23_s(find(M23_s==max(M23_s)):end));
k = 1;
for j = 4:length(df)
    if abs(df(j)) > 50
        M23_s(find(M23_s==max(M23_s))+j+1) = "NaN";
    end
end
```

Plotting of stress relaxation for all products

```
figure(1)
plot(T11(:,1),T11_s/max(T11_s));
hold on;
plot(T12(:,1),T12_s/max(T12_s));
plot(T13(:,1),T13_s/max(T13_s));
xlabel('Time (s)','FontSize',18)
ylabel('Percent of Max Stress','FontSize',18)
title('Traditional 1','FontSize',18)
legend('Trial 1','Trial 2','Trial 3','Location','SouthEast','FontSize',14)
xlim([0 70])
ylim([0 1.1])

figure(2)
plot(T21(:,1),T21_s/max(T21_s));
hold on;
plot(T22(:,1),T22_s/max(T22_s));
plot(T23(:,1),T23_s/max(T23_s));
xlabel('Time (s)','FontSize',18)
ylabel('Percent of Max Stress','FontSize',18)
```

```
title('Traditional 2','FontSize',18)
legend('Trial 1','Trial 2','Trial 3','Location','SouthEast','FontSize',14)
xlim([0 70])
ylim([0 1.1])

figure(3)
plot(T31(:,1),T31_s/max(T31_s));
hold on;
plot(T32(:,1),T32_s/max(T32_s));
plot(T33(:,1),T33_s/max(T33_s));
xlabel('Time (s)','FontSize',18)
ylabel('Percent of Max Stress','FontSize',18)
title('Traditional 3','FontSize',18)
legend('Trial 1','Trial 2','Trial 3','Location','SouthEast','FontSize',14)
xlim([0 70])
ylim([0 1.1])

figure(4)
plot(T41(:,1),T41_s/max(T41_s));
hold on;
plot(T42(:,1),T42_s/max(T42_s));
plot(T43(:,1),T43_s/max(T43_s))
xlabel('Time (s)','FontSize',18)
ylabel('Percent of Max Stress','FontSize',18)
title('Traditional 4','FontSize',18)
legend('Trial 1','Trial 2','Trial 3','Location','SouthEast','FontSize',14)
xlim([0 70])
ylim([0 1.1])

figure(5)
plot(M11(:,1),M11_s/max(M11_s));
```

```
hold on;
plot(M12(:,1),M12_s/max(M12_s));
plot(M13(:,1),M13_s/max(M13_s))
xlabel('Time (s)','FontSize',18)
ylabel('Percent of Max Stress','FontSize',18)
title('Mesh 1','FontSize',18)
legend('Trial 1','Trial 2','Trial 3','Location','SouthEast','FontSize',14)
xlim([0 70])
ylim([0 1.1])

figure(6)
plot(M21(:,1),M21_s/max(M21_s));
hold on;
plot(M22(:,1),M22_s/max(M22_s));
plot(M23(:,1),M23_s/max(M23_s))
xlabel('Time (s)','FontSize',18)
ylabel('Percent of Max Stress','FontSize',18)
title('Mesh 2','FontSize',18)
legend('Trial 1','Trial 2','Trial 3','Location','SouthEast','FontSize',14)
xlim([0 70])
ylim([0 1.1])
```

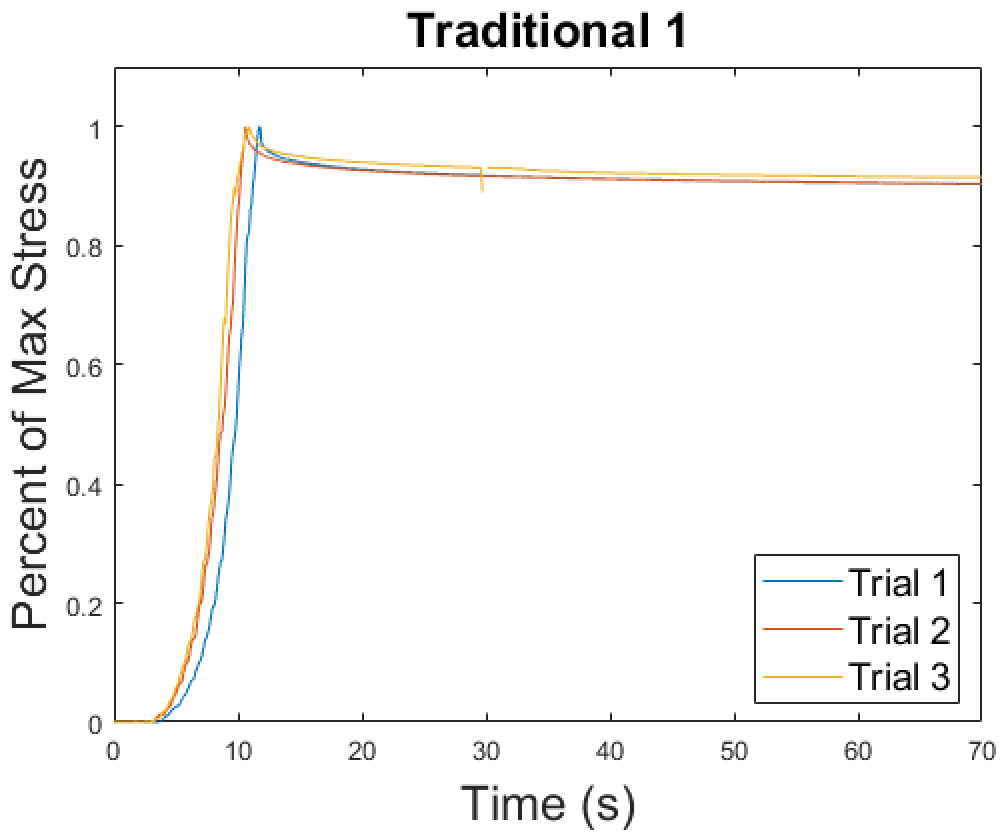
Traditional 1
Percent of Max Stress
Time (s)
0
0.2
0.4
0.6
0.8
1
0
10
20
30
40
50
60
70
Trial 1
Trial 2
Trial 3

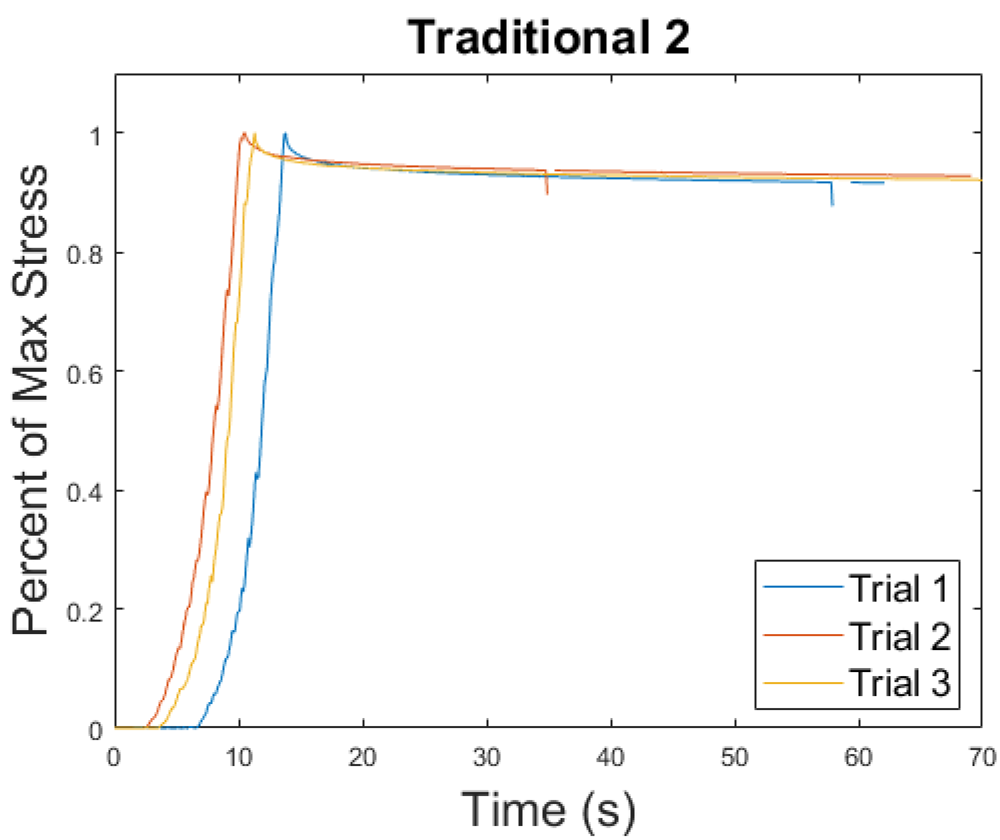
Traditional 2
Percent of Max Stress
Time (s)
0
0.2
0.4
0.6
0.8
1
0
10
20
30
40
50
60
70
Trial 1
Trial 2
Trial 3

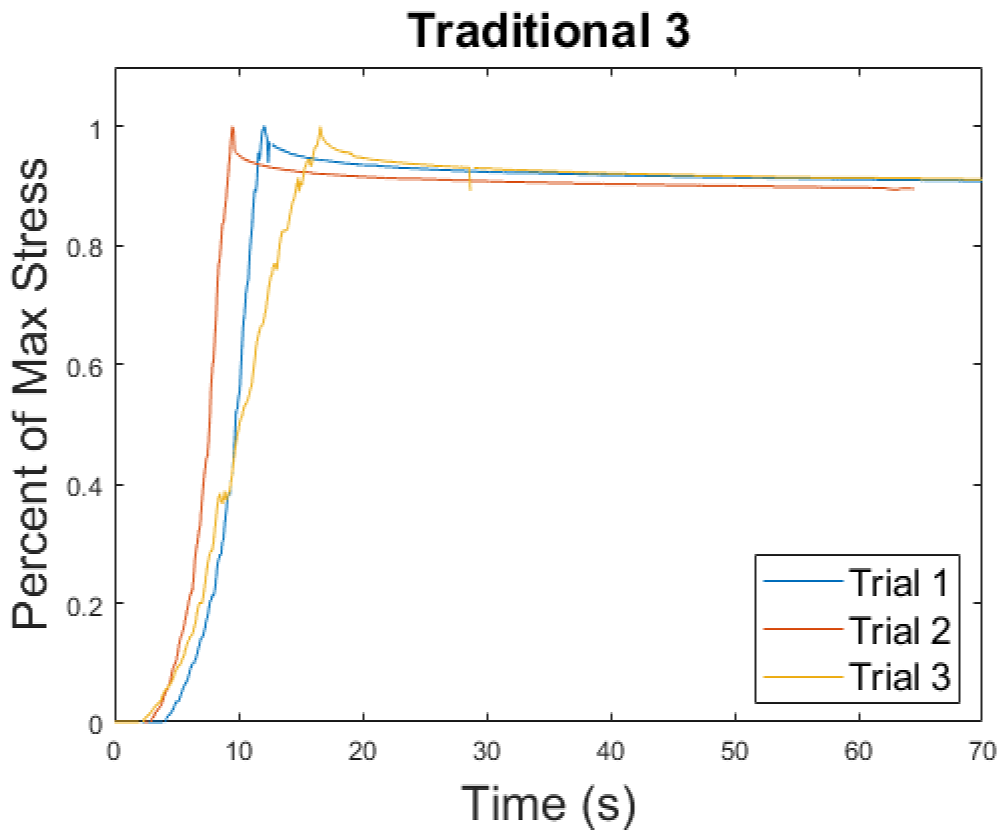
Traditional 3
Percent of Max Stress
Time (s)
0
0.2
0.4
0.6
0.8
1
0
10
20
30
40
50
60
70
Trial 1
Trial 2
Trial 3

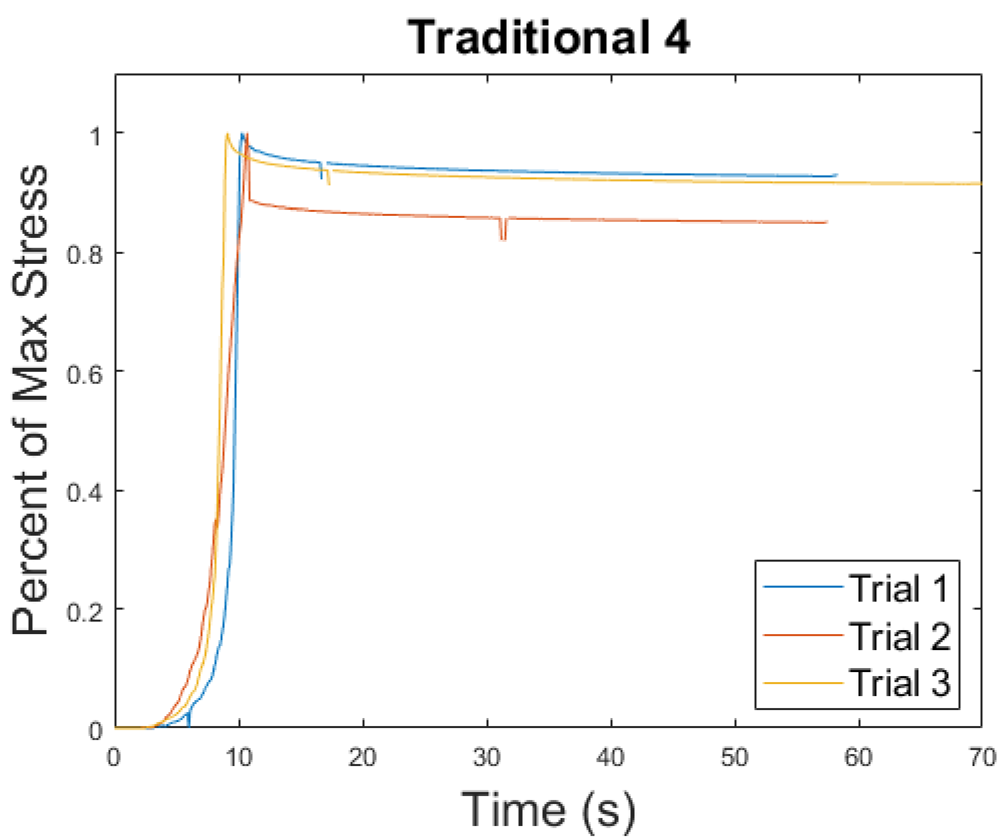
Traditional 4
Percent of Max Stress
Time (s)
0
0.2
0.4
0.6
0.8
1
0
10
20
30
40
50
60
70
Trial 1
Trial 2
Trial 3

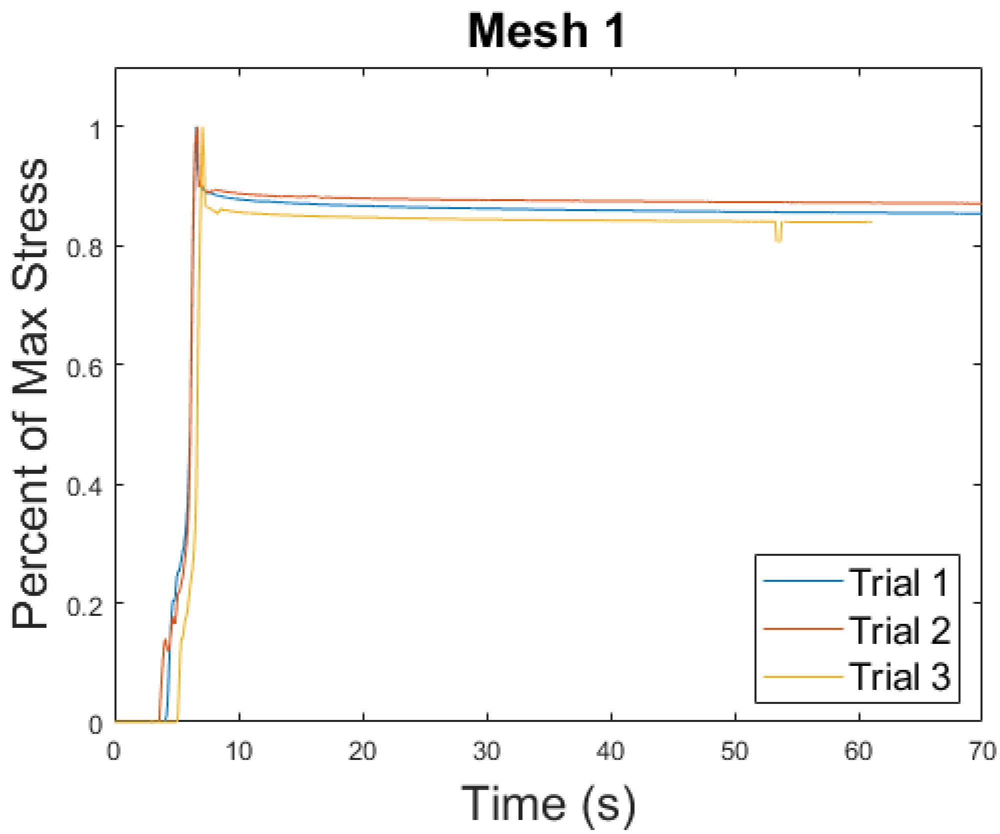
Mesh 1
Percent of Max Stress
Time (s)
0
0.2
0.4
0.6
0.8
1
0
10
20
30
40
50
60
70
Trial 1
Trial 2
Trial 3

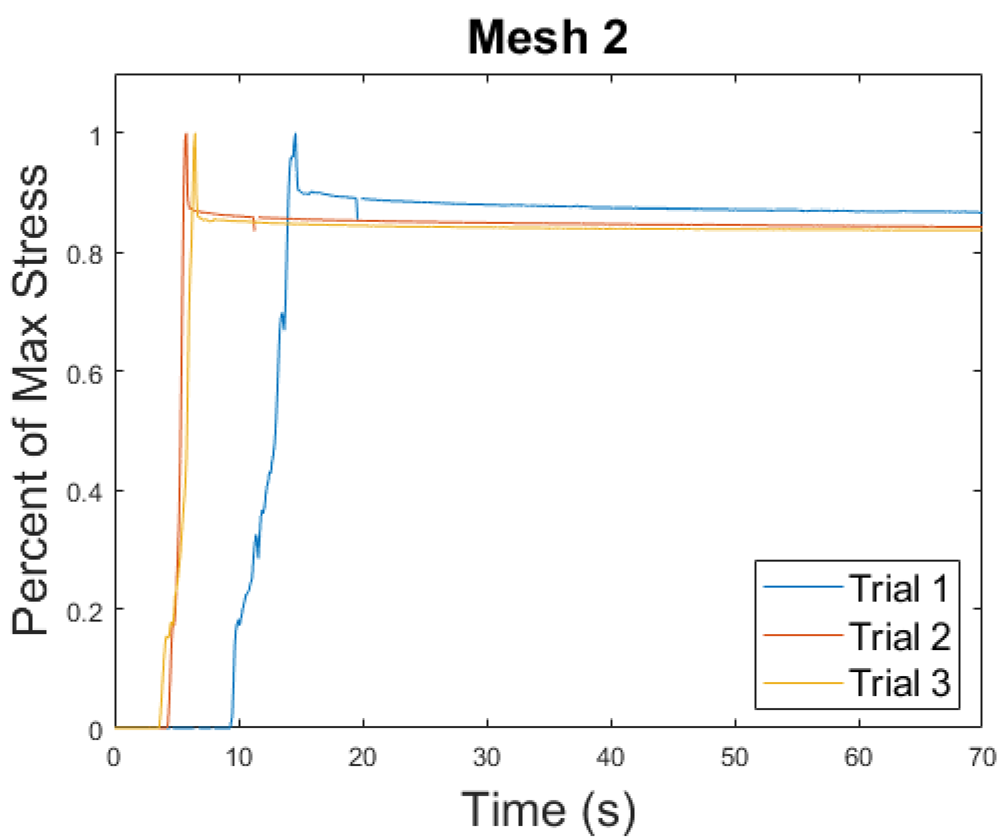
Mesh 2
Percent of Max Stress
Time (s)
0
0.2
0.4
0.6
0.8
1
0
10
20
30
40
50
60
70
Trial 1
Trial 2
Trial 3

130

Published with MATLAB® R2020a

APPENDIX I

Product Cross-Sectional Photographs

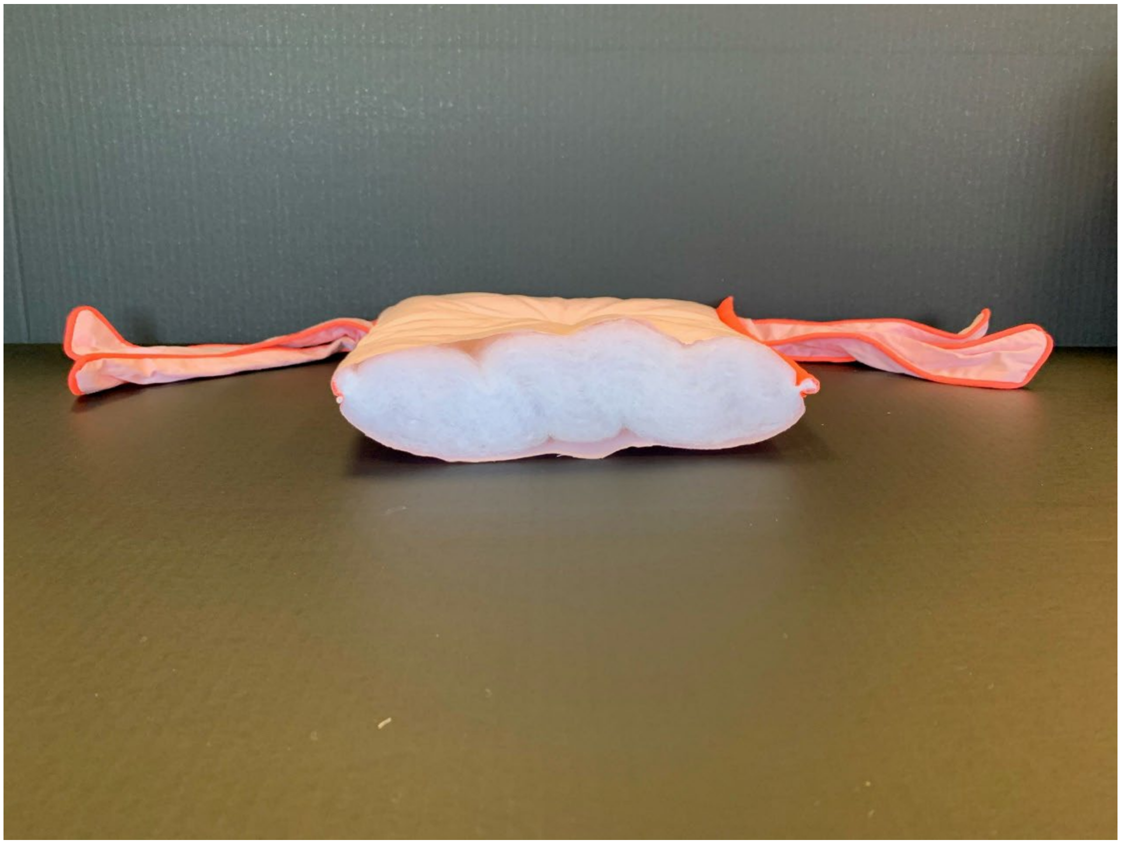

Figure I.1 Cross Sectional Photo of Traditional 1.

Figure I.2 Cross Sectional Photo of Traditional 2.

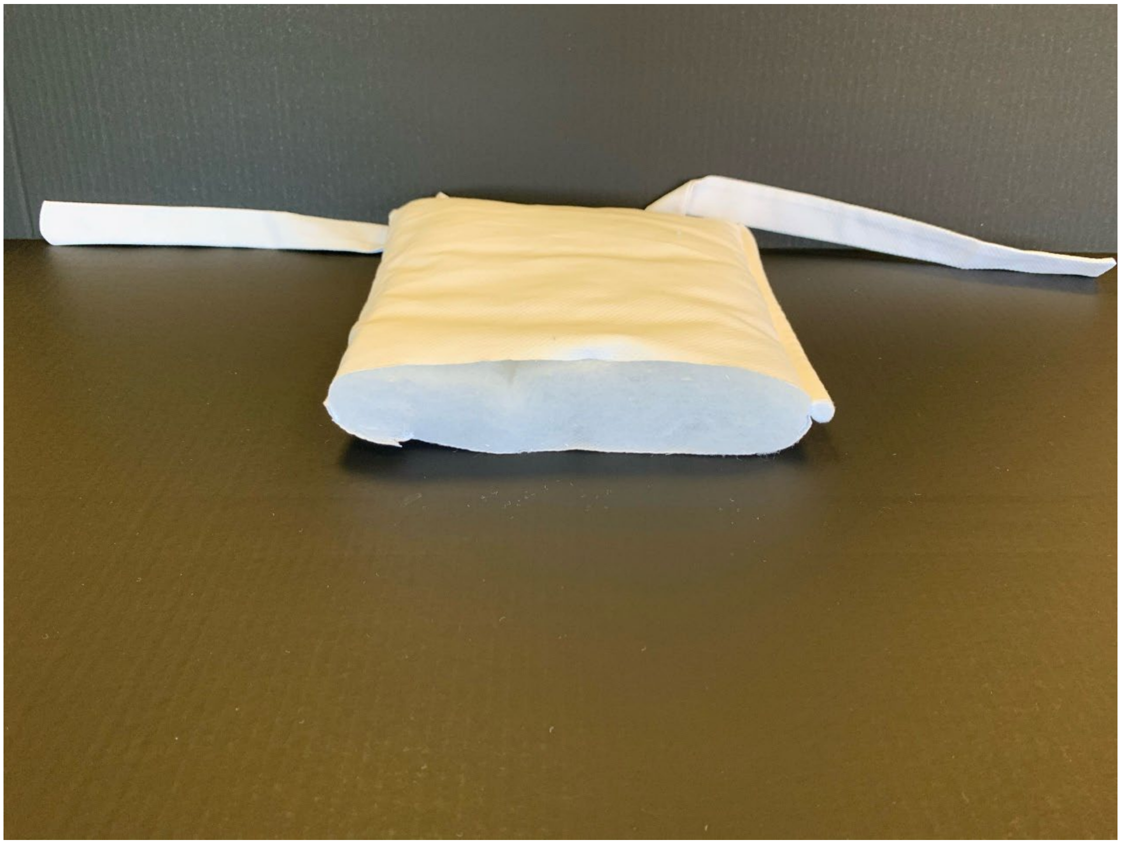

Figure I.3 Cross Sectional Photo of Traditional 3.

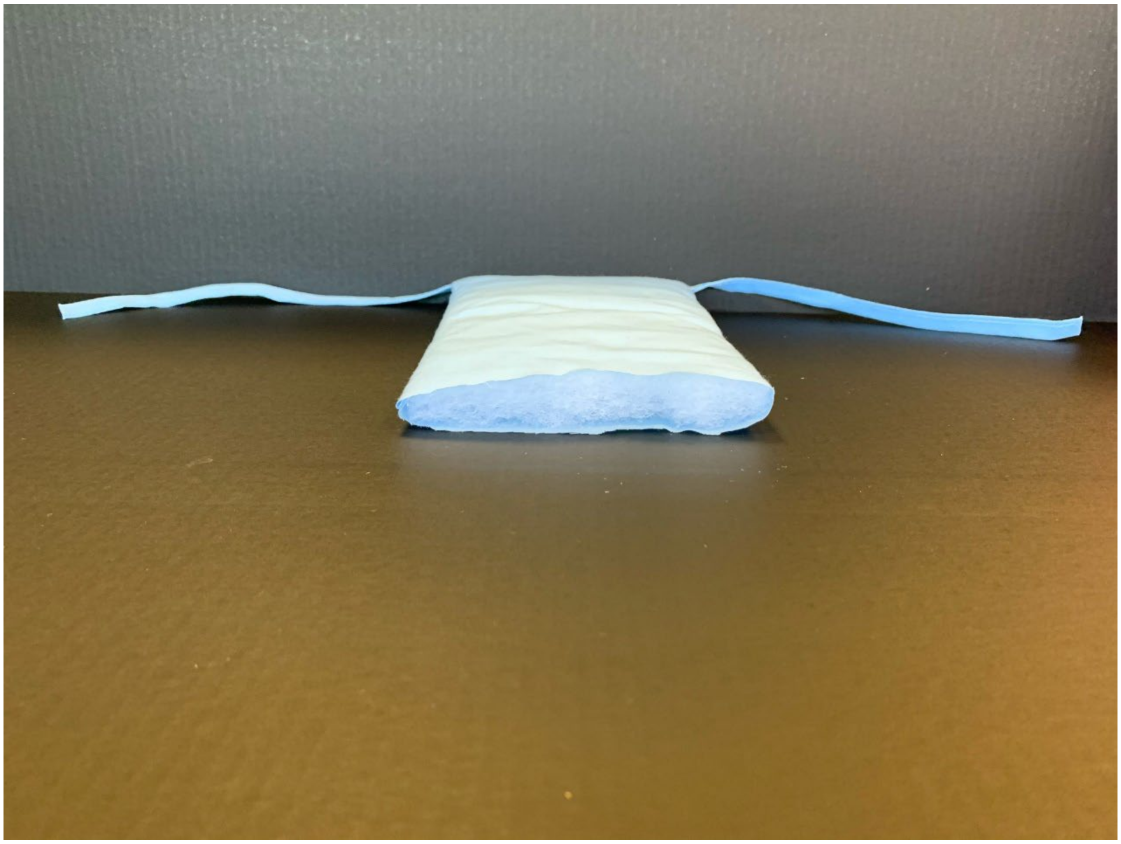

Figure I.4 Cross Sectional Photo of Traditional 4.

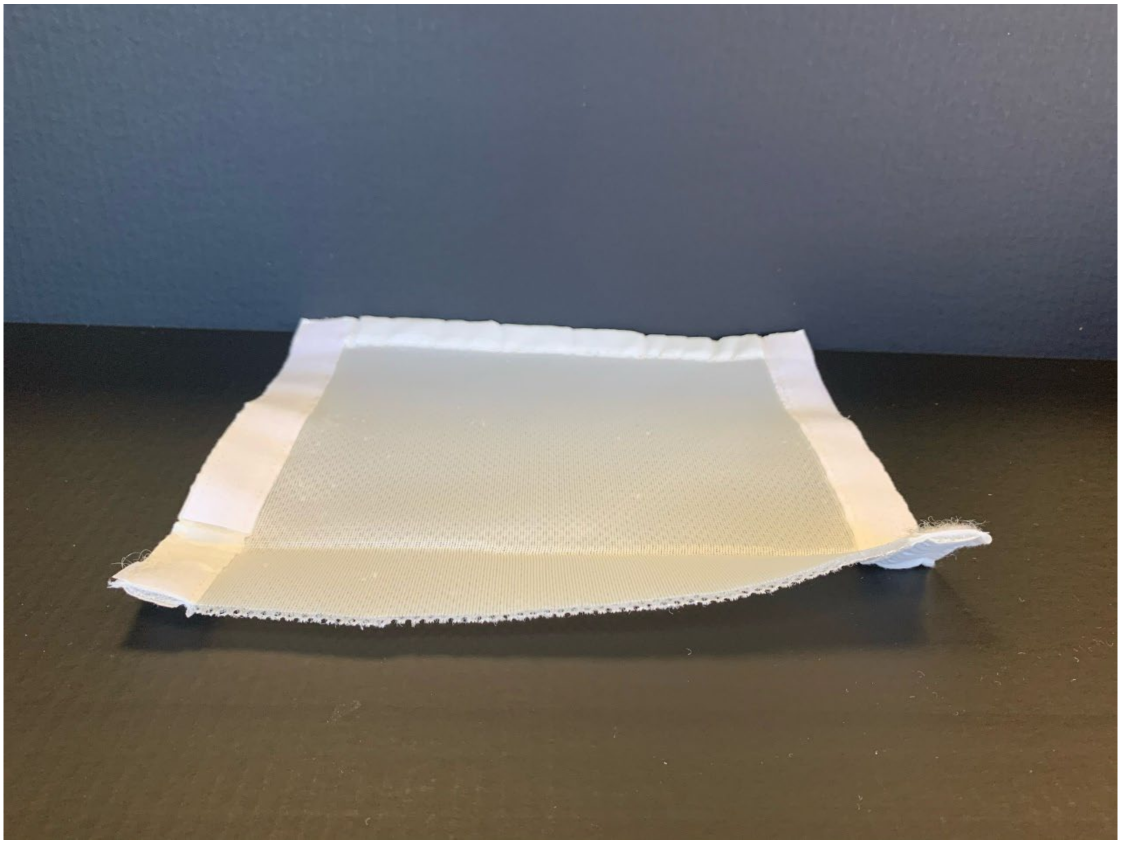

Figure I.5 Cross Sectional Photo of Mesh 1.

Figure I.6 Cross Sectional Photo of Mesh 2.